INTERACTIONS AMONG CLIMATE, FIRE, AND VEGETATION IN THE

ALASKAN BOREAL FOREST

A

THESIS

Presented to the Faculty

of the University of Alaska Fairbanks

in Partial Fulfillment of the Requirements

for the Degree of

DOCTOR OF PHILOSOPHY

By

Paul Arthur Duffy, B.A., M.A.

Fairbanks, Alaska

August 2006

UMI Number: 3240324

Copyright 2007 by

Duffy, Paul Arthur

All rights reserved.

INFORMATION TO USERS

The quality of this reproduction is dependent upon the quality of the copy submitted. Broken or indistinct print, colored or poor quality illustrations and photographs, print bleed-through, substandard margins, and improper alignment can adversely affect reproduction.

In the unlikely event that the author did not send a complete manuscript and there are missing pages, these will be noted. Also, if unauthorized copyright material had to be removed, a note will indicate the deletion.

UMI®

UMI Microform 3240324

Copyright 2007 by ProQuest Information and Learning Company.

All rights reserved. This microform edition is protected against unauthorized copying under Title 17, United States Code.

ProQuest Information and Learning Company
300 North Zeeb Road
P.O. Box 1346
Ann Arbor, MI 48106-1346

INTERACTIONS AMONG CLIMATE, FIRE, AND VEGETATION IN THE

ALASKAN BOREAL FOREST

By

Paul Arthur Duffy

RECOMMENDED:

_____

_____

_____

_____

_____
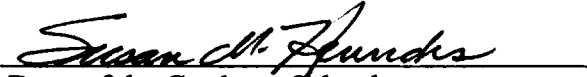Advisory Committee Chair

_____
Chair, Department of Forest Sciences

APPROVED:

_____
Dean, School of Natural Resources and Agricultural Sciences

_____
Dean of the Graduate School

_____
Date   August 3, 2006

Abstract

The boreal forest covers 12 million km^2 of the northern hemisphere and contains roughly 40% of the world's reactive soil carbon. The Northern high latitudes have experienced significant warming over the past century and there is a pressing need to characterize the response of the disturbance regime in the boreal forest to climatic change. The interior Alaskan boreal forest contains approximately 60 million burnable hectares and, relative to the other disturbance mechanisms that exist in Alaska, fire dominates at the landscape-scale. In order to assess the impact of forecast climate change on the structure and function of the Alaskan boreal forest, the interactions among climate, fire and vegetation need to be quantified. The results of this work demonstrate that monthly weather and teleconnection indices explain the majority of observed variability in annual area burned in Alaska from 1950-2003. Human impacts and fire-vegetation interactions likely account for a significant portion of the remaining variability. Analysis of stand age distributions indicate that anthropogenic disturbance in the early 1900's has left a distinct, yet localized impact. Additionally, we analyzed remotely sensed burn severity data to better understand interactions among fire, vegetation and topography. These results show a significant relationship between burn severity and vegetation type in flat landscapes but not in topographically complex landscapes, and collectively strengthen the argument that differential flammability of vegetation plays a significant role in fire-vegetation interactions. These results were used to calibrate a cellular automata model based on the current conceptual model of interactions among weather, fire and vegetation. The model generates spatially explicit maps of simulated stand ages at 1 km resolution across interior Alaska, and output was validated using observed stand age distributions. Analysis of simulation output suggests that significant temporal variability of both the mean and variance of the stand age distribution is an intrinsic property of the stand age distributions of the Alaskan boreal forest. As a consequence of this non-stationarity, we recommend that simulation based methods be used to analyze the impact of forecast climatic change on the structure and function of the Alaskan boreal forest.

Table of Contents

List of Figures

List of Tables

Introduction

The boreal forest covers 12 million km^2 of the northern hemisphere and contains roughly 40% of the world's reactive soil carbon, an amount similar to that held in the atmosphere (Melillo et al. 1993, McGuire et al. 1995, IPCC 2001). The biophysical phenomena affecting carbon storage and high latitude albedo make the boreal forest an integral component of the global climate system (IPCC 2001). Observational evidence suggests that the Northern high latitudes have experienced significant warming over the past century that is largely due to shifts in atmospheric circulation (Serreze et al. 2000). Abrupt shifts in climate patterns can modify feedbacks among climate, vegetation, and disturbance factors. These changes in the short-term interactions are collectively referred to as transient ecosystem dynamics (TED). In the boreal forest, TED may persist for decades to centuries after an abrupt climate change (Kittel et al. 2000) because of the lags caused by species migrations (Rupp et al. 2001), soil development (Zhuang et al. 2003), and impacts on permafrost (Osterkamp and Romanovsky 1999, Osterkamp et al 2000). Because of interactions among these and other factors, the response of the boreal forest to climatic change is complex and also exerts an influence on the global carbon cycle (Fan et al. 1998, Goulden et al. 1998, Rapalee et al. 1998, Harden et al. 2000, Michalek et al. 2000, IPCC 2001). Consequently, there is a pressing need to characterize the sensitivities and potential responses of the disturbance regime of the boreal forest to climatic change (Schimel et al. 1997, Fosberg et al. 1999, Gower et al, 2001, Chapin et al. 2003).

Disturbance regimes often govern the TED within ecosystems, and relative to the other disturbance mechanisms (e.g., beetlekill and windthrow) that exist in Alaska, fire dominates at the landscape-scale (Van Cleve et al. 1991, Payette 1992). Within the North American boreal forest, Interior Alaska (i.e., the region between the Alaska and Brooks Ranges) contains roughly 60 million burnable hectares and includes the largest National Parks and Wildlife Refuges in the United States. For the period of 1950-2003, wildland fires burned an average of roughly 270,000 hectares in Interior Alaska each year. Fires routinely threaten the lives, property, and timber resources of the sparse but growing

population, yet they play a crucial role in the maintenance of the Alaskan boreal forest ecosystem through influences on secondary succession (Chrosciewicz 1974, Dyrness and Norum 1983, Van Cleve and Viereck 1983, Zasada et al. 1983, Foster 1985, Payette 1992, Van Cleve et al. 1996, Greene and Johnson 1999, Mann and Plug 1999, Johnstone et al. 2004, Johnstone and Kasischke 2005), stand age (Kurz and Apps 1999, Goodale et al. 2002), and carbon cycling (McGuire et al. 2004, Csiszar et al. 2000). Despite the pervasive economic and ecological impacts, fundamental aspects of the fire regime in Interior Alaska remain poorly understood. The first chapter of this work refines the conceptual model of the Alaskan boreal forest ecosystem by quantifying critical aspects of interactions among fire, climate and forest vegetation.

In the Alaskan boreal forest, the influence of climate is felt on both fire and vegetation at varying temporal scales. The link between climate and vegetation exists at a much longer timescale (i.e., decades to centuries) relative to the influence of climate on fire (i.e., months to hours). Despite the lower temporal frequency, the link between climate and vegetation has been shown to vicariously influence the historical fire regime in Alaska through modification of the dominant forest species (Lynch et al. 2003, Lynch et al. 2004). Outside of Alaska in the Canadian boreal forest, there is evidence that, on timescales of hundreds to thousands of years, climate has a more direct influence on fire regime (Carcaillet and Richard 2000, Carcaillet et al. 2001). Hence, climate differentially exerts influences on both vegetation composition and fire regime depending on the location within the boreal forest as well as the resolution of the timescale of interest. Quantification of the role of climate with respect to the fire regime in Alaska is of critical importance for the conceptual model development of the boreal forest ecosystem.

As a mechanism that modifies atmospheric circulation patterns at large spatial scales, atmospheric teleconnections affect weather throughout the northern hemisphere (Hurrell 2003). Teleconnections are correlated anomalies of geopotential height (Wallace and Gutzler, 1981, Barnston and Livezey, 1987) that impact regional weather through

recurring and persistent shifts in pressure and circulation across large spatial scales. Links between disturbance and weather that are modified by teleconnections include droughts and fire in Canada (Bonsal et al. 1993, Bonsal and Lawford 1999, Skinner et al. 2002, Girardin et al. 2004), fires in the Pacific Northwestern US (Hessl et al. 2004) and fires in the Southwestern US (Swetnam and Betancourt 1990). In Alaska, deviations from synoptic weather patterns have been correlated with the Pacific Decadal Oscillation (Papineau 2001, Hartmann and Wendler 2003) as well as the El Niño/Southern Oscillation and Pacific/North America patterns (Hess et al. 2001). Specifically, the occurrence of large fire years has been correlated with the presence of strong to moderate El Niño conditions (Hess et al. 2001). This work moves a step further and quantifies the impact of these signals on the annual area burned in Alaska through the development of a statistical regression model.

Quantification of the influence of weather on annual area burned provides a necessary part of the foundation for deeper understanding of fire regime in Alaska. Although weather plays a dominant role in the flammability of the Alaskan landscape, interactions between fire and vegetation potentially play an important role as well. Specifically, heterogeneity of burn severity within fire perimeters results in differential ecological impacts that are significant with respect to secondary succession (Chrosciewicz 1974, Dyrness and Norum 1983, Van Cleve and Viereck 1983, Zasada et al. 1983, Foster 1985, Payette 1992, Johnstone et al. 2004). Previous studies of burn severity in boreal forests have resulted in several different metrics of quantification: from the amount of organic matter consumed to the amount of the soil surface and vegetation that is charred (Michalek et al. 2000, Miyanishi and Johnson 2002, Greene et al. 2004, van Wagtendonk et al. 2004, Epting and Verbyla 2005, Johnstone and Kasischke 2005). A driving factor for the existence of different metrics is that critical ecological processes (e.g., post-fire succession and carbon cycling) are differentially influenced depending on the specific characterization of burn severity. For example, if the amount of carbon immediately released by a fire is the variable of interest, then the amount of organic matter consumed

is a more appropriate metric to use for burn severity (Michalek et al. 2000). If, however, it is of interest to characterize the relationship between burn severity and post-fire succession, then the amount of the soil surface that is charred may be a more appropriate metric of burn severity.

Many of the factors that drive post-fire succession are also strongly related to topography (e.g., water availability for seedlings, solar radiation and burn severity); hence these patterns need to be characterized across a large spatial domain (Bridge and Johnson 2000). Specifically, the existence of patterns of burn severity associated with different positions on the landscape (Miyanishi and Johnson 2002) provides additional motivation for the quantification of burn severity across large spatial domains that sufficiently represent the range of topographic diversity. The existence of topographically controlled factors driving succession suggests a certain amount of stability in dominant forest type with respect to post-fire succession (i.e., self-replacement). Observational data show this is often the case (Van Cleve and Viereck 1983, Greene and Johnson 1999); however, extremely severe burns can preclude the asexual sprouting that is the dominant mechanism for self-replacement in broadleaf stands (Johnstone et al. 2004, Johnstone and Kasischke 2005). Additionally, extremely severe burns resulting in a charred and exposed mineral soil surface can destroy the serotinous cones that often serve as the seed source for self-replacement in conifer-dominated stands. This allows for aerially dispersed seeds of broadleaf trees to colonize the burned site (Lutz 1956, Viereck 1973, Zasada et al. 1983, Johnstone et al. 2004). As a consequence, relay-floristics (i.e., the post-fire germination and subsequent canopy dominance of broadleaf vegetation from seed on sites previously dominated by conifers) also operates as a post-fire successional pathway (Van Cleve and Viereck 1983, Van Cleve et al. 1996). Hence, burn severity is a factor that is influenced but not completely controlled by topography (Miyanishi and Johnson 2002), and as such plays a critical role in the modification of vegetation patterns on the landscape through time. To better understand the relationship between large-scale patterns of burn severity and vegetation dynamics, it is essential that the metric of burn

severity used be able to estimate burn severity across large spatial domains. The second chapter of this work uses remotely sensed burn severity data to evaluate large-scale patterns of burn severity as a function of topography and vegetation type across three spatial resolutions (90m, 500m and 1km).

The initiation of succession by fire, with its subsequent shifts in stand age structure and dominant species, modifies carbon flux from boreal forests across multiple temporal scales (McGuire et al. 2004, Csiszar et al. 2004). As stand age increases, the ability to sequester carbon decreases and the susceptibility to disturbance increases (Kurz and Apps 1999). The importance of the relationship between stand age distribution and disturbance is underscored by modeling results suggesting a shift in Canadian forest ecosystems from a sink during 1920-1980 to a source from 1980-1989 that is attributed to a change in the disturbance regime (Kurz and Apps 1999). Field data support the importance of the link between disturbance and carbon flux and during the late 1980-1990's growth in the relatively unmanaged forests of Canada and Eastern Russia was offset by an increase in disturbance (Goodale et al. 2002). The importance of the linkages between stand age, disturbance and carbon flux is clear and these interactions play a critical role in understanding the impact of future climate change. A key question in the ongoing conceptual model development relating fire-disturbance and carbon flux in the Alaskan boreal forest is: Does stand flammability change as a function of time since fire? And, more specifically, does the susceptibility to fire increase through time?

Numerous studies have used stand origin reconstructions to better understand the local disturbance regimes in the boreal forest (Van Wagner, 1978, Yarie 1981, Johnson and Van Wagner 1985, Larsen 1997, Reed 1997, Reed et al. 1998, Reed 1998, Polakow and Dunne 1999, Bergeron 2000, Weir et al. 2000, Parisien and Sirois 2003, Bergeron et al. 2004, Grenier et al. 2005). These studies, to a large extent, used parametric methods to analyze stand age data or time since last fire (TSLF) data. Analysis using the distributional models of TSLF data allows inference regarding properties of the fire

regime (e.g., hazard functions) in the area of interest. However, the application of standard parametric methods requires selection of a distributional model for the data and stationarity of the underlying process being studied. Stationarity in this context refers to the mean and variance being roughly constant through time. The utility of subsequent analyses rests on not only the degree to which the selected model fits the observed data but also the validity of the stationarity assumption. Due to the strong relationship between annual area burned and short term weather that exists in the boreal forest (Skinner et al. 1999, Hess et al. 2001, Skinner et al. 2002, Girardin et al. 2004, Duffy et al. 2005), there is often a significant lack of fit between the data and corresponding distributional models (Boychuk et al. 1997). The annual distribution of area burned in Alaska is skewed with the majority of the area burned coming in a relatively small percentage of the years (Kasischke et al. 2006). Even when interior Alaska as a whole is considered as the area of interest, climatic anomalies and the corresponding large areas burned from decades ago produce spikes in the distribution of stand ages, which drive a significant lack of fit for distributional models (Boychuk et al.1997, Johnson et al. 1998). Ignoring a lack of fit and proceeding with distributional modeling can convey a false impression about the intrinsic variability and more importantly potential stationarity of the fire regime. When parametric modeling efforts result in a significant lack of fit, or the stationarity assumptions are not valid, the resulting analyses can lead to a false perception regarding the stability of critical aspects of the fire regime.

An additional factor that can influence the structure of the boreal forest is the impact of anthropogenic disturbance (Drobyshev et al. 2004, Bergeron et al. 2004, Grenier et al. 2005). In Alaska, the current impact of humans on fire regimes near cities is fire suppression, which results in a reduction of the area burned (DeWilde and Chapin, in press). However, the impact of historical anthropogenic disturbance on the current structure of the boreal forest is less clear. Aboriginal settlements have existed across interior Alaska for thousands of years. In a sense, this activity could be considered part of the "natural" fire regime since it is thought to have been relatively low impact with

respect to area burned (Natcher 2004). One of the goals of this work is to assess the impact of mining-related anthropogenic disturbance that has occurred in the past one hundred years. There are numerous examples within interior Alaska of places where mining camps have been set up and, after a couple of decades, have essentially disappeared. These situations provide a unique opportunity to examine the legacy of anthropogenic disturbance with respect to stand age distributions in the boreal forest.

The final chapter of this work combines information from the first two chapters with additional analyses to characterize critical linkages among humans, climate, fire and the distribution of forest stand ages across the landscape of interior Alaska. Specifically, the importance of age-dependent flammability is assessed, and incorporated into a spatially explicit cellular automata simulation model (ALFRESCO). The simulation is calibrated using a backcast of annual area burned generated by a statistical representation of the relationship between climate and annual area burned in Alaska. The simulation output is then validated using observed stand age data collected across a climatic gradient within interior Alaska. The simulation output provides a baseline of the historical variability and, as a consequence, future changes in stand age distributions can now be assessed in this context. For example, the impact of different fire-management policies on forest structure can be examined with respect to the historical variability. Additionally, the estimation of changes in the average stand age through time provides essential information regarding aspects of boreal carbon cycling related to stand age distributions in the boreal forest.

CHAPTER 1

IMPACTS OF LARGE-SCALE ATMOSPHERIC-OCEAN VARIABILITY ON ALASKAN FIRE SEASON SEVERITY[1]

1.1   Abstract

Fire is the keystone disturbance in the Alaskan boreal forest and is highly influenced by summer weather patterns. Records from the last fifty-three years reveal high variability in the annual area burned in Alaska and corresponding high variability in weather occurring at multiple spatial and temporal scales. Here we use multiple linear regression (MLR) to systematically explore the relationships among weather variables and the annual area burned in Alaska. Variation in the seasonality of the atmospheric circulation-fire linkage is addressed through an evaluation of both the East Pacific teleconnection field and a Pacific Decadal Oscillation index keyed to an annual fire index. In the MLR, seven explanatory variables and an interaction term collectively explain 79% of the variability in the natural logarithm of the number of hectares burned annually by lightning-caused fires in Alaska from 1950-2003. Average June temperature alone explains one-third of the variability in the logarithm of annual area burned. The results of this work suggest that the Pacific Decadal Oscillation and the East Pacific teleconnection indices can be useful in determining a priori an estimate of the number of hectares that will burn in an upcoming season. This information also provides insight into the link between ocean-atmosphere interactions and the fire disturbance regime in Alaska.

1.2   Introduction

The boreal forest covers 12 million km^2 of the northern hemisphere and contains roughly 40% of the world's reactive soil carbon, an amount similar to that held in the atmosphere (Melillo et al. 1993, McGuire et al. 1995, IPCC 2001). The biophysical phenomena affecting carbon storage and high latitude albedo make the boreal forest an integral component of the global climate system (IPCC 2001). Fire-initiated succession underlies the biophysical factors, and there is a pressing need to characterize sensitivities and potential responses of the boreal forest disturbance regime to climatic change (Schimel et al. 1997, Fosberg et al. 1999, Gower et al. 2001, Chapin et al. 2003). The impact of forecast climatic warming on fire regimes in North America varies from a prediction for increased burning for Alaska and Canada (Flannigan et al. 2000, Flannigan et al. 2001) to reduced fire frequency in eastern Canada (Carcaillet et al. 2001). Quantification of the links between climate and fire in Alaska is not only essential for understanding the dominant landscape-scale disturbance processes in Alaska, but it is also a valuable tool for planning fire management activities and developing a better understanding of how forecast climate change might impact the dominant disturbance mechanism.

Within the North American boreal forest, interior Alaska (i.e., the region between the Alaska and Brooks Ranges) contains roughly 60 million burnable hectares and includes the largest National Parks and Wildlife Refuges in the United States. Most of this huge area is roadless. For the period of 1950-2003, wildland fires burned an average of roughly 270,000 hectares in interior Alaska each year and they routinely threaten the lives, property, and timber resources of the sparse but growing population. Wildland fires can threaten human values, yet they play a crucial role in the maintenance of interior Alaskan ecosystems. Despite the pervasive economic and ecological impacts, fundamental aspects of the fire regime in interior Alaska are poorly understood.

Fire regimes consist of many components including frequency, duration, intensity, severity, seasonality, extent, and spatial distribution. When complicating factors such as interactions with other components of the ecosystem (e.g., human impacts, weather, vegetation) and the importance of spatial and temporal scales are taken into account, the characterization of a fire regime requires a tremendous amount of data and appropriate analysis. One of the most basic aspects of a fire regime is the fire cycle (i.e., the amount of time it takes to burn an area equivalent to the study area). There are only a few field studies from interior Alaska that utilize fire-scar and/or tree age distributions to infer fire cycle (Yarie 1981, DeVolder 1999, Mann and Plug 1999). These studies were scattered over a region the size of Montana and show that fire cycles in Alaska are probably >250 years in the relatively moist, southern parts of the state (Mann personal communication), 80-100 years near Fairbanks in the central interior (Mann et al. 1995), and <80 years for the Porcupine River valley in the northeastern portion of the state (Yarie 1981). These estimates are consistent with the results of Kasischke et al. (2002) who used fire perimeter data (from aerial photography and remotely sensed data) from the past five decades to estimate fire cycles for different ecoregions of the interior. The uncertainty associated with these fire cycle estimates is unknown.

At longer temporal scales but somewhat more coarse resolution, charcoal and pollen analyses from varved lake sediments reveal critical information about the fire frequency and interactions among fire, climate and vegetation. Due to the limited dispersal of charcoal particles that are used in these analyses, the results apply to limited spatial scales. Within interior Alaska, there have only been a few studies that utilize sediment cores to gain insight about the fire regime. Pollen and charcoal data from several sediment cores in interior Alaska reveal shifts in vegetation (i.e., increased dominance of *Picea mariana*) around 2400 yr BP are associated with a corresponding shift in the fire regime (Lynch et al. 2003). The implication is that climatic change occurring at decadal to centennial time scales influenced the fire regime through shifts in dominant vegetation. This yields the counter-intuitive result that cooler and moister

climate results in higher fire frequency due to the increased dominance of the relatively more flammable *Picea mariana*. This response appears to extend outside interior Alaska to forests South of the Alaska Range as well (Lynch et al. 2004). These studies provide evidence that climatically-induced shifts in dominant vegetation within the boreal forest over a period of decades to centuries can potentially modify the fire regime. Outside of Alaska in the Canadian boreal forest, there is evidence that, on timescales of hundreds to thousands of years, climate has a more direct influence on fire regime (Carcaillet and Richard 2000, Carcaillet et al. 2001). Hence, climate differentially exerts influences on both vegetation composition and fire regime depending on the location within the boreal forest as well as the resolution of the timescale of interest.

As a mechanism that modifies atmospheric circulation patterns at large spatial scales, atmospheric teleconnections affect weather throughout the northern hemisphere (Hurrell 2003). Teleconnections are correlated anomalies of geopotential height (Wallace and Gutzler, 1981, Barnston and Livezey, 1987) that impact regional weather through recurring and persistent shifts in pressure and circulation across large spatial scales. Links between disturbance and weather that are mediated by teleconnections include; droughts and fire in Canada (Bonsal et al. 1993, Bonsal and Lawford 1999, Skinner et al. 2002, Girardin et al. 2004), fires in the Pacific Northwestern US (Hessl et al. 2004) and fires in the Southwestern US (Swetnam and Betancourt 1990). In Alaska, deviations from synoptic weather patterns have been correlated with the Pacific Decadal Oscillation (Papineau 2001, Hartmann and Wendler 2003) as well as the El Niño/Southern Oscillation and Pacific/North America patterns (Hess et al. 2001). Specifically, the occurrence of large fire years has been correlated with the presence of strong to moderate El Niño conditions (Hess et al. 2001). Our work moves a step further and quantifies the impact of these signals on the annual area burned in Alaska through the development of a statistical regression model.

Experience and common sense dictate that fire responds to local weather conditions but modeling results indicate that the link between weather and fire does not easily translate to the landscape scale (Flannigan and Harrington 1988, Hely et al. 2001, Westerling et al. 2002). Yet at large spatial scales, statistical relationships quantifying these links at an annual temporal resolution in Alaska have not been established. It is important to stress the spatio-temporal scale at which this analysis is relevant since the dynamics of interactions among climate, fire and vegetation change depending on the spatial and temporal scale of interest. This work quantifies the relationship among monthly teleconnection indices, specifically the East Pacific teleconnection and the Pacific Decadal Oscillation, and the annual area burned by lightning caused fires in Alaska through the development of a statistical regression model. To this end, a Multiple Linear Regression (MLR) model is developed, with the natural logarithm of the number of hectares burned annually as the response variable and monthly climatic indices for explanatory variables. We used a sequential selection procedure to evaluate linkages between teleconnection indices and monthly temperature and precipitation. In doing so, we characterize the linkages among components of the climate system that exert an influence on short-term surface weather in Alaska. The statistical model presented in this work represents a simple first step in quantifying the complex linkages between climate and fire in interior Alaska, where fire is the dominant agent of landscape-level change (Van Cleve et al. 1991, Payette 1992) and dictates the composition of the forest vegetation through determination of the successional trajectory (Zackrisson 1977, Van Cleve and Viereck 1983, Payette 1992, Mann and Plug 1999).

1.3   Methods

1.3.1   Fire Data

The Alaska Fire Service (AFS) maintains a database of fires for the state of Alaska dating back to 1950. These data are commonly referred to as the Large Fire Data Base (LFDB) and can be found at the Alaska Geospatial Data Clearinghouse (AGDC:

http://agdc.usgs.gov/data/blm/fire/index.html) (Kasischke et al. 2002). The period of analysis for our study is 1950-2003 (Figure 1.1). For each year and for each fire recorded in the AGDC, there are many pieces of information recorded including, ignition source (i.e., human or lightning) and a record of the approximate size of each fire. Estimates of the annual number of hectares burned in Alaska that are used in this analysis come from summing the number of hectares burned from each lightning-caused fire within a given year. Because lightning is the natural ignition source, part of the climate-fire link includes the climatic conditions that are favorable for lightning-caused ignitions (Johnson 1992, Nash and Johnson 1996, Wierzchowski et al. 2002). Lightning caused fires are rare both north of the Brooks Range and south of the Alaska Range and as a consequence the majority of fires burn between these mountain ranges within the region known as interior Alaska (Figure 1.1).

Human-caused fires were excluded since the analysis is focused on the link between climate and fire. Historically, the exclusion of human-caused fires has a relatively small impact on the number of hectares burned annually. However, in 2001 and 2002, over 95 % and 40% of the respective area burned was caused by non-lightning ignition sources. Another factor to consider regarding the use of the LFDB is that reliability of source determination can reasonably be assumed to be more questionable for the early part of the record. Only fires that burned an area greater than 50 hectares (0.5 km^2) were included in the analysis. This was done so the results of this work could be used in conjunction with the frame-based spatially explicit ecosystem model ALFRESCO (Starfield and Chapin 1996, Rupp et al. 2000), which operates on a spatial resolution of 1 km^2. The exclusion of fires smaller than 50 hectares (0.5 km^2) has a negligible impact on the output of the statistical model.

1.3.2 Climate Data

Alaskan climate station data that are both homogeneous and complete for the past half-century are sparse. Data were obtained from the Western Region Climate Center

(WRCC: http://www.wrcc.dri.edu/summary/climsmak.html). There are fewer than a dozen climate stations in Alaska with sufficient data for our modeling purposes (Figure 1.1). The requirement for selection of a climatic station was that no more than 5% of the monthly observations from 1950-2003 were missing. Based on this selection criteria and spatial representativeness with respect to fires that have burned over the period of record, the following seven stations were used: Bettles, Delta Junction, Fairbanks, McGrath, Nome, Northway and Tanana (Figure 1.1).

The question of how to represent both the temperature and precipitation of Alaska based on these seven stations is not a trivial one. We are essentially determining from a small number of stations a spatial zone of weather influence for the area burned annually in Alaska. Several methods for calculating representative weather were evaluated. Different weighting schemes for the climate data were considered based on the spatial location of fires for a given year. As an example, if the majority of fires burned near Tanana in a given year, then a weighting scheme would give the data from Tanana greater weight than the other six stations when assembling the weather data for that year. Of the different methods evaluated for assembling the climate data, the simplest and most effective in terms of explaining the greatest variability was a simple average of the data for a given month from the seven stations. This results in a "statewide" average of both temperature and precipitation for each month in a given year. This procedure essentially integrates any spatial information regarding intrastate variability over interior Alaska into a single estimate. For each station, the average monthly temperatures from the WRCC are calculated as the average of all the average daily temperatures in a given month. The monthly precipitation for each station was calculated as the sum of the precipitation amounts recorded daily at each station for each day in the month. The average monthly precipitation for the MLR was then taken to be the average of the monthly precipitation recorded for each of the seven stations.

Additionally, we re-fit our regression model using monthly temperature and precipitation data from the Climate Research Unit (CRU) in place of the seven-station average. The CRU data consist of data-based model estimates of monthly temperature and precipitation values for half-degree cells and are a distance weighted average of all available station data in Alaska. Hence, a different number of stations are used depending on which data are available for a given month. We averaged the monthly values for cells covering the region of interior Alaska where fires burn (Figure 1.1) to produce a CRU based dataset that is capable of driving our statistical model. The reduction in variability explained by the statistical model when the CRU dataset is used was less than 5%. This shows that the results of the regression model are robust with respect to the method of spatially integrating the climate data, and it also shows that the simple seven-station average does the best job of representing the weather signals that explain inter-annual variability in area burned.

1.3.3 East Pacific (EP) Teleconnection Data

Monthly teleconnection indices were obtained from the National Oceanic and Atmospheric Administration (NOAA) Climate Prediction Center (CPC: http://www.cpc.ncep.noaa.gov/data/teledoc/telecontents.html). Each teleconnection identified by the CPC (e.g., the North Atlantic Oscillation, East Atlantic, East Atlantic Jet, East Atlantic/Western Russia, Scandinavian, Polar/Eurasia, Asian Summer, West Pacific, East Pacific, North Pacific, Pacific/North America, Tropical/Northern Hemisphere, and the Pacific Transition) was evaluated for its ability to explain variability in the natural logarithm of the number of hectares burned annually in Alaska. The monthly indices for the East Pacific (EP) teleconnection collectively explained the greatest amount of variability. Since the EP has a strong center near Alaska and a comparable but oppositely signed locus between Hawaii and the Baja peninsula (Figure 1.2, after Barnston and Livezy 1987), this finding is physically plausible. Strong positive phases of the EP pattern are associated with upper airflow that is more meridional over the northeastern Pacific. This results in enhanced ridging over Alaska and the western

coast of North America. Alternatively, negative phases of the EP pattern are associated with increased zonal flow and strengthened westerlies in the Eastern North Pacific as a consequence of negative height anomalies to the north and positive anomalies to the south of 40-45°N. The negative phase is also associated with an eastward displacement of the Aleutian Low (AL), in the North Pacific.

1.3.4 Pacific Decadal Oscillation

Significant covariability exists between Sea Surface Temperatures (SSTs) and North American climate (Bonsal et al. 1993, Livezy and Smith 1999). Specifically, there is correlation between SSTs in the North Pacific and weather in Alaska (Papineau 2001). The Pacific Decadal Oscillation reflects differences in the circulation and location of anomalous warm/cool SSTs across the Pacific Ocean (Figure 1.3). To quantify the impact of North Pacific SSTs on area burned in Alaska, indices for the Pacific Decadal Oscillation (PDO: http://jisao.washington.edu/pdo/PDO.latest) were examined as explanatory variables in the MLR. Multiple temporal scales (i.e., one, two, three and four-month averages) of the PDO index were evaluated as explanatory variables in the MLR model. Some degree of statistical similarity exists between the signal for the PDO and El Niño events. Because of this El Niño indices (both pressure-based and SST) were evaluated for their potential as explanatory variables in the statistical model. The metric used to quantify the PDO was more statistically significant.

Depending on the phase of the PDO, certain atmospheric circulation patterns in the North Pacific are favored. During cool phases of the PDO, ridging is more frequent whereas in the warm phase, the development of troughs is more likely (Bond and Harrison, 2000). The cool phase is characterized by cool SSTs in the Gulf of Alaska (GOA) and warm temperatures in the North Pacific. Alternatively, warm SSTs in the GOA and cool temperatures in the North Pacific characterize the warm phase of the PDO (Figure 3). The strength and location of the AL is also correlated with the phase of the PDO. During cool phases of the PDO, the AL is, on average, located around the western

extent of the Aleutian Islands. When the PDO shifts from a cool phase to a warm phase, the AL strengthens and moves to the east (Trenberth 1990, Niebauer 1998).

1.3.5 Statistical Model and Spatiotemporal Scaling

The allowable number of explanatory variables in the MLR was fixed at roughly fifteen percent of the total number of data points. Standard subset selection techniques were used to evaluate significance of monthly temperature/precipitation and teleconnection indices within the MLR model. By fixing the number of parameters, we are essentially evaluating a subset of all possible models. In the context of information criteria (e.g., AIC) we have fixed the penalty function and are maximizing the likelihood within this subset of models. There are numerous methods with differing criteria that can be used to fit models. The success of any model selection exercise can be best evaluated by cross-validation. The results of sequential cross-validation along with other model diagnostics (e.g., residual analyses) show that the regression model is relatively robust and does not violate any of the regression assumptions.

The natural logarithm transformation is applied to the annual area burned data to both minimize heteroskedasticity and decrease the potential for bias in variable selection based on the relatively small number of years where the majority of area burned. This transformation results in more reliable tests of parameter significance since the variability of the response is no longer a nonconstant function of the expected value estimated by the regression. All references to statistical significance are made at the 0.10 type I error level.

The spatial and temporal scales of the MLR need to be considered when interpreting the results. The statistical model is essentially a point model in that it integrates values of climatic explanatory variables across both space (i.e., interior Alaska) and time. The model integrates across space through the calculation of a simple average of monthly climate indices for weather stations that in this sense represent interior Alaska

(Figure 1.1). This method represents a first-order integration of spatial information regarding intra-state variability into a single point estimate. The model integrates across time through the use of monthly averages for the temporal scale of explanatory variables and the use of annual values for response variables. The use of monthly indices lacks explicit consideration of intra-monthly variability. Extreme fire behavior can and often does occur at a less than monthly temporal scale (Alvarado et al. 1998, Flannigan and Harrington 1988). Nonetheless, important linkages between pressure anomalies and fire behavior on monthly/seasonal timescales have been identified in Canada (Johnson and Wowchuk 1993, Skinner et al.1999).

The goal of the statistical model is to identify variables that collectively explain the greatest amount of variability in the natural logarithm of the number of hectares burned for a given year. The structure and spatio-temporal scaling of the model were selected to be both pragmatic and parsimonious. Pragmatically, it is of interest to quantify the link between weather variables and the area burned for fire management activities and a greater understanding of fire-weather interactions. Another pragmatic aspect is that the antecedent nature of the various climatic variables gives the results application in long-range (monthly-to-seasonal) prediction of annual area burned in Alaska. As a starting point, integrating both the response and explanatory variables across space provides a clear definition of the spatial scale of interest and a simple interpretation of the model results. Across the numerous temporal scales evaluated, the current state of the model maximizes the predictive relationship between fire and climate.

1.4   Results

Seven climatic variables and an interaction term collectively explain 79% of the variability in the natural logarithm of number of hectares burned annually. The explanatory variables in order of most to least significant (Table 1.1) are Average June Temperature (AJT), Delta EP Teleconnection (DEP), Average April Temperature, (AAT), the interaction between DEP and AAT, Average May Temperature (AMT),

Average PDO index for January and February (PDOWIN), Average July Temperature (AJLT), and Average June Precipitation (AJP). DEP is defined as the January EP index minus the April EP index. The low p-value for the F-test (Table 1.1) indicates that the deterministic component of the statistical model explains a significant percentage of the variability in the natural logarithm of the number of hectares burned per year. Comparison between observed values of the number of hectares burned annually (Figure 1.4, circles) and transformed model estimates (Figure 1.4, diamonds with connecting lines) shows that the transformed estimates from the statistical model provide a reasonable estimate of the number of hectares burned annually. The estimated values (Figure 1.4, diamonds with connecting lines) are an exponentiation of the fitted values produced by the MLR. Since the regression was performed on the natural logarithm of the number of hectares burned annually, a "back-transformation" was used to obtain estimates in the original space. There are numerous ways to "back-transform" data and this one, although the simplest, does produce a negatively biased estimate under the assumption of lognormality. Hence, predictions made using this simple back-transformation will produce slight underestimates under the assumption that the area burned data are lognormally distributed.

1.4.1 Explanatory Variables

1.4.1.1 Teleconnection Indices

The time series of the EP index (Figure 1.5) and the estimated partial autocorrelation function shows that the EP teleconnection is an autoregressive process with maximal temporal correlations occurring at one and three-month lags. DEP is defined as the January EP index minus the April EP index, and provides a metric of shifts in atmospheric circulation from winter to spring. Through its influence on atmospheric circulation, a shift from the negative phase of the EP index in winter to a positive phase in spring increases the likelihood of blocking ridges forming in the following summer. Hence negative values of DEP indicate a tendency toward drier-than-normal conditions

for the months of March through August (Figure 1.6). Along with drier than normal conditions, negative values of DEP are also associated with increased temperatures for the months of May and June (Figure 1.7). The cumulative impact of the warmer and drier spring/summer conditions associated with negative values of DEP is a greater area burned (Table 1.2). The negative value of the parameter estimate for DEP (Table 1.1) implies that a shift from negative to positive EP values between January and April favors a greater area burned in the upcoming summer.

Monthly PDO indices were evaluated for use as explanatory variables in the MLR and winter indices displayed the largest signal with respect to explaining variability in the natural logarithm of the number of hectares burned annually in Alaska. The months of January and February were the most significant explanatory variables among the monthly PDO indices and since the estimates were of the same sign, the average of these monthly indices (PDOWIN) was used as a single explanatory variable in the regression. The negative value for the parameter estimate of PDOWIN indicates that cool phases of the PDO are associated with a greater area burned. There is positive correlation between PDOWIN and the average precipitation for May and June (Figure 1.8). Hence cool phases of the PDO are associated with drier summer conditions. Additionally, the phase of the PDO is also associated with a shift in the correlation between winter and summer precipitation. During the cool phase of the PDO, there is significant negative correlation between precipitation in summer and precipitation in winter, but no correlation exists during the warm phase (Figure 1.9).

1.4.1.2 Temperatures

The MLR analysis found the average temperatures for the months of April, May, June and July (AAT, AMT, AJT and AJLT respectively) to be significant explanatory variables for the logarithm of the number of hectares burned (Table 1.1). Among the parameter estimates for these monthly temperatures only AAT has a negative value. AJT was the most significant explanatory variable identified by the MLR and by itself it

explains over 34% of the variability in the response. Attempts to combine the average temperatures from months (across two, three and four month periods) yielded explanatory variables with comparatively lower explanatory capability. Hence, monthly temperatures exert differential impacts on the annual area burned.

The parameter estimate for AAT is negative indicating that lower April temperatures are associated with greater area burned (Table 1.1) but the interpretation is made difficult by non-linear interactions with DEP. When zonal flow is dominant in the spring (DEP >0) April temperatures are positively correlated with area burned whereas when meridional flow is building, April temperatures are negatively correlated with area burned. The reason for this shift is not fully understood but is likely due to interactions with the precipitation signal associated with the EP. When zonal flow is dominant, precipitation is more likely and higher April temperatures can signal the beginning of break-up and result in an earlier fire season. When meridional flow is dominant, precipitation is less likely and elevated April temperatures may result in snowmelt before the organic horizon is thawed enough to accept the meltwater as recharge. The impact of spring snowmelt on fire dynamics is a subject that requires further study.

Temperatures for the months of May, June and July are positively correlated with area burned. May is the month when deciduous trees typically break dormancy in the interior. In the period between snowmelt and leafout, deciduous stands can have greater flammability than conifers. This is partially because deciduous stands are more prevalent on south facing slopes, which respond rapidly when warm, dry spring conditions exist. Elevated temperatures in May decrease available moisture for ground cover and increase progressive drying of deeper organic layers. Elevated May temperatures can be sufficient to develop convective thunderstorm activity, although the majority of lightning strikes in the interior typically occur during June and July (Reap 1991). Average June and July temperatures probably exert their influence through drying of the organic layer and development of convective activity.

1.4.1.3 Precipitation

As the sole precipitation variable in the regression model, average June precipitation (AJP) was the least significant among the other variables (Table 1.1). Depending on the thaw depth of the organic layer, June precipitation data can yield information regarding moisture status of organic layers. Temperature is also an integral component of moisture status and in general, area-averaged anomalies of monthly temperature and precipitation are negatively correlated in high latitudes during summer. A common factor in anomalies of both variables is cloudiness, which is associated with lower temperatures and greater precipitation during summer. This correlation is primarily driven by the prevalence of frontal low-pressure systems that typically have large areas of cloud cover and relatively spatially homogenous precipitation. Alternatively, convective storms associated with surface heating can result in highly localized cloud cover and precipitation, which reduces the effectiveness of monthly precipitation as an explanatory variable.

Intra-monthly variability of precipitation is also an important factor with respect to moisture status of the organic layer (Flannigan and Harrington 1988). A month receiving average precipitation that occurs on only several days can have a greater potential for fire than a month in which the same total rainfall is distributed evenly throughout the month. In general, months with more precipitation will also have greater intra-monthly variability. This hinders attempts to determine the relative importance of total monthly precipitation versus timing. The lack of information regarding intra-monthly variability in precipitation is partly obviated by the use of the EP monthly indices, which implicitly contain information about circulation and the potential for blocking highs associated with reduced precipitation (Johnson and Wowchuk 1993, Skinner et al. 1999).

1.5 Discussion

This analysis provides a framework for understanding the influence of ocean-atmosphere interaction on the fire regime of interior Alaska. Our study is the first to build a statistical model quantifying the link among teleconnections, weather, and area burned in interior Alaska. Intuitively, one assumes that, in the short-term, less precipitation and higher temperatures increase fire danger. This work extends such reasoning to the antecedent ocean-atmosphere interactions that influence short-term weather, and it quantifies the influences of these factors on the annual area burned. Teleconnections modify atmospheric circulation and the statistically significant relationships between teleconnection indices and monthly weather provide plausible physical mechanisms for the teleconnections to influence area burned. The relationships between teleconnections, weather, and conditions that are favorable for large area burned are considered below.

1.5.1 Teleconnection Influences on Weather

Positive phases of the EP teleconnection correspond with upper airflow that is meridional whereas negative phases are associated with zonal circulation and strengthened westerlies in the eastern North Pacific. The meridional flow is conducive to the formation of blocking highs that impact short-term weather and fire behavior in interior Alaska. Blocking highs typically persist for several days to several weeks and influence the fire potential across regions of 100-1000 km (Johnson and Wowchuk 1993). In summer, surface blocking high-pressure systems bring warm temperatures and low precipitation that can cause deep drying of the organic layer. Hence, mid-tropospheric anomalies and the surface high-pressure systems that accompany them increase fire danger at a landscape scale. Shifts from positive to negative EP indices in the spring (DEP < 0) are associated with greater precipitation and cooler temperatures across interior Alaska.

With respect to the EP teleconnection, the antecedent atmospheric circulation pattern most strongly correlated with a large area burned is a negative EP index in the winter that shifts to a positive EP index in the spring. To quantify this, DEP is defined as the January EP index minus the April EP index. DEP measures the change in atmospheric circulation from winter to spring. The negative value of the parameter estimate for DEP (Table 1.1) shows that a shift from a negative EP index in January to a positive EP index in April is correlated with greater area burned in the following summer. This shift represents a departure from the positive seasonal correlation that is characteristic of the autoregressive EP teleconnection (Figure 1.5). As a consequence of the impact on atmospheric circulation, negative values of DEP are associated with drier-than-normal conditions for the months of March through August (Figure 1.6) and increased temperatures for the months of May and June (Figure 1.7). Shifts in the EP index from negative phases in winter to positive phases in spring modify atmospheric circulation and increase the likelihood of blocking ridges forming in the following summer. In general, warmer and drier early summer conditions favor a progressive drying of deeper organic layers. As the length of a dry spell increases, there is greater potential for widespread, intense combustion due to increased homogeneity of favorable fuel conditions. In the boreal forest of Alaska, the majority of fires are dependent on combustion of the organic layer; however, during extreme fire events fires can burn in the canopy without consuming much soil organic matter. Hence DEP likely influences the number of hectares burned in interior Alaska through its effects on moisture conditions in the organic layer. The cumulative impact of the warmer and drier summer conditions associated with negative values of DEP is a greater area burned (Table 1.2).

Like the EP teleconnection, the PDO also influences the number of hectares burned in interior Alaska through modification of weather. Of the PDO indices evaluated, the index comprised of the average for the winter months of January and February (PDOWIN) explains the greatest amount of variability in the MLR. Like the EP teleconnection, the PDO dictates certain aspects of atmospheric circulation.

Specifically, ridging in the North Pacific is more frequent during cool phases of the PDO, whereas in the warm phase the development of troughs in this region is more likely (Bond and Harrison, 2000). The PDOWIN index is positively correlated to late-spring precipitation (Figure 1.8) in Alaska.

The phase of the PDO also influences correlation between winter and summer precipitation amounts for interior Alaska (Figure 1.9). With respect to precipitation in interior Alaska, these two times of year are critical. In the winter, there is a monotonic decrease in the average monthly precipitation from October to May, and the majority of winter precipitation comes in the months of October and November. Although the average temperature for October is below freezing, precipitation events during this month can contribute to moisture content at the soil surface. Impacts of the interaction between winter and summer precipitation on the area burned require further evaluation but are possibly driven by soil moisture dynamics in the organic horizons. Specifically, differences in snow pack can potentially influence soil moisture in the following spring. For soils with organic horizons, the ability of snowmelt water to percolate into the active layer depends on quantity of ice in soil pores (Kane 1980). Moisture content at the soil surface has been observed to increase throughout the winter with this effect being most pronounced for wet soils. Hence, higher soil moisture contents correspond to greater amounts of ice present in the frozen soil, which in turn reduces the infiltration rate and the saturated hydraulic conductivity (Kane 1980). Similar results have been found for mineral soils in boreal forests (Zhao and Gray 1999). Additionally, after winters with little snowfall, it is possible for organic layers at high latitudes to remain frozen into July (Nyberg et al. 2001). Hence the importance of summer precipitation can depend on the development and persistence of winter snowpack. Wetter soils during freeze-up in the fall coupled with above-average precipitation during the winter can potentially result in drier soil organic layers in the following spring. Soil moisture of organic layers plays a critical role in the smoldering combustion of deeper organic horizons (Miyanishi and Johnson, 2002). Fires that smolder in deeper organic horizons are more likely to persist

through rainfall events that may occur. Although the correlation between winter and summer precipitation is significantly different between warm and cool phases of the PDO, none of the fall or winter monthly precipitation variables were significant in the regression. Hence if the relationship between the PDO and the correlation between winter and summer precipitation influences area burned in the subsequent year, the mechanism is likely complex and has yet to be definitively characterized.

The majority of summer precipitation in Alaska comes in the months of July and August, and during this time area-averaged anomalies of monthly temperature and precipitation are negatively correlated. As a consequence, elevated temperatures typically accompany low precipitation and both are conducive to increased area burned. During cool phases of the PDO, there is a strong negative correlation between cumulative precipitation amounts for October-November and July-August (Figure 1.9). Hence in cool phases, dry winters are likely to be followed by wet summers and dry summers are likely preceded by relatively wet winters. Simply put, it is less likely to have both a wet winter and a wet summer during cool phases of the PDO than it is during warm phases of the PDO. Following the reasoning in the previous paragraph, the relationship between winter and summer precipitation during the cool phase of the PDO can potentially more favorable conditions for greater area burned since wet winters are likely to be followed by dry summers (Figure 1.9). Alternatively, during the warm phase of the PDO, there is negligible correlation between winter and summer precipitation (Figure 1.9), and it is less likely that a warm summer will follow a wet winter. Shifts in sea-ice dynamics off the West coast of Alaska have been linked to changes in the phase of the PDO (Niebauer 1998) and it is possible that the shift in intra-annual correlation between precipitation signals is related to the impact of the PDO on sea-ice extent.

1.5.2 The Pacific Decadal Oscillation and the Aleutian Low

The phase of the PDO is positively correlated with spring precipitation (Figure 1.8) in Alaska. One mechanism that can explain these short term-weather anomalies is

impacts of the PDO on the location and intensity of the Aleutian Low (Niebauer 1998, Papineau 2001). In the period used for this study, there were only 5 (1957-1958, 1969-1970, 1976-1977, 1990-1991, 1999-2000) times where substantial (greater than a 1.6 unit shift in the PDOWIN metric for sequential years) shifts from cool to warm phase of the PDO occurred. One of the consequences of this type of shift was that the Aleutian Low intensified and moved southeast of its former position. This shift causes a more easterly (less southerly) flow component across interior Alaska and is associated with regional summer droughts. The years of 1957, 1969, 1977, 1990 and 1999 had the 1st, 4th, 5th, 2nd, and 12th, largest fire years (respectively) of the period from 1950-2003. One of the most extreme cases of this was in the summer of 1977 when the Kotzebue weather station recorded 0.03 inches of total precipitation for the months of June and July (http://www.wrcc.dri.edu/cgi-bin/cliMAIN.pl?akkotz). Not surprisingly, many fires that burned that summer were located in the NW part of the state near Kotzebue.

1.5.3   Model Development

A key component of any model development lies in testing of the final model. This is especially important when developing a statistical model through the sequential elimination of explanatory variables based on significance tests. The potential always exists for the chance selection of statistically significant variables that are of little practical importance. By the definition of statistical significance, the probability of this happening increases as more potential explanatory variables are evaluated. A first step in exploring the potential for the selection of explanatory variables that are not practically significant is to consider plausible mechanisms for the selected variables to influence the response. All of the variables included in the regression model (Table 1.1) have plausible physical mechanisms for influencing annual area burned (Figures 1.6-1.9, Table 1.2) and the identification of these variables will help guide future exploration of the link between climate and fire in different boreal systems.

Another potential issue is that of correlation among explanatory variables, or collinearity. When dealing with monthly temperature data, correlation between months should be expected since months are somewhat arbitrary designations for discretizing the year. For example, a high pressure ridge bringing warm and dry weather at the end of May will likely have a similar influence on the weather in the beginning of June. The collinearity that exists among explanatory variables can influence model output in several ways including the selection of variables with little practical significance. A quantitative way to assess the impact of both collinearity and the potential for selection of variables with little practical significance is through cross-validation. If explanatory variables of little practical significance have been selected due to collinearity or chance, cross-validation routines often reveal this. Based on our cross-validation results, the impact of collinearity on model predictions seems negligible and there do not appear to be any variables selected that are not significant both practically and statistically.

1.5.4 Forecasting with the Model

The results of this paper can be used for long-range (monthly-to-seasonal) forecasts of the magnitude (area burned) of the upcoming fire season. As an example, consider two forecasts for the upcoming 2004 fire season, one at the end of April and one at the end of May. Estimates of the other necessary monthly variables are obtained by interpreting the Climate Prediction Center prognostic discussion for long-lead seasonal outlooks (http://www.cpc.ncep.noaa.gov/products/predictions/90day/fxus05.html). Based on the prognostic discussions, the 60th percentile of the May, June and July Temperatures will be used for the first forecast (made at the end of April) and the 70th percentile will be used for the June and July temperature for the second forecast (made at the end of May). The median June precipitation will be used for first forecast and the 40th percentile will be used for the second. Based on this information, the first forecast (end of April) is for 41,000 hectares and the second forecast (end of May) is for 135,000 hectares. Both of these are well below average (270,000 hectares). In fact, as of the end of July 2004, the total area burned has already reached roughly 1,780,000 hectares (2nd

overall since 1950). In Fairbanks, June 2004 was the second hottest in the past 100 years. In addition to the hot weather, lightning activity has been record breaking as well. On the 14th of June, 8,589 lightning strikes were recorded throughout the state and one month later on July 15th, over 9,000 strikes were recorded (courtesy of the National Weather Service http://pafg.arh.noaa.gov/). These represent two of the largest single-day outbreaks on record for the state. With the values for June inserted in the statistical model (and using the 70th percentile for July Temperature), the estimate of hectares burned is 2,100,000 hectares. This exercise demonstrates the importance of June temperature in the statistical model. Attempts to use this model for planning should incorporate multiple plausible scenarios for June temperatures in order to appropriately plan for the upcoming season.

1.6   Conclusion

Climate, fire and vegetation in the boreal forest of interior Alaska interact on multiple spatial and temporal scales. It is clear from this work that teleconnections operating on multiple timescales influence the annual area burned across interior Alaska. The results presented in this paper provide evidence linking the East Pacific teleconnection and the Pacific Decadal Oscillation to several weather variables that are directly related to the annual area burned in interior Alaska. The most likely, ultimate mechanisms for these linkages are shifts in atmospheric circulation. Strong positive phases of the EP pattern are conducive to the development of blocking highs that impact short-term weather and fire behavior. Negative phases of the EP pattern are associated with strengthened westerlies in the Eastern North Pacific as a consequence of a more zonal upper airflow over the region south of Alaska. The shift in sign of the EP teleconnection over a period of several months in winter exerts a significant signal on both temperature and precipitation during the spring and summer in interior Alaska.

The Pacific Decadal Oscillation exerts a direct influence on winter temperatures and summer precipitation and also modifies the correlation between winter and summer

precipitation. During cool phases of the PDO, there is strong negative correlation between winter and summer precipitation. One possible explanation for the importance of above average winter precipitation is that decreased percolation due to ice in the soil pores can potentially leave the organic layers more susceptible to warm, dry temperatures in May and June. This scenario is more likely during cool phases of the PDO and consequently 69% of the area burned for the period of this study occurred when the PDOWIN metric was less than zero (i.e., cool phases of the PDO). The interactions among moisture content of the soil organic layers, winter precipitation and fire extent in the following year remains unclear and merits further study.

This work represents a first step in quantifying the links among weather and fire in Alaska. The multiple linear regression model used to characterize this link is a simple tool for taking this first step. The model lacks a spatially explicit component as monthly temperatures and precipitation represent averages from a relatively small number of sites located throughout the Alaskan interior. The use of broader circulation indices reduces the reliance on, and possible concerns about, the representativeness of local (single-point) surface-based measurements made in a heterogeneous landscape. The interactions between weather and fire characterized in this work were developed conditional on the current spatial distribution of vegetation across interior Alaska. Debate exists as to the importance of age-dependant flammability in the boreal forest (Johnson 1992, Johnson et al. 1998, Hely et al. 2000a, Hely et al. 2000b, Johnson et al. 2001, Ward et al. 2001). If stand flammability does indeed change as a function of age, the spatial distribution of such vegetation would modify the relationship between climate and fire. Cross-validation of the model suggests that collinearity and spurious variable selection are not serious issues and model predictions can provide input to fire management officials charged with developing resource allocation plans for upcoming fire seasons. Due to the strong dependence of area burned on weather, forecasts of area burned produced by the model are only as reliable as the forecasts for temperature and precipitation used in the model. Specifically, June temperature plays a critical role in the magnitude of area

burned. Future attempts to forecast area burned in Alaska should focus on identifying those atmospheric mechanisms that most strongly influence June temperature. A next step is to apply similar MLR procedures for tundra versus forest vegetation to identify the climatological characteristics that drive the burning of different vegetation types.

1.7 Figures
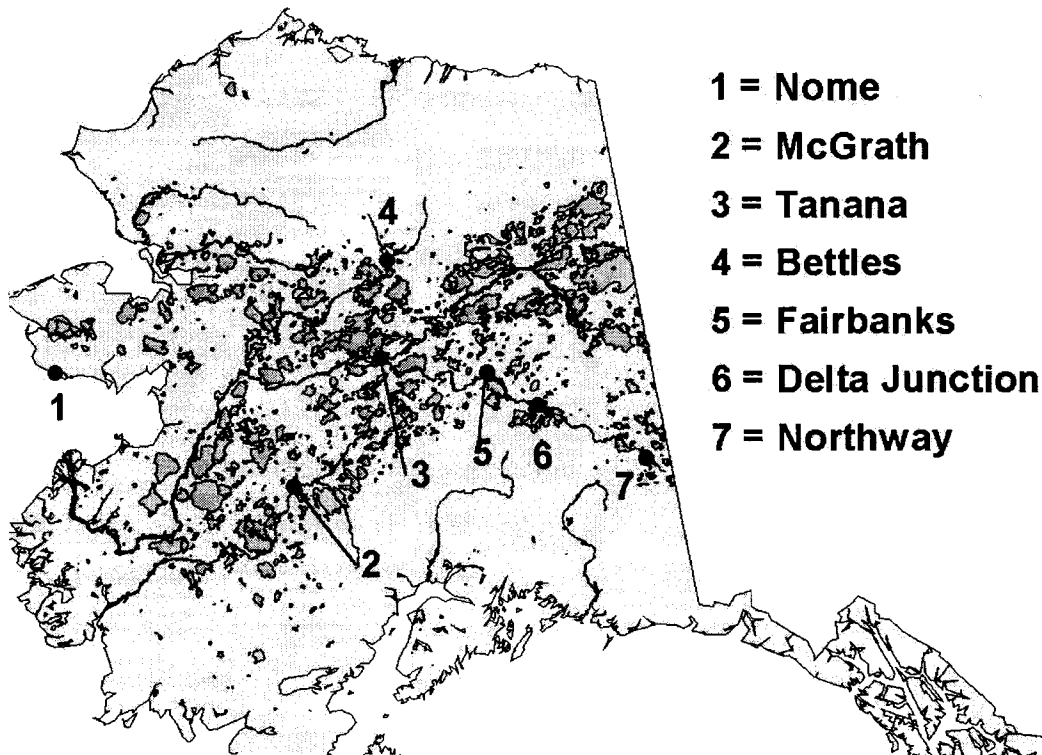
Figure 1.1 Map of Alaska identifying the seven climate stations used in the statistical analyses. The polygons represent individual fire perimeters from 1950-2003.
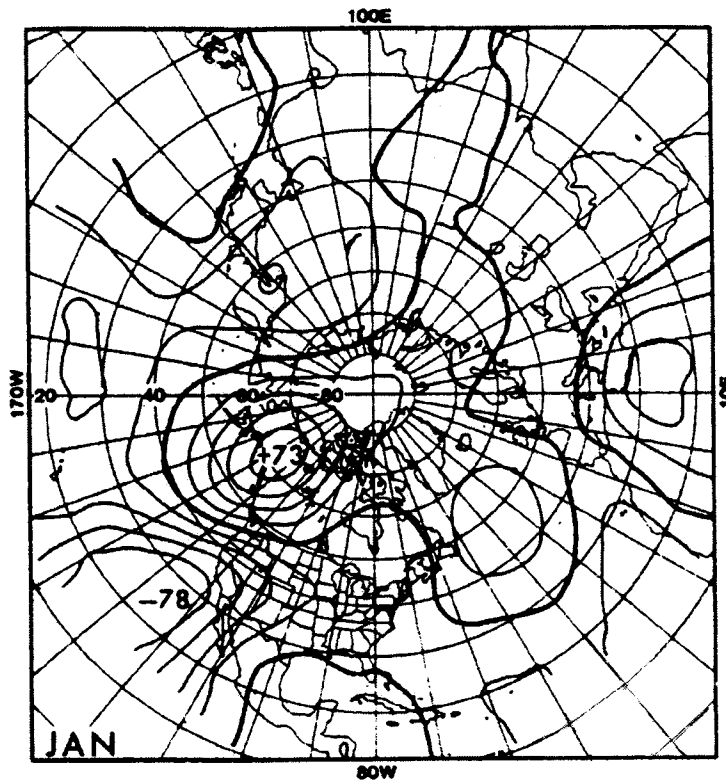
Figure 1.2   East Pacific Pattern in January, taken from Barnston and Livezy (1987). Values are correlations between 70kPa (700 millibar) heights at grid points and the rotated principal component time series of the East Pacific teleconnection. The 70 kPa heights approximate the actual height of a pressure surface above mean sea level. These heights correspond to the middle troposphere at roughly 3000 meters. Height anomalies at the 70 kPa level influence the movement of surface weather systems.
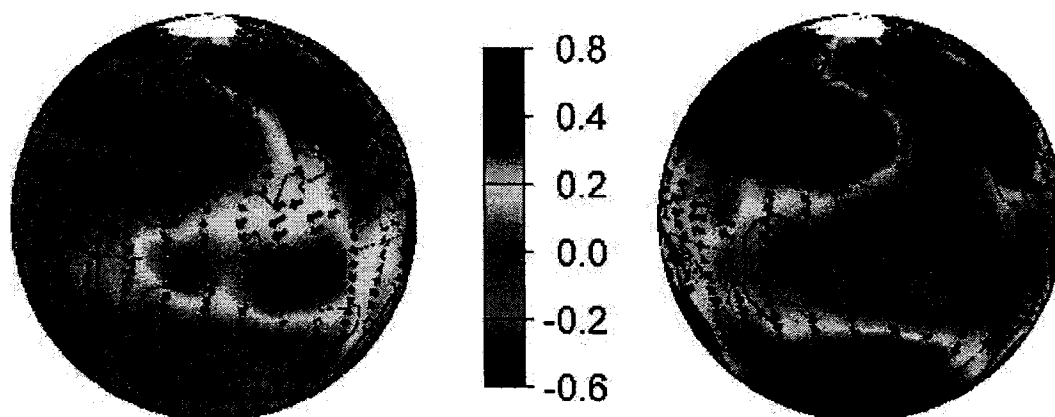
Figure 1.3   Typical wintertime Sea Surface Temperature (colors), Sea Level Pressure (contours) and surface windstress (arrows) anomaly patterns during both warm (left) and cool (right) phases of the Pacific Decadal Oscillation. Obtained with permission from the University of Washington's Joint Institute for the Study of the Atmosphere and Oceans: http://tao.atmos.washington.edu/PDO/. This image was created by Dr. Steven Hare, International Pacific Halibut Commission.
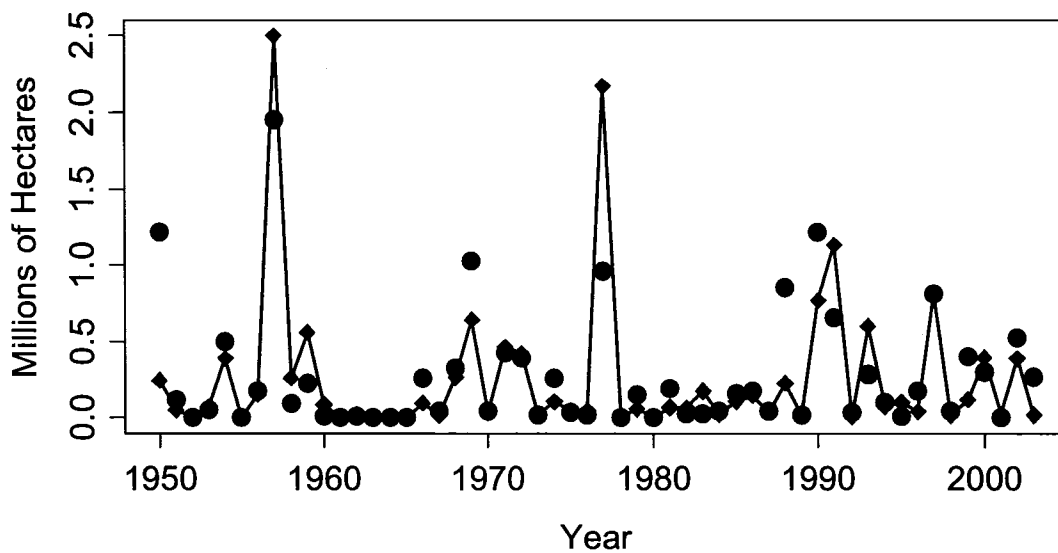
Figure 1.4   Time series plot showing the number of hectares burned annually (circles) and transformed estimates (diamonds with connecting lines) based on the predicted values from the multiple linear regression (MLR) model. The estimated values (diamonds) in this plot are an exponentiation of the fitted values produced by the MLR. Since the regression was performed on the natural logarithm of the number of hectares burned annually, a "back-transformation" was used to obtain estimates in the original space.
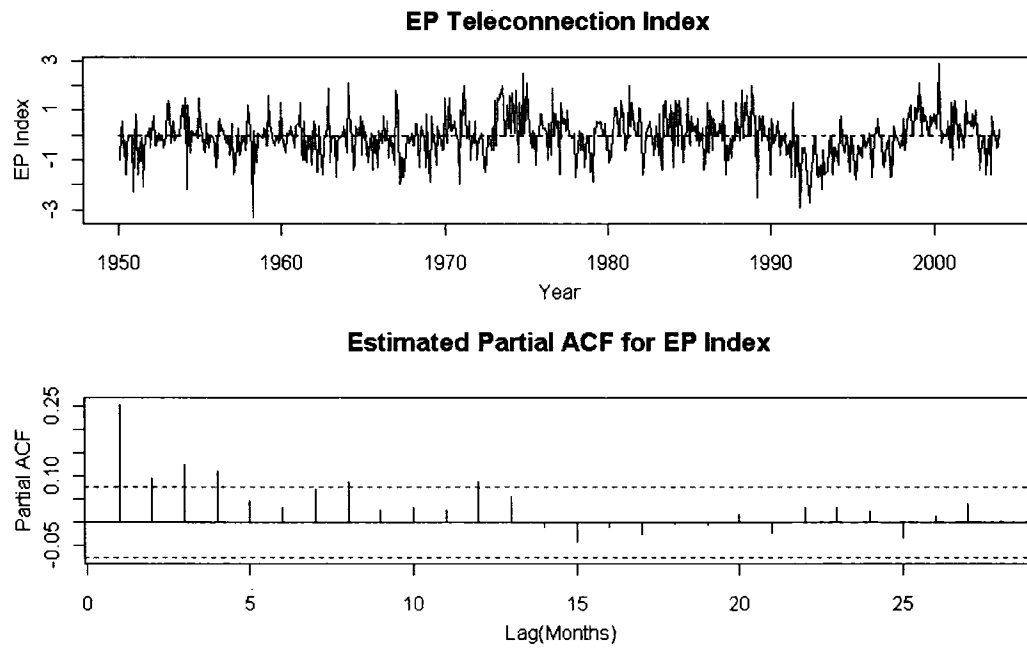
Figure 1.5   Time series of East Pacific index and estimated partial autocorrelation function (PACF). Dashed lines in PACF plot represent 95% confidence intervals for the estimated correlation at a given lag.
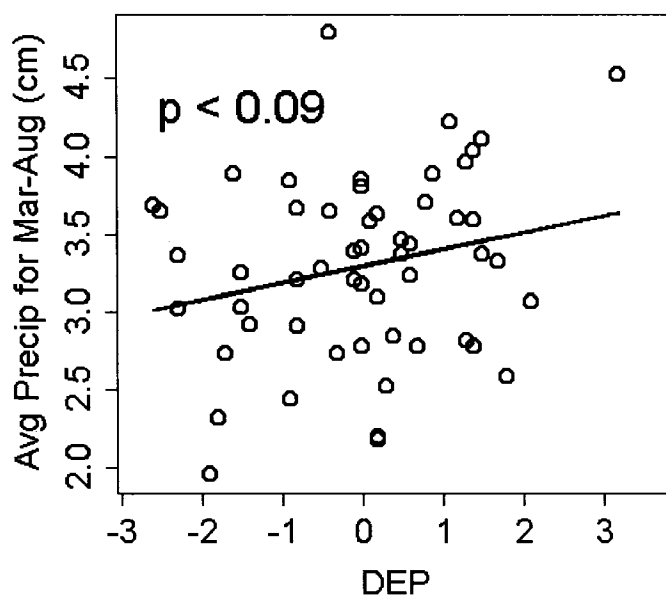
Figure 1.6   Scatterplot of average precipitation for the months of March through August versus DEP (January East Pacific teleconnection index minus April East Pacific teleconnection index). Shifts from negative values of the EP in January to positive values of the EP in April (negative DEP) are associated with decreased precipitation from March through August. Least squares regression line and p-value (corresponding to test of slope equal to zero) are presented.
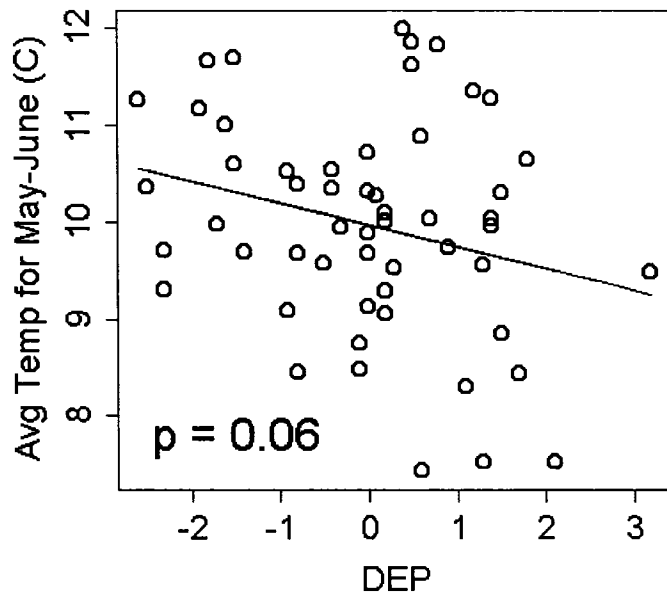
Figure 1.7 Scatterplot of average spring (May and June) temperatures versus DEP (January East Pacific teleconnection index minus April East Pacific teleconnection index). Shifts from negative values of the EP in January to positive values of the EP in April (negative DEP) are associated with increased temperatures in May and June. Least squares regression line and p-value (corresponding to test of slope equal to zero) are presented.
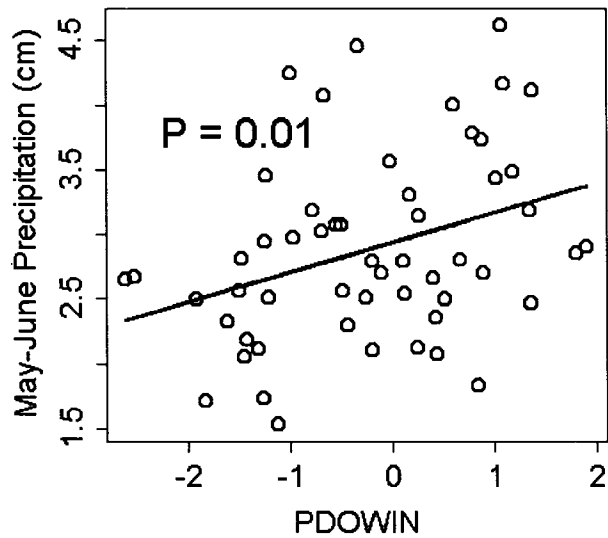
Figure 1.8 Scatterplot of average precipitation for May and June versus the average of the PDO index for the months of January and February. Cool phases of the PDO (negative *PDOWIN*) are associated with decreased precipitation for the months of May and June. Least squares regression line and p-value (corresponding to test of slope equal to zero) are presented.
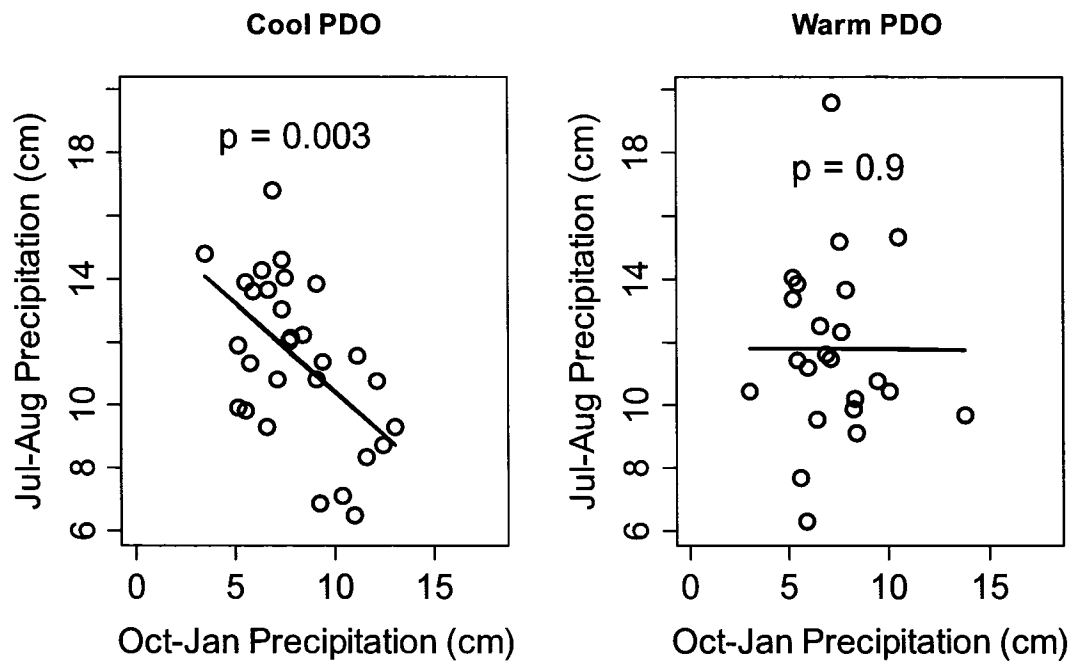
Figure 1.9   Scatterplots of July-August precipitation versus previous September-January precipitation. Plots are partitioned based on the sign of the average PDO values for the months of January and February (*PDOWIN*). The negative correlation between winter and summer precipitation exists only during cool phases of the PDO. Hence during cool phases of the PDO, it is less likely that a dry winter will be followed by a dry summer. Least squares regression line and p-value (corresponding to test of slope equal to zero) are presented.

1.8 Tables

Table 1.1 Statistical output for the multiple linear regression (MLR) model with response variable of natural logarithm of the number of hectares burned annually. The R-squared value of 0.79 implies that the deterministic component of the MLR (consisting of the explanatory variables listed below) model explains 79% of the total variability in the response variable.

Explanatory Variables	Estimate	Std. Error	t value	Pr(T>|t|)
Intercept	-41.368	7.352	-5.626	1.12E-06
Average June Temperature	0.617	0.098	6.302	1.11E-07
Delta EP	-4.803	0.914	-5.254	3.93E-06
Average April Temperature	-0.199	0.041	-4.855	1.49E-05
Delta EP* Average April Temperature	0.159	0.034	4.712	2.38E-05
Average May Temperature	0.235	0.056	4.201	1.24E-04
Average PDO of January and February	-0.465	0.151	-3.071	3.61E-03
Average July Temperature	0.252	0.089	2.836	6.81E-03
Average June Precipitation	-1.195	0.458	-2.606	1.24E-02
Residual standard error: 1.098 on 45 degrees of freedom				
R-Squared: 0.790				
F-statistic: 21.14 on 8 and 45 DF, p-value: 7.112 e-13				

Table 1.2 DEP data have been partitioned into "big" and "small" fire years with respect to 100,000 hectares. Years with area burned greater than 100,000 ha are classified as "big" fire years and years with area burned less than 100,000 ha are classified as "small" fire years. Positive values for DEP signify increased zonal flow from spring to summer whereas; negative values of DEP indicate more meridional flow and increased potential for ridges to develop (Figures 1.6 and 1.7). DEP values for big fire years are significantly different (and less than) than DEP values for small fire years (p-value < 0.0002 for Welsh's modification (unequal variances) to a two-sided, two-sample t-test).

	Minimum	Median	Mean	Maximum
"Small" Fire Years	-1.50	0.60	0.64	3.20
"Big Fire" Years	-2.60	-0.65	-0.60	1.50

Table 1.3   List of acronyms

AAT	Average April Temperature
AGDC	Alaska Geospatial Data Clearinghouse
AFS	Alaska Fire Service
AMT	Average May Temperature
AJLT	Average July Temperature
AJT	Average June Temperature
AJP	Average June Precipitation
AL	Aleutian Low
CPC	Climate Prediction Center
CRU	Climate Research Unit
DEP	Delta EP = January East Pacific Teleconnection index minus the April East Pacific Teleconnection index. This index measures changes in atmospheric circulation from winter to spring
EP	East Pacific: This is a teleconnection index used to quantify atmospheric circulation
GOA	Gulf Of Alaska
IPCC	Intergovernmental Panel on Climate Change
LFDB	Large Fire Data Base
MLR	Multiple Linear Regression
NOAA	National Oceanic and Atmospheric Administration

PDO	Pacific Decadal Oscillation
PDOWIN	Average PDO value for the months of January and February
WRCC	Western Region Climate Center

1.9   Acknowledgements

1.10 Literature Cited

Alvarado, E., D. V. Sandberg, and S. G. Pickford. 1998. Modeling large forest fires as extreme events. Northwest Science 72 (Special Issue): 66-74.

Barnston, A. G., and R. E. Livezey. 1987. Classification, seasonality and persistence of low-frequency atmospheric circulation patterns. Monthly Weather Review 115: 1083-1126.

Bond, N. A., and D. E. Harrison. 2000. The Pacific decadal oscillation, air-sea interaction and central North Pacific winter atmospheric regimes. Geophysical Research Letters 27: 731-734.

Bonsal, B. R., A. K. Chakravarti, and R. G. Lawford. 1993. Teleconnections between North Pacific SST anomalies and growing season extended period dry spells on the Canadian prairies. International Journal of Climatology 13: 865-878.

Bonsal, B. R., and R. G. Lawford. 1999. Teleconnections between El Niño and La Niña Events and Summer Extended Dry Spells on the Canadian Prairies. International Journal of Climatology 19(13): 1445-1458.

Carcaillet, C., and P. J. H. Richard. 2000. Holocene changes in seasonal precipitation highlighted by fire incidence in eastern Canada. Climate Dynamics 16: 549-559.

Carcaillet, C., Y. Bergeron, P. J. H. Richard, B. Frechette, S. Gauthier, and Y. T. Prairie. 2001. Changes of fire frequency in the Eastern Canadian boreal forest during the Holocene: Does vegetation composition or climate trigger the fire regime. Journal of Ecology 89: 930-946.

Chapin III, F. S., T. S. Rupp, A. M. Starfield, L. DeWilde, E. S. Zavaleta, N. Fresco, J. Henkelman, and A. D. McGuire. 2003. Planning for resilience: modeling change in human-fire interactions in the Alaskan boreal forest. Frontiers in Ecology and the Environment 1(5): 255-261.

DeVolder, A. 1999. Fire and climate history of lowland black spruce forests, Kenai National Wildlife Refuge, Alaska, Dissertation. Northern Arizona University, Flagstaff, Arizona, USA.

Flannigan, M. D., and J. B. Harrington. 1988. A study of the relation of meteorological variables to monthly provincial area burned by wildfire in Canada 1953-80. Journal of Applied Meteorology: 441-452.

Flannigan, M. D., B. J. Stocks, and B. M. Wotton. 2000. Climate change and forest fires. The Science of the Total Environment 262: 221-229.

Flannigan, M. D., I. Campbell, B. M. Wotton, C. Carcaillet, P. Richard, and Y. Bergeron. 2001. Future fire in Canada's boreal forest: Paleoecology results and general circulation model-regional climate model simulations. Canadian Journal of Forest Research 31: 854-864.

Girardin, M-P., J. Tardif, M. D. Flannigan, B. M. Wotton, and Y. Bergeron. 2004. Trends and periodicities in the Canadian Drought Code and their relationships with atmospheric circulation for the southern Canadian boreal forest. Canadian Journal of Forest Research 34: 103-119.

Gower, S. T., O. Krankina, R. J. Olson, M. Apps, S. Linder, and C. Wang. 2001. Net primary production and carbon allocation patterns of boreal forest ecosystems. Ecological Applications 11(5): 1395-1411.

Hartmann, B., and G. Wendler. 2003. Manifestation of the Pacific Decadal Oscillation shift of 1976 in Alaskan climatology. Seventh AMS Conference on Polar Meteorology and Climatology, Hyannis, MA, American Meteorological Society.

Hely, C., Y. Bergeron, and M. D. Flannigan. 2000a. Coarse woody debris in the southeastern Canadian boreal forest: Composition and load variations in relation to stand replacement. Canadian Journal of Forest Research 30: 674-687.

Hely, C., Y. Bergeron, and M. D. Flannigan. 2000b. Effects of stand composition on fire hazard in mixed-wood Canadian boreal forest. Journal of Vegetation Science 11: 813-824.

Hely, C., M. Flannigan, Y. Bergeron, and D. McRae. 2001. Role of vegetation and weather on fire behavior in the Canadian mixedwood boreal forest using two fire behavior prediction systems. Canadian Journal of Forest Research 31: 430-441.

Hess, J. C., C. A. Scott, G. L. Hufford, and M. D. Fleming. 2001. El Niño and its impact on fire weather conditions in Alaska. International Journal of Wildland Fire 10: 1-13.

Hessl, A. E., D. McKenzie, and R. Schellhaas. 2004. Drought and Pacific Decadal Oscillation linked to fire occurrence in the inland Pacific Northwest. Ecological Applications 14(2): 425-442.

Hurrell, J. W., Y. Kushnir, G. Ottersen, and M., Visbeck. 2003. The North Atlantic Oscillation: Climatic significance and environmental impact. Geophysical Monograph Series. American Geophysical Union. Washington D.C. USA.

IPCC. 2001. Climate Change 2001: Technical Summary of the Working Group I Report. WMO/UNEP. Cambridge, Cambridge University Press.

Johnson, E. A. 1992. Fire and vegetation dynamics: Studies from the North American boreal forest, Cambridge University Press.

Johnson, E. A., and D. R. Wowchuk. 1993. Wildfires in the southern Canadian Rocky Mountains and their relationship to mid-tropospheric anomalies. Canadian Journal of Forest Research 23: 1213-1222.

Johnson, E. A., K. Miyanishi, and J. M. H. Weir. 1998. Wildfires in the western Canadian boreal forest: Landscape patterns and ecosystem management. Journal of Vegetation Science 9: 603-610.

Johnson, E. A., K. Miyanishi, and S. R. J. Bridge. 2001. Wildfire regime in the boreal forest and the idea of suppression and fuel buildup. Conservation Biology 156: 1554-1557.

Kane, D. L. 1980. Snowmelt infiltration into seasonally frozen soils. Cold Regions Science and Technology 3(2-3): 153-161.

Kasischke, E. S., D. Williams, and D. Barry. 2002. Analysis of the patterns of large fires in the boreal forest region of Alaska. International Journal of Wildland Fire 11: 131-144.

Livezey, R. E., and T. M. Smith. 1999. Covariability of aspects of North American climate with global sea surface temperatures on interannual to interdecadal timescales. Journal of Climate 12: 289-302.

Lynch, J. A., J. S. Clark, N. H. Bigelow, M. E. Edwards, and B. P. Finney. 2003. Geographic and temporal variations in fire history in boreal ecosystems of Alaska. Journal of Geophysical Research 108(D1-1851): 8-1:8-17.

Lynch, J. A., J. L. Hollis, and F. S. Hu. 2004. Climatic and landscape controls of the boreal forest fire regime: Holocene records from Alaska. Journal of Ecology 92: 477-489.

Mann, D. H., C. L. Fastie, E. L. Roweland, and N. H. Bigelow. 1995. Spruce succession, disturbance and geomorphology on the Tanana River floodplain, Alaska. Ecoscience 22: 184-199.

Mann, D. H., and L. J. Plug. 1999. Vegetation and soil development at an upland taiga site, Alaska. Bioscience 6(2): 272-285.

McGuire, A. D., J. M. Melillo, and L. A. Joyce. 1995. The role of nitrogen in the response of forest net primary production to elevated atmospheric carbon dioxide. Annual Review of Ecology and Systematics 26: 472-503.

Melillo, J. M., A. D. McGuire, D. W. Kicklighter, B. Moore III, C. J. Vorosmarty, and A. L. Schloss. 1993. Global climate change and terrestrial net primary production. Nature 63: 234-240.

Miyanishi, K., and E. A. Johnson. 2002. Process and patterns of duff consumption in the mixedwood boreal forest Canadian Journal of Forest Research 32: 1285-1295.

Nash, C. H., and E. A. Johnson. 1996. Synoptic climatology of lightning-caused forest fires in subalpine and boreal forests. Canadian Journal of Forest Research 26: 1859-1874.

Niebauer, H. J. 1998. Variability in Bering Sea ice cover as affected by a regime shift in the North Pacific in the period 1947-1996. Journal of Geophysical Research 103(c12): 27171-27737.

Nyberg, L., M. Stahli, P.-E. Mellander, and K. H. Bishop. 2001. Soil frost effects on soil water and runoff dynamics along a boreal forest transect: 1. Field investigations. Hydrological Processes 15: 909-926.

Papineau, J. M. 2001. Wintertime temperature anomalies in Alaska correlated with ENSO and PDO. International Journal of Climatology 21: 1577-1592.

Payette, S. 1992. Fire as a controlling process in the North American boreal forest. In 'A systems analysis of the global boreal forest'. (Eds. H. H. Shugart, R. Leemans, G. B. Bonan), Cambridge University Press, Cambridge, U.K. pp. 145-169.

Reap, R. M. 1991. Climatological characteristics and objective prediction of thunderstorms over Alaska. Weather and Forecasting 6(3): 309-319.

Rupp, T. S., A. M. Starfield, and F. S. Chapin III. 2000. A frame-based spatially explicit model of subarctic vegetation response to climatic change: comparison with a point model. Landscape Ecology 15: 283-400.

Schimel, D. S., B. H. Braswell, and VEMAP participants. 1997. Continental scale variability in ecosystem processes: Models, data, and the role of disturbance. Ecological Monographs 67(2): 251-271.

Skinner, W. R., B. J. Stocks, D. L. Martell, B. Bonsal, and A. Shabbar. 1999. The association between circulation anomalies in the mid-troposphere and the area burned by wildfire in Canada. Theoretical and Applied Climatology: 3-17.

Skinner, W. R., M. D. Flannigan, B. J. Stocks, D. L. Martell, B. M. Wotton, J. B. Todd, J. A. Mason, K. A. Logan, and E. M.Bosch. 2002. A 500 hPa synoptic wildland fire climatology for large Canadian forest fires, 1959-1996. Theoretical and Applied Climatology 71: 157-169.

Starfield, A. M., and F. S. Chapin III. 1996. Model of transient changes in arctic and boreal vegetation in response to climate and land use change. Ecological Applications 6(3): 842-864.

Swetnam, T. W., and J. L. Betancourt. 1990. Fire-Southern Oscillation relations in the Southwestern United States. Science 249(4972): 1017-1020.

Trenberth, K. E. 1992. Climate System Modeling. Cambridge, Cambridge University Press.

Van Cleve, K., and L. A. Viereck. 1983. A comparison of successional sequences following fire on permafrost-dominated and permafrost-free sites in interior Alaska. Pages 1286-1291 in Proceedings of the Permafrost: Fourth International Conference.

Van Cleve, K., F.S. Chapin III, C. T. Dyrness, and L.A.Viereck.1991. Element cycling in Taiga forests: State-factor control. Bioscience 41(2): 78-88.

Wallace, J. M., and D. S. Gutzler. 1981. Teleconnections in the geopotential height field during the Northern Hemisphere winter. Monthly Weather Review 109: 784-812.

Ward, P. C., A. G. Tithecott, and B. M. Wotton. 2001. Reply - A re-examination of the effects of fire suppression in the boreal forest. Canadian Journal of Forest Research 31: 1467-1480.

Westerling, A. L., A. Gershunov, D. R. Cayan, and T. P. Barnett. 2002. Long lead statistical forecasts of area burned in western US wildfires by ecosystem province. International Journal of Wildland Fire 11: 257-266.

Wierzchowski, J., M. Heathcott, and M. D. Flannigan. 2002. Lightning and lightning fire, central cordillera, Canada. International Journal of Wildland Fire 11: 41-51.

Yarie, J. 1981. Forest fire cycles and life tables: a case study from interior Alaska. Canadian Journal of Forest Research 11(3): 554-562.

Zackrisson, O. 1977. Influence of forest fires on the North Swedish boreal forest. Oikos 29: 22-32.

Zhao, L., and D. M. Gray. 1999. Estimating snowmelt infiltration into frozen soils. Hydrological processes 13: 1827-1842.

CHAPTER 2

ANALYSIS OF ALASKAN BURN SEVERITY PATTERNS USING REMOTELY SENSED DATA[1]

2.1 Abstract

Wildland fire is the dominant large-scale disturbance mechanism in the Alaskan boreal forest, and it strongly influences forest structure and function. In this research, patterns of burn severity in the Alaskan boreal forest are characterized. First, the relationship between burn severity and area burned is quantified using a linear regression. Second, the spatial correlation of burn severity as a function of topography is modeled using a variogram analysis. Finally, the relationship between vegetation type and spatial patterns of burn severity is quantified using linear models where variograms account for spatial correlation. These results show that: 1) average burn severity increases with the natural logarithm of the area of the wildfire, 2) burn severity is more variable in topographically complex landscapes than in flat landscapes, and 3) there is a significant relationship between burn severity and vegetation type in flat landscapes but not in topographically complex landscapes. These results strengthen the argument that differential flammability of vegetation exists in the boreal forest of Alaska. Additionally, these results suggest that through feedbacks between vegetation and burn severity, the distribution of forest vegetation through time is likely more stable in the flats than it is in more complex topography.

2.2 Introduction

Fire is the dominant disturbance agent in the boreal forest of interior Alaska. As a consequence, the spatial distribution of vegetation across the landscape is a mosaic of previous burns and subsequent secondary succession (Zackrisson 1977, Payette 1992). Most studies of the fire regime in the Alaskan boreal forest have appropriately focused on characterizing the frequency and size distributions of fires (Yarie 1981, Mann and Plug 1999, Kasischke et al. 2002). The inter-annual variability of area burned in Alaska is tightly coupled to weather patterns (Duffy et al. 2005) and consequently displays significant variability on both spatial and temporal scales (Johnson 1990, Johnson and Wowchuk 1993, Bessie and Johnson 1995, Kasischke et al. 2002). Despite this variability in space and time, fire return intervals have been estimated for different regions across Alaska (Yarie, 1981, Mann et al. 1995, Kasischke et al. 2002). The frequency-area distribution of fires in Alaska roughly follows a power law (Malamud et al. 1998) and in a given year relatively few large fires typically account for the majority of the area burned. However, in years with a greater area burned, there are not only larger fires but a greater number of fires as well (Kasischke et al. 2002). Collectively, these results show that years with a large area burned are relatively infrequent (roughly once a decade), but when they do occur, not only are there more fires, the average fire size also increases. Hence the mean and variability of the fire size distribution in a given year changes as a function of the total area burned.

Despite its role as a keystone disturbance, some aspects of the fire regime of the Alaskan boreal forest are still poorly understood. Foremost among these, is burn severity, which plays a critical role in the key ecosystem process of secondary succession (Chrosciewicz 1974, Dyrness and Norum 1983, Van Cleve and Viereck 1983, Zasada et al. 1983, Foster 1985, Payette 1992, Johnstone et al. 2004). Previous studies of burn severity in boreal forests have resulted in several different ways to quantify burn severity: from the amount of organic matter consumed to the amount of the soil surface and vegetation that is charred (Michalek et al. 2000, Miyanishi and Johnson 2002, Greene et

al. 2004, van Wagtendonk et al. 2004, Epting and Verbyla 2005, Johnstone and Kasischke 2005). A driving factor for the existence of different metrics used to quantify burn severity is that critical ecological processes (e.g., post-fire succession and carbon cycling) are differentially influenced depending on the specific characterization of burn severity. For example, if the amount of carbon immediately released by a fire is the variable of interest, then the amount of organic matter consumed is a more appropriate metric to use for burn severity (Michalek et al. 2000). If, however, it is of interest to characterize the relationship between burn severity and post-fire succession, then the amount of the soil surface that is charred may be a more appropriate metric of burn severity. This works focuses on the metric of burn severity that most likely influences subsequent patterns of secondary succession.

Many of the factors that drive post-fire succession are strongly related to topography (e.g., water availability for seedlings, solar radiation and burn severity); hence these patterns need to be characterized across a large spatial domain (Bridge and Johnson 2000). Specifically, the existence of patterns of burn severity associated with different positions on the landscape (Miyanishi and Johnson 2002) provides additional motivation for the quantification of burn severity across large spatial domains that sufficiently represent the range of topographic diversity. The existence of topographically controlled factors driving succession suggests a certain amount of stability in dominant forest type with respect to post-fire succession (i.e., self-replacement). Observational data show this is often the case (Van Cleve and Viereck 1983, Greene and Johnson 1999); however, extremely severe burns can preclude the asexual sprouting that is the dominant mechanism for self-replacement in broadleaf stands (Johnstone et al. 2004, Johnstone and Kasischke 2005). Additionally, extremely severe burns resulting in a charred and exposed mineral soil surface can destroy the serotinous cones that often serve as the seed source for self-replacement in conifer-dominated stands. This allows for aerially dispersed seeds of broadleaf trees to colonize the burned site (Lutz 1956, Viereck 1973, Zasada et al. 1983, Johnstone et al. 2004). As a consequence, relay-floristics (i.e., the post-fire

germination and subsequent canopy dominance of broadleaf vegetation from seed on sites previously dominated by conifers) also operates as a post-fire successional pathway (Van Cleve and Viereck 1983, Van Cleve et al. 1996). Hence, burn severity is a factor that is influenced but not completely controlled by topography (Miyanishi and Johnson 2002), and as such plays a critical role in the modification of vegetation patterns on the landscape through time. The first step towards a better understanding of the relationship between large-scale patterns of burn severity and vegetation dynamics is through the development of statistical models and hypothesis tests. In order to accomplish this, it is essential that the metric of burn severity used be able to estimate burn severity across large spatial domains. In this paper we use single scene post-fire imagery from the Landsat TM to compute the Normalized Burn Ratio (NBR) (Key and Benson 2004) and evaluate large-scale patterns of burn severity at three spatial resolutions (90m, 500m and 1km). The use of a remotely sensed index allows for the burn severity to be quantified at multiple spatial resolutions across large spatial domains.

2.3   Methods

2.3.1   Overview

The goal of this work is to characterize several critical aspects of fire-vegetation interactions across interior Alaska. This is accomplished through tests of three hypotheses: 1) Average burn severity is not significantly correlated with the area of the wildfire, 2) There is no significant difference in the variability of burn severity for fires that burn topographically complex landscapes versus fires that burn in flat landscapes, and 3) The relationship between burn severity and vegetation type does not change as a function of topography.

Each of these hypotheses deals with a remotely sensed measure of burn severity. The metric of burn severity used here is the single scene Normalized Burn Ratio (NBR) (Key and Benson 2004). The NBR is computed using the near and the shortwave IR

portions of the electromagnetic spectrum (bands 4 and 7 of the Landsat TM sensors, respectively) [Equation 2.1].

$$NBR = \frac{(R_4 - R_7)}{(R_4 + R_7)}$$ [2.1]

There are several advantages to the use of this remotely sensed product. First, entire burned regions can be studied in a single Landsat scene. Additionally, the mid-infrared band is sensitive to moisture and since moisture conditions are radically altered following fire, TM7 is a valuable channel for mapping burn severity. As a consequence, in a comparison (using fires from interior Alaska) with twelve other remotely sensed indices the NBR had the highest correlation to the ground-based measurement of the composite burn index (CBI) (Epting et al. 2005). Finally, due to the long-running nature of the Landsat program, historical fires after approximately 1980 can be studied.

2.3.2 Data Assembly and Preparation

Landsat TM data were obtained for twenty-four wildfires (Table 2.1) that burned across interior Alaska. The primary limitation for the selection of data was the availability of cloud free imagery within one or two years of the burn. The Landsat imagery is available at a 30m spatial resolution. Fire perimeters were outlined manually using onscreen digitizing and for each pixel within the fire perimeter, the normalized burn ratio (NBR) was computed as a metric of burn severity for each pixel in the image.

Maps of pre-fire vegetation were assembled to characterize the relationship between vegetation and burn severity. The vegetation maps were generated using Landsat MSS, Landsat TM, and SPOT MSS data. Seven datasets were combined, all of which had either a spatial resolution of 50m or 127m. The vegetation map products were re-sampled at 30m to match the resolution of the NBR product. The resampling was performed such that each 30m cell contained both NBR and vegetation data. Vegetation classes used in

this analysis included 1) closed conifer, 2) open conifer, 3) broadleaf forest, 4) shrub, and 5) herbaceous communities. Remotely sensed vegetation classification was verified using either a field based assessment or digital photographs. Closed conifer forest includes black and white spruce (*Picea mariana* and *Picea glauca*, respectively) stands characterized by at least 25% cover. Open conifer also contains black and white spruce, but the trees represent only 10 - 25% total cover. Broadleaf forest is characterized as a stand consisting of more than 75% broadleaf trees. These include quaking aspen (*Populus tremuloides*), paper birch (*Betula papyrifera*), and balsam poplar (*Populus balsamifera*). This vegetation type was not divided into closed and open stands because only a negligible number of stands were open. Shrub vegetation is dominated by shrubs and contains less than 10% tree cover. The final class, herbaceous, includes areas dominated by herbaceous vegetation such as grasses or sedges with no more than 25% shrub cover and less than 10% tree cover. Herbaceous classes were typically in wetland areas where *Calamagrostis* grass and various sedges and sedge relatives were dominant. Scrub and herbaceous communities collectively account for a relatively small percentage (~ 15%) of the vegetation classes.

The 30m NBR and vegetation data were then aggregated to the 90m, 500m and 1 km spatial resolution. When aggregating from finer to more coarse spatial resolution, an average of the smaller pixels contained within the new larger pixel was used to compute the NBR. For vegetation, the mode (i.e., the most frequently observed) of the vegetation type for the smaller pixels was used as the vegetation type for the new larger pixel. By aggregating the NBR metric and using a mean, the potential for results to be driven by measurement error that can exist in the classification algorithms associated with remotely sensed products is reduced. Additionally, since many of the factors that drive post-fire succession are strongly related to topography (e.g., water availability for seedlings, solar radiation and burn severity), large spatial domains need to be considered when characterizing fire-vegetation interactions (Bridge and Johnson 2000). Finally, by performing the analysis at three different spatial resolutions, differences in fire-vegetation

dynamics across spatial scales can be examined. If no differences among spatial scales are observed, then future analyses can be designed accordingly.

2.3.3 Statistical Analyses

Hypothesis 1: Average burn severity is not significantly correlated with the natural logarithm of the area of the wildfire. The relationship between the average NBR and the area burned by a fire is modeled using a linear regression. Average NBR was computed for each fire and then regressed on the natural logarithm of area burned. The p-value for the explanatory variable 'area burned' in the regression corresponds to a test of the null hypothesis that average burn severity is unrelated to the natural logarithm of fire size. In order to assess sensitivity of the results to potentially influential points, a cross-validation was performed. For each of the 10,000 iterations of the cross-validation, three randomly selected fires were excluded and the regression parameters were re-estimated. From each of these 10,000 regression models, there is a corresponding p-value. From this list of 10,000 p-values, the median was used to assess the results of the cross-validation. This test was only performed at the 90 m spatial resolution because the average NBR for a fire is relatively invariant to the size of the pixels within the fire used to compute the average.

Hypothesis 2: There is no significant difference in the variability of burn severity for fires that burn topographically complex landscapes versus fires that burn in flat landscapes. The terrain over which each fire burned was categorized a priori as either 1) flat or 2) hilly/mountainous. Of the twenty-four fires, ten occurred on flat terrain and fourteen occurred on hilly/mountainous terrain. In order to assess differences in the spatial correlation structure of fires burning in different topography, a variogram analysis was performed. Variograms can be used to characterize changes in the spatial correlation of a variable (e.g., NBR) as a function of distance. In this application, the variogram quantifies the similarity of NBR values as a function of distance between pixels. Variograms can be computed using the following formula [Equation 2.2]

$$\gamma(d_1 - d_2) = \left(\frac{1}{2}\right) \mathrm{var}(Z(d_1) - Z(d_2)) \qquad [2.2]$$

where Z is a random spatial process (NBR in this example), and d_i in this case represents a unique location in 2-D space. The difference between two d_i's is computed as the sum of the squared distances of both the horizontal and vertical component. In general, most classical statistical tests (e.g., t-tests and ANOVA) assume that the variogram is essentially a horizontal line and that the average of the values on this line is the estimate of the variability in the response. When this is the case and the variogram is 'flat', the data are assumed to be independent. This assumption can be formally tested with regression models or a non-parametric 'runs test'. Typically, estimates of the variogram are obtained by discretizing the distances into classes or bins. Hence an estimate of the variogram is computed for all possible pairs with distances that fall into a given bin (e.g., pixels with centers that are between 500 and 1,000 meters apart). In this example, a bin width of 500 m was used. This variogram analysis was performed using the geoR package (Ribeiro and Diggle 2001) in the R statistical computing language.

In order to assess differences in the spatial correlation structure of burn severity as a function of topography, a 'composite' variogram was calculated for fires burning in both flat and hilly/mountainous terrains. The composite variogram is the weighted average of the empirical variograms from each fire within the topographic class. The first step in computing the composite variogram is to compute the empirical variogram (of NBR) for each fire. To do this, the possible distances between pixels within a single fire are partitioned into evenly spaced bins. The spacing used for bins (500 m) is identical for each fire, which facilitates averaging the individual variograms into the composite. Next, within each distance bin, the value of the variogram is computed by taking the variance (of the NBR) for each pair of points [Equation 2.2] that are within the given distance specified by the bins. Each point in each empirical variogram has a number of pairs

associated with it (i.e., the number of pairs used to estimate the value of the variogram for that bin). To obtain the composite variogram for a given topographic class, the total number of pairs for each bin was summed across all fires in a given topographic class (e.g., flat). Then a weighted average was computed across fires for each bin. The weighting was performed based on the number of pairs in that bin for a given fire. For example, a fire with twenty pairs in a given bin contributes more to the composite than a fire with ten pairs in that bin. This process results in two composite variograms: one for each topographic class. The advantage to this weighting scheme, as opposed to a simple average of variograms across fires, is that it reflects the number of pairs that went into the estimate of each point in each of the empirical variograms.

These two composite variograms each represent an average of the empirical variograms for the respective topographic categories (i.e., flat or hilly/mountainous). The difference between the two composite variograms was quantified by taking the sum of the squared differences between the empirical variograms [Equation 2.3].

$$D = \sum_{i=1}^{n} \left(\gamma_{flat}(i) - \gamma_{hilly}(i) \right) \qquad [2.3]$$

Where γ is defined as in equation [2.2], and n is the number of bins in the empirical variogram. Hence, the difference between these two composite variograms is mapped to a single value computed [Equation 2.3]. The null distribution of the test statistic 'D' was simulated by discarding the original topographic information and randomly dividing the variograms into two groups. Once the fires are randomly divided into two groups of size ten and fourteen (identical to the respective number of fires from each topographic category in the original data set) the value of the test statistic is re-calculated. This produces a realization from the distribution of this test statistic under the null hypothesis that there is no difference between the composite variograms for the two topographic categories. This process was repeated 10,000 times to generate 10,000 realizations of the

null distribution. Using this distribution, and the observed value of the test statistic [Equation 2.3], a p-value for the test of the null hypothesis, 'There is no difference between the spatial correlation structure of burn severity for fires burning in flat versus hilly/mountainous terrain' is computed. Comparison of composite variograms for flat versus hilly/mountainous terrain was performed at all three spatial resolutions.

Hypothesis 3: The relationship between burn severity and vegetation type does not change as a function of topography. Linear models were fit (using the spatial correlation of NBR to explicitly account for correlation in the error structure) to quantify the relationship between burn severity and vegetation type. In this analysis, only three vegetation classes are used: closed conifer, open conifer, and broadleaf. The shrub and herbaceous classes were eliminated to simplify the interpretation of the analysis, and focus on the differences between burn severities of forest types and only use vegetation classes with enough data to yield a meaningful analysis.

The first step in this analysis is to fit a simple ANOVA model where no spatial correlation is taken into account. In this ANOVA model, the response variable is burn severity and the forest types: closed conifer, open conifer, and broadleaf are levels of the factor 'vegetation type'. If the p-value corresponding to the test of the equality of the NBR across vegetation types is significant for this simple ANOVA, then a more sophisticated model that accounts for spatial correlation is fit. The impact of the explicit inclusion of the spatial correlation in the linear model is an increase in the estimate of the variability associated with the parameter estimates in the model. This increase in variability results in smaller test statistics and larger p-values. In other words, ignoring significant spatial correlation in the response variable results in an artificially low estimate of the variability of the parameter estimates in the model. As a consequence, the results of hypothesis tests for parameter significance that use non-spatial ANOVA models, when spatial correlation is present, can be misleading since the p-values are artificially decreased. The end result is often inappropriately rejected null hypotheses.

Hence, if in the presence of significant spatial correlation, the non-spatial ANOVA model has a non-significant p-value, the incorporation of a spatial component will usually result in a larger and hence less significant p-value.

The application of the spatial ANOVA begins with a second test. This test deals with the similarity of the correlation structure between vegetation classes within each fire. For each fire, differences in the spatial correlation of burn severity between forest vegetation classes were assessed by considering the closed conifer forest as a baseline and pooling the open conifer and broadleaf forest into a separate single category. The closed conifer was used as a baseline since it is the most ubiquitous; hence this method provides results for the greatest number of fires. The test for differences in the spatial correlation of vegetation classes (i.e., the variograms) was performed using the re-sampling method detailed under hypothesis 2. If the results of this test were significant, then a spatial ANOVA model that allows for a distinct correlation structure for each of the different forest vegetation classes was fit. Otherwise, a spatial ANOVA with a single correlation structure across forest vegetation classes was fit. In either case, the resulting model allows for estimation of the differences in average NBR within a given fire for the three forest vegetation types. This is essentially an ANOVA model where the lack of independence is accounted for through the construction of a separate variogram model for each fire. The parameters in the ANOVA model are estimated using restricted maximum likelihood estimation (REML) (Smyth and Verbyla 1995).

At a given spatial resolution, each fire must have twenty-five cells for each forest vegetation class included in the analysis. Twenty-five was selected arbitrarily, but provided a balance between robustness of results and the number of fires that were able to be used in this analysis. If fewer than twenty-five cells of a vegetation class were present in a given fire, that vegetation class is omitted from the analysis of that fire at that spatial resolution. At the 90m spatial resolution some of the fires were analyzed through resampling due to the large size of the datasets. For these fires, 150 different sets of 1000

pixels were randomly sampled without replacement and analyzed using the modeling approach described above. For each of these 150 different sub-samples, there is a distinct spatial ANOVA model and corresponding p-value for the test of equality of mean NBR for each vegetation type. From this list of 150 p-values, the median is used to assess the weight of evidence against the null hypothesis: 'There is no difference between the average NBR for each of the forest vegetation classes'. At the 500m and 1km spatial resolutions, the size of the datasets is such that a single analysis using the entire data set was tractable. Therefore, the re-sampling approach described above was not necessary.

2.4   Results

Hypothesis 1: Average burn severity is not significantly correlated with the natural logarithm of the area of the wildfire. The linear regression of average NBR on the natural logarithm of area burned provides a test of the null hypothesis that there is no relationship between average NBR and area burned. As values of the NBR become more negative, the severity of the burn increases. The analysis was performed using twenty-four fires from across interior Alaska (Figure 2.1 and Table 2.1). With a p-value of 0.02 there is sufficient evidence to reject this hypothesis and conclude that larger fires have a higher average burn severity. These results suggest there is a moderately strong linear relationship between the natural logarithm of the size of a fire and the average burn severity (Figure 2.2). Based on this regression model we expect that for every unit increase in the logarithm of fire size, there is a corresponding decrease of 51 in the average NBR associated with that fire. Cross-validation was performed where three randomly selected fires were repeatedly omitted and the linear model was refit with each randomly selected subset of twenty-one fires. This was repeated 10,000 times and the median of the 10,000 p-values from the cross validation was computed as 0.02. Large fires are more likely to contain areas that are more severely burned than smaller fires as opposed to a uniform increase in overall burn severity (Figure 2.3). This difference was quantified using the non-parametric quantile test (p < 0.0001) at the 80th quantile (Johnson et al. 1987).

Hypothesis 2: There is no significant difference in the variability of burn severity for fires that burn in topographically complex landscapes versus fires that burn in flat landscapes. There is a significant difference in the composite variograms of NBR between fires that burn on flat and hilly/mountainous terrain (Figure 2.4) across all three spatial resolutions (90m: $p = 0.04$, 500m: $p = 0.04$ and 1km: $p = 0.05$). Fires burning in the flats have a higher degree of spatial correlation across a range of distances.

Hypothesis 3: The relationship between burn severity and vegetation type does not change as a function of topography. At the 90 m resolution, only one of the fourteen (7%) hilly/mountainous fires indicate a difference in burn severity across vegetation classes, whereas nine of the ten (90%) flat terrain fires indicate such differences (Table 2.1). At the 500 m resolution, enough data were available to perform this analysis for eighteen of the twenty-four fires. Of the ten hilly/mountainous fires, only one (or 10%) indicated differences in burn severity across vegetation classes, whereas five of the eight (or 62.5 %) of the flat terrain fires indicated such differences (Table 2.1). At the 1 km resolution, enough data were available to perform this analysis on nine fires. None of the three fires in the hilly/mountainous terrain indicated a difference in burn severity across vegetation classes, whereas four of the six (66.7 %) flat terrain fires indicated such differences (Table 2.1). In general, regardless of scale, the difference in burn severity, as a function of vegetation type is considerably higher for fires that burn on flat terrain.

2.5 Discussion

2.5.1 Conceptual Model of the Boreal Forest

At large spatial scales, the boreal forest can be viewed as a system of several spatially explicit interacting components. In a simple conceptualization, the list of components includes, weather, fire and forest vegetation type. With respect to fire and weather, atmospheric teleconnections and monthly weather explain roughly two-thirds of the observed inter-annual variability in area burned over the past five decades (Duffy et

al. 2005). This work further refines the conceptual model through tests of hypotheses that characterize and quantify fire-vegetation interactions across several spatial scales within interior Alaska.

The annual area burned in Alaska is highly variable due to the strong forcing by atmospheric teleconnections (Duffy et al. 2005). During summers when a large area burns across interior Alaska, not only are there more fires, but the average fire size also increases (Kasischke et al. 2002). Since the fire size distribution in a given year changes as a function of the total area burned, differences in fire-vegetation interactions that exist as a function of fire size would play a fundamental role in the determination of forest structure. If average burn severity of a fire is related to area burned, then successional trajectory, through its relationship to burn severity (Johnstone et al. 2004), may also be related to fire size. Our results suggest a significant relationship between the size of a fire and its average burn severity (Figure 2.2), with larger fires being associated with more severe burning (more negative NBR) due to the existence of subregions within large fires that burn at a level of severity not seen in smaller fires (Figure 2.3). The positive correlation between fire size and severity is likely a consequence of the larger fires burning later into the summer during years when the synoptic late-summer precipitation is below average (Kasischke et al. 2002). Conversely, when the synoptic summer precipitation is present, conditions are likely to be less favorable for severe burning. As a consequence, the atmospheric teleconnections that influence annual area burned likely impact succession and carbon cycling vicariously through impacts on differential burn severity.

A significant portion of interior Alaska has negligible topographic relief (e.g., Yukon flats, Tanana Flats). Outside of the flats where topographic features do exist there are differences in the physical environments associated with different combinations of slope, aspect and elevation. In these places, species composition is often a consequence of the influence of topography and physical site characteristics on secondary succession

(Van Cleve and Viereck 1983). In addition to species composition, topography also influences fire behavior (Van Wagner 1977). Because of the heterogeneity in both species composition and fire behavior, lower spatial correlation of burn severity exists in hilly or mountainous regions, as opposed to the flats where both vegetation and burn severity should be more homogeneous (Figure 2.4). For fires that burn in the flats, the broadleaf vegetation has a lower average burn severity than coniferous vegetation. In general, when both broadleaf and coniferous species were present before fire (i.e., there are not any physical characteristics of the site which preclude either broadleaf or coniferous species), intermediate burn severities tend to favor the dominance of broadleaf species through asexual re-sprouting (Zasada et al. 1983) and more severe burns have been shown to favor post-fire dominance of coniferous species (Johnstone et al. 2004).

Finally, the relationship between burn severity and vegetation type is examined for fires that burn in both flat and complex topography. In this portion of the analysis, the spatial correlation of burn severity is accounted for and what is left is essentially a test of the influence of the topography on the relationship between burn severity and vegetation. This result coupled with the greater spatial correlation of burn severity (as measured by the variograms, Figure 2.4) that exists in the flats, suggests stability with respect to the vegetation distribution in the flats relative to the distribution of vegetation that exists in more complex topography. This does not preclude the same type of 'inertia' from existing in topographically complex regions, however pattern formation of forest vegetation types in topographically complex regions is more likely to be driven by physiological constraints associated with gradients of solar insolation and moisture (Van Cleve and Viereck 1983).

The fire vegetation interactions presented here hold for spatial resolutions varying across several orders of magnitude, which has implications for future data collection and analysis. These results also provide critical information for spatially explicit simulation studies of burn severity. Additionally, for tests of hypotheses involving data collected

across a large spatial domain, the characterization of spatial correlation is essential in order to ensure that hypothesis-testing techniques are applied appropriately. Although this work provides specific information regarding the link between burn severity and vegetation for fires that burn in flat terrain, more work needs to be done to characterize the more complex relationship that exist when fires burn in complex terrain.

2.5.2 Burn Severity and Carbon Cycling

The boreal forest covers 12 million square km of the northern hemisphere and contains roughly 40% of the world's reactive soil carbon, an amount similar to that held in the atmosphere (Melillo et al. 1993, IPCC 2001). This carbon is vulnerable to release from disturbance. Fire is an important disturbance in boreal forests and plays a critical role in the carbon cycle of boreal forests (McGuire et al. 2004, Csiszar et al. 2004). For example, it has been estimated that changes in fire regime and other disturbance regimes played an important role in shifting the forest ecosystems of Canada from a long-term carbon sink (from 1920-1980) to a source (from 1980-1989) (Kurz and Apps 1999). Fire influences carbon cycling in the boreal forest through initial carbon loss, and shifts in both species composition and stand age distribution. Large-scale biogeochemical models have traditionally treated the initial carbon loss in fire as fractions of above-ground and below-ground carbon that are defined regionally as the average of studies that have been conducted in the region (e.g., McGuire et al. 2004). The ability to estimate the temporal and spatial variability of initial carbon loss after fire within a region has been limited by knowledge of how initial carbon loss varies in time and space. The results of this study represent progress in helping to define how initial carbon loss varies in time and space. Now that we better understand how a satellite-derived measure of burn severity varies in time and space, an important next step will be to verify how NBR relates to carbon loss after fire. Approximately 10% of the boreal forest in interior Alaska burned during the fire seasons of 2004 and 2005, and a number of studies are now being conducted to estimate initial carbon loss after fire and are attempting to relate these to NBR. The results of those studies combined with the results of our study should allow large-scale

biogeochemical models to better estimate how fire influences carbon cycling within the Alaska boreal forest.

2.6   Conclusion

This characterization of fire-vegetation interactions across large spatial domains provides critical information for a conceptual model of the Alaskan boreal forest. The results of a linear regression of average burn severity on the natural logarithm of average fire size show that burn severity increases with fire size. This is a consequence of subregions of larger fires burning more severely as opposed to a uniform increase in burn severity. Topography plays a critical role in the determination of fire-vegetation interactions and fires burning in the flats have greater spatial correlation (as measured by variogram analysis) of burn severity than those burning in hilly/mountainous terrain. This relationship was significant across three spatial resolutions 90m, 500m and 1km. Additionally, fires burning in the flats showed significant differences between burn severities of vegetation classes. Conversely, fires burning in more complex terrain did not have significant differences between burn severities as a function of vegetation types. Topographically mediated differences in burn severity as a function of vegetation type imply that with respect to vegetation distribution, there are stronger feedback mechanisms in the flats as opposed to more topographically complex terrain.

Collectively these results underscore the importance of fire size and topography as important factors in the determination of fire-vegetation interactions, and strengthen the argument that differential flammability of vegetation plays a significant role in the boreal forest of Alaska. Specifically, the role of fire size and topography as determinants of burn severity underscores their relevance to both carbon cycling and secondary succession. Because of the link between vegetation and burn severity in the flats, fire induced shifts in the dominant forest species in the flats have a greater potential to influence direct carbon emissions than corresponding changes in dominant forest type that occur in more complex topography. This work characterizes the variability of burn

severity for fires burning in both flat and complex terrain. However, for fires that burn in complex terrain, there does not appear to be a link between burn severity and vegetation. As a next step, models need to be constructed that examine burn severity as a function of different combinations of slope, aspect, and elevation, in order to characterize spatial patterns of burn severity for fires in complex topography. Future modeling efforts should take into account the role of fire size and topography as modifiers of fire-vegetation interactions.

2.7 Figures
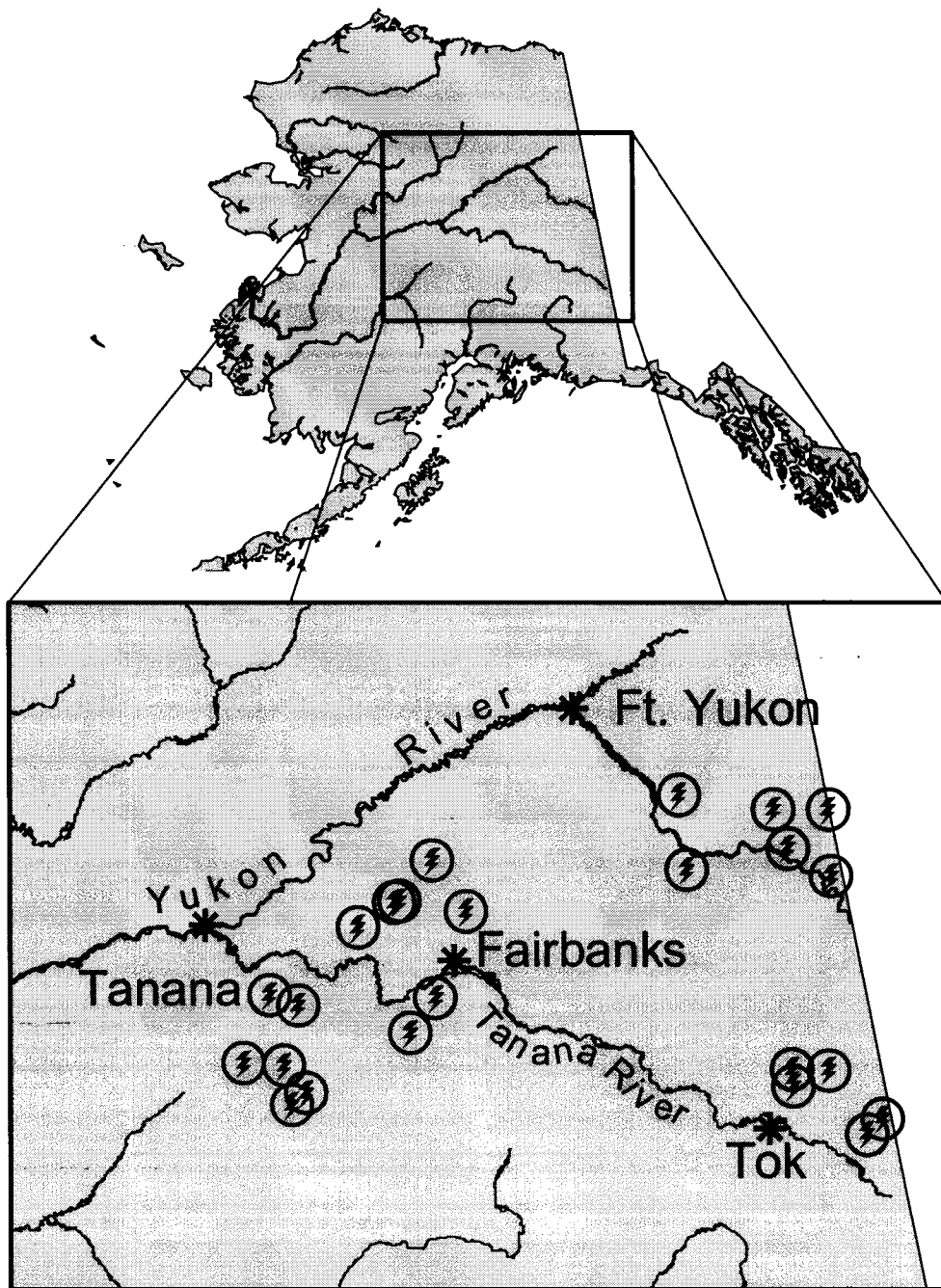
Figure 2.1 Locations of twenty-four fires used in this analysis.
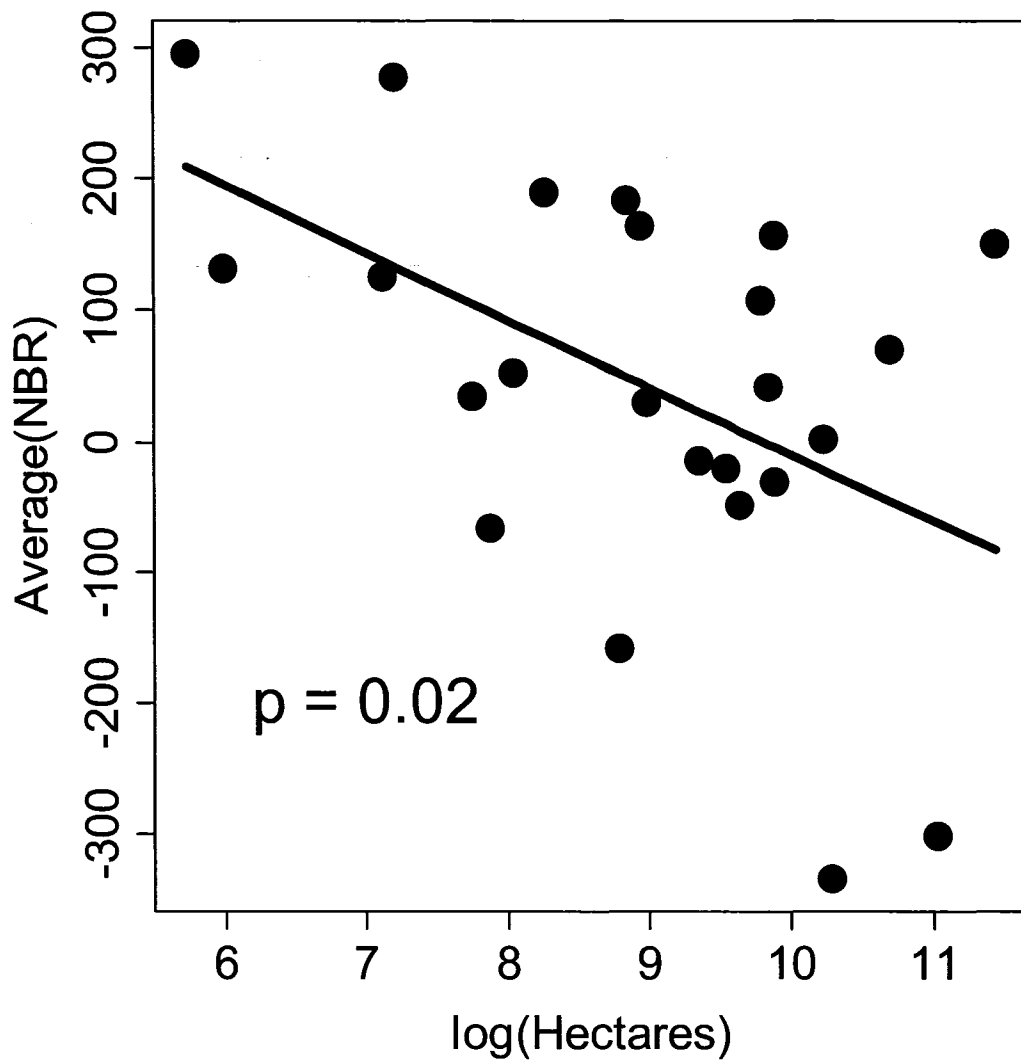
Figure 2.2   Scatterplot and line corresponding to regression of average normalized burn ratio (NBR) on the natural logarithm of hectares burned. Negative values of NBR correspond to more severe burning and there is a significant relationship between NBR and the natural logarithm of fire size with larger fires burning more severely. Cross-validation was performed where three randomly selected fires were excluded from the analysis and the regression parameters were re-estimated using the randomly selected subset. This was repeated 10,000 times giving a median p-value of 0.02.

5 Biggest Fires (27,000 - 94,000 ha)

5 Smallest Fires (300 - 2,300 ha)
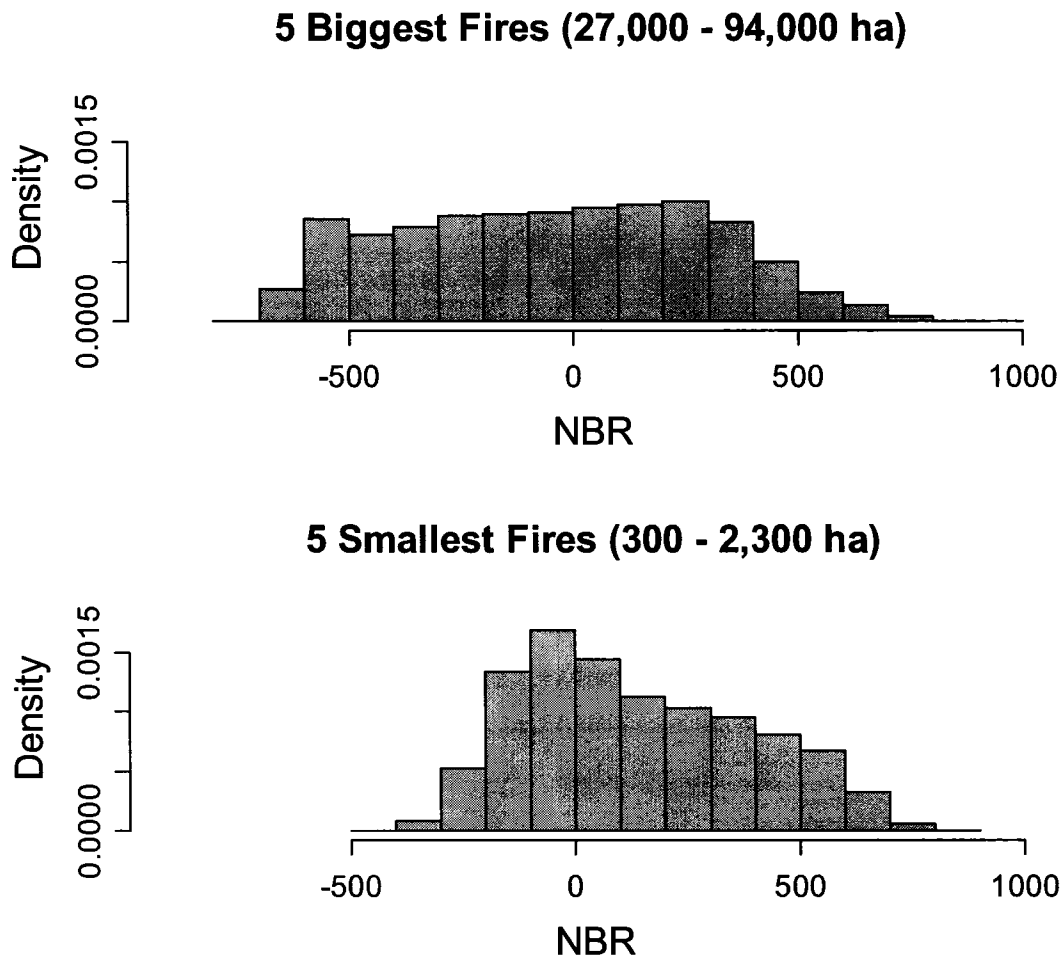
Figure 2.3   Histograms of pooled data for the five biggest and five smallest fires analyzed. Comparison of the pooled histograms for the biggest and smallest fires shows that the largest fires contain subregions that burn more severely (large negative values of NBR) than any region within the smallest fires. This difference was quantified using the non-parametric quantile test (p < 0.0001) at the 20th quantile (Johnson et al. 1987).
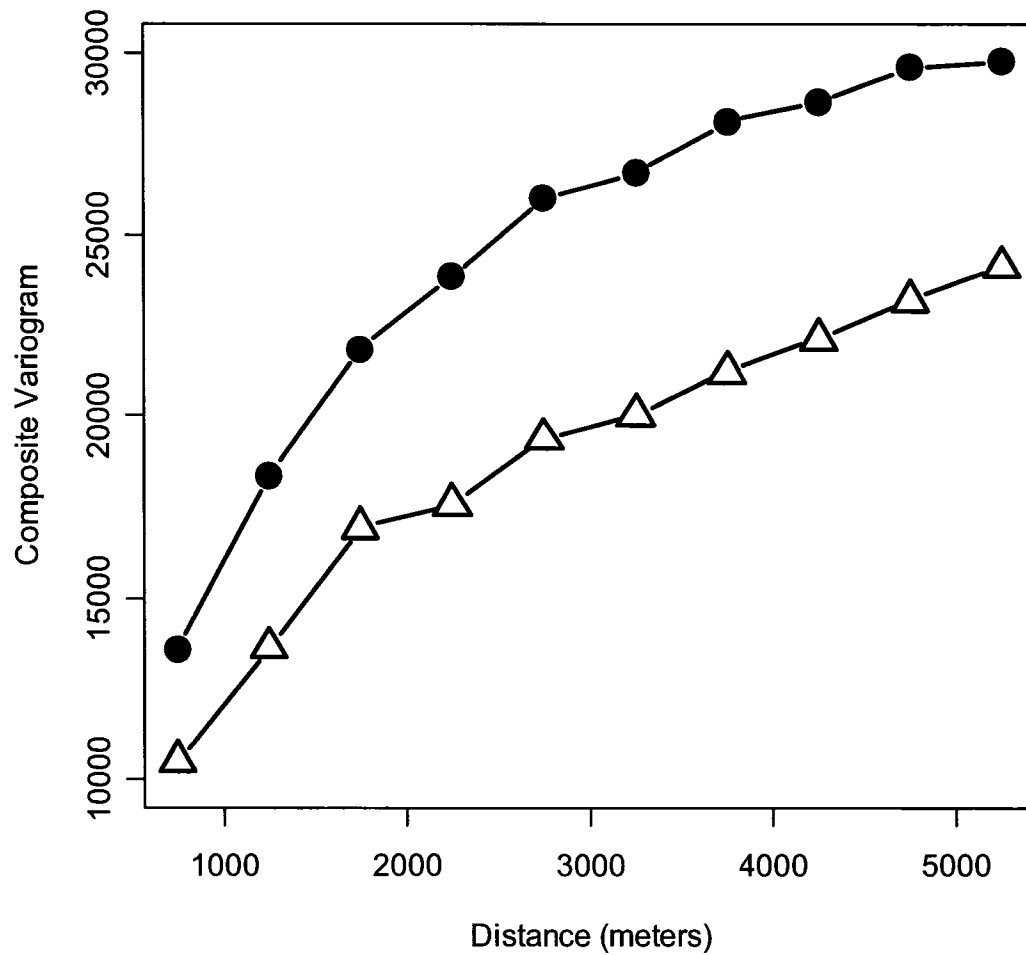
Figure 2.4 Composite variograms for burn severity as measured by normalized burn ratio (NBR) of fires that burn on both flat (shown as triangles) and hilly/mountainous (shown as circles) terrain were compared at 90m, 500m and 1km spatial resolutions. The variograms are significantly different at all three spatial resolutions (90m: $p = 0.04$, 500m: $p = 0.04$ and 1km: $p = 0.05$). Results shown here are for the 1 km resolution.

2.8   Tables

Table 2.1   Results from spatial ANOVA at multiple resolutions. Variograms were fit to model spatial correlation and then restricted maximum likelihood (REML) was used to estimate parameters in a spatial ANOVA model. The p-value from the spatial ANOVA corresponds to a test of the hypothesis that the average burn severity is equal for each vegetation class in a given fire.

Fire Name	Year	Area (Ha)	Landsat TM info			Spatial ANOVA p-value			Terrain class
			Date	Path	Row	90m	500m	1km	
Tolovana West	2000	308	8/16/2000	70	14	NS^A	--	--	Hill/Mtn
Chatanika	1999 ^{D}	400	8/16/2000	70	14	NS	--	--	Hill/Mtn
Minto	1999	1,242	8/16/2000	70	14	0.01^A	NS^A	--	Flat
Tolovana East	2000	1,344	8/16/2000	70	14	0.01	--	--	Flat
Forty Mile	1998	2,340	8/4/1999	64	16	NS	--	--	Hill/Mtn
Taylor Hwy	1999	2,643	8/4/1999	64	16	NS	--	--	Hill/Mtn
Laude River	1999	3,110	8/4/1999	64	16	NS	NS^A	--	Hill/Mtn
Toklat East	2000	3,889	7/21/2002	70	15	NS	NS^C	--	Flat
Square Lake	2002	6,583	7/21/2002	70	15	NS	NS^A	--	Hill/Mtn
Toklat West	2000	6,898	7/21/2002	70	15	0.00	--	--	Flat
Chena	1999	7,584	8/16/2000	70	14	NS	NS	--	Hill/Mtn
Webber Creek	1993	7,975	6/11/1994	66	14	NS	NS^A	NS^A	Hill/Mtn
Gardiner Creek	1998	11,559	8/4/1999	64	16	NS	NS	NS^A	Hill/Mtn
Prindle Volcano	1998	13,998	8/4/1999	64	16	NS^A	NS^A	NS^A	Hill/Mtn
Kantishna	2000	15,451	7/21/2002	70	15	0.00^A	NS^A	NS^A	Flat
Yukon West	1999	17,862	9/10/1999	67	14	NS^A	NS^A	--	Hill/Mtn
Yukon 242	1999	18,907	9/10/1999	67	14	NS	NS	--	Hill/Mtn
Yukon 260	1999	19,676	9/10/1999	67	14	NS	NS^B	--	Hill/Mtn
Yukon East	1999	19,737	9/10/1999	67	14	0.07	0.10	--	Hill/Mtn
Fish Creek	2001	27,831	7/21/2002	70	15	0.00	0.00	0.02^A	Flat
Twin Lakes	2002	29,617	7/21/2002	70	15	0.00	0.00^A	0.00^A	Flat
Survey Line	2001	44,445	7/21/2002	70	15	0.00	0.00	0.00	Flat
Bear Lake	2000	61,670	6/16/2000	70	15	0.00	0.00	0.00	Flat
Paddle Creek	1993	93,655	6/11/1994	66	14	0.02	0.00	NS^A	Flat

Table 2.1 (cont)

-- not enough data
NS = not significant at the 0.05 level
A = closed conifer vs. open conifer
B = closed conifer vs. broadleaf
C = open conifer vs. broadleaf
D = date is estimated

2.9   Acknowledgements

2.10   Literature Cited

Bessie, W. C., Johnson, E. A., 1995. The relative importance of fuels and weather on fire behavior in subalpine forests. Ecology 76 (3): 747-762.

Bridge, S. R. J., Johnson, E. A., 2000. Geomorphic principles of terrain organization and vegetation gradients. Journal of Vegetation Science 11: 57-70.

Chrosciewicz, Z., 1974. Evaluation of fire-produced seedbeds for Jack Pine regeneration in central Ontario. Canadian Journal of Forest Research 4: 455-457.

Csiszar, I., C. O. Justice, A. D. McGuire, M. A. Cochrane, D. P. Roy, F. Brown, S. G. Conard, P. G. H. Frost, L. Giglio, C. Elvidge, M. D. Flannigan, E. Kasischke, D. J. McRae, T. S. Rupp, B. J. Stocks, and D. L. Verbyla, Ed. 2004. Land use and fires. In 'Land Change Science: Observing, Monitoring, and Understanding Trajectories of Change on the Earth's Surface'. (Eds. Gutman, G., Janetos, A. C., Justice, C. O., Moran, E. F., Mustard, J. F., Rindfuss, R. R., Skole, D., Turner II, B. L., Cochrane, M. A.), pp. 329-350, Dordrecht, Netherlands, Kluwer Academic Publishers.

Duffy, P. A., Walsh, J. E., Graham, J. M., Mann, D. H., Rupp, T. S. 2005. Impacts of large-scale atmospheric-ocean variability on Alaskan fire season severity. Ecological Applications 15(4): 1317-1330.

Dyrness, C. T., Norum, R. A. 1983. The effects of experimental fires on black spruce forest floors in interior Alaska. Canadian Journal of Forest Research 13: 879-893.

Epting, J., Verblya, D., Sorbel, B. 2005. Evaluation of remotely sensed indices for assessing burn severity in interior Alaska using Landsat TM and ETM+. Remote Sensing of Environment 96: 328-339.

Epting, J., Verbyla, D. 2005. Landscape-level interactions of prefire vegetation, burn severity, and postfire vegetation over a 16-year period in interior Alaska. Canadian Journal of Forest Research 35: 1367-1377.

Foster, D. R. 1985. Vegetation development following fire in Picea mariana (black spruce)-Pleurozium forests of South-Eastern Labrador Canada. Journal of Ecology 73: 517-534.

Greene, D. F., Johnson, E. A. 1999. Modeling recruitment of Populus tremuloides, Pinus banksiana, and Picea mariana following fire in the mixedwood boreal forest. Canadian Journal of Forest Research 29: 462-473.

Greene, D. F., Noel, J., Bergeron, Y., Rousseau, M., Gauthier, S. 2004. Recruitment of Picea mariana, Pinus banksiana, and Populus tremuloides across a burn severity gradient following wildfire in the southern boreal forest of Quebec. Canadian Journal of Forest Research 34: 1845-1857.

IPCC 2001. 'Climate Change 2001: Technical Summary of the Working Group I Report'. WMO/UNEP. Cambridge, Cambridge University Press.

Johnson, R. A., Verrill, S., Moore II, D. H. 1987. Two-sample rank tests for detecting changes that occur in a small proportion of the treated population. Biometrics 43(3): 641-655.

Johnson, L. B. 1990. Analyzing spatial and temporal phenomena using geographical information systems. Landscape Ecology 4(1): 31-43.

Johnson, E. A., Wowchuk, D. R., 1993. Wildfires in the southern Canadian Rocky Mountains and their relationship to mid-tropospheric anomalies. Canadian Journal of Forest Research 23: 1213-1222.

Johnstone, J. F., Chapin III, F. S., Foote, J., Kemmett, S., Price, K., Viereck, L. 2004. Decadal observations of tree regeneration following fire in the boreal forest. Canadian Journal of Forest Research 34: 267-273.

Johnstone, J. F., Kasischke, E. S. 2005. Stand-level effects of soil burn severity on postfire regeneration in a recently burned black spruce forest. Canadian Journal of Forest Research 35(9): 2151-2163.

Kasischke, E. S., Williams, D., Barry, D. 2002. Analysis of the patterns of large fires in the boreal forest region of Alaska. International Journal of Wildland Fire 11: 131-144.

Key, C. H., Benson, N. C. 2004. 'Landscape assessment: ground measure of severity, the composite burn index; and remote sensing of severity, the normalized burn ratio'. USDA Forest Service General Technical Report RMRS-GTR-XXX. D. C. Lutes, Keane, R. E., Caratti, J. F., Key, C. H., Benson, N. C., Gangi, L. J.

Kurz, W. A., Apps, M. J. 1999. A 70-year retrospective analysis of carbon fluxes in the Canadian forest sector. Ecological Applications 9(2): 526-547.

Lutz, H. J. 1956. Ecological effects of forest fires, USDA - FS: 121.

Malamud, B. D., Morein, G., Turcotte, D. L. 1998. Forest fires: An example of self-organized critical behavior. Science 281: 1840-1842.

Mann, D. H., Fastie, C. L., Roweland, E. L., Bigelow, N. H. 1995. Spruce succession, disturbance and geomorphology on the Tanana River floodplain, Alaska. Ecoscience 2(2): 184-199.

Mann, D. H., Plug, L. J. 1999. Vegetation and soil development at an upland taiga site, Alaska. Bioscience 6(2): 272-285.

McGuire, A. D., M. Apps, F. S. Chapin III, R. Dargaville, M. D. Flannigan, E. S. Kasischke, D. Kicklighter, J. Kimball, W. Kurz, D. J. McRae, K. McDonald, J. Melillo, R. Myneni, B. J. Stocks, D. L. Verbyla, and Q. Zhuang, Ed. 2004. Land cover disturbances and feedbacks to the climate system in Canada and Alaska. In 'Land Change Science: Observing, Monitoring, and Understanding Trajectories of Change on the Earth's Surface'. (Eds. Gutman, G., Janetos, A. C., Justice, C. O., Moran, E. F., Mustard, J. F., Rindfuss, R. R., Skole, D., Turner II, B. L., Cochrane, M. A.), pp. 139-161. Dordrecht, Netherlands, Kluwer Academic Publishers.

Melillo, J. M., McGuire, A. D., Kicklighter, D. W., Moore III, B., Vorosmarty, C. J., Schloss, A. L. 1993. Global climate change and terrestrial net primary production. Nature 63: 234-240.

Michalek, J. L., N. H. F. French, E. S. Kasischke, R. D. Johnson, J. E. Colwell, 2000. Using Landsat TM data to estimate carbon release from burned biomass in an Alaskan spruce forest complex. International Journal of Remote Sensing 21: 323-328.

Miyanishi, K., Johnson, E. A. 2002. Process and patterns of duff consumption in the mixedwood boreal forest. Canadian Journal of Forest Research 32: 1285-1295.

Payette, S. 1992. Fire as a controlling process in the North American boreal forest. In 'A systems analysis of the global boreal forest'. (Eds. H. H. Shugart, R. Leemans, G. B. Bonan), Cambridge University Press, Cambridge, U.K. pp. 145-169.

Ribeiro, Jr. P. J., Diggle, P. J. 2001. geoR: A package for geostatistical analysis. R-News (http://cran.r-project.org/doc/Rnews) 1(2).

Smyth, G. K., Verblya, A. P. 1996. A conditional approach to residual maximum likelihood estimation in generalized linear models. Journal of the Royal Statistical Society B 58: 565-572.

Van Cleve, K., Viereck, L. A. 1983. A comparison of successional sequences following fire on permafrost-dominated and permafrost-free sites in interior Alaska. Permafrost: Fourth International Conference, Proceedings, 1286-1291.

Van Cleve, K., Vierick, L. A., Dyrness, C. T. 1996. State factor control of soils and forest succession along the Tanana River in interior Alaska, U.S.A. Arctic and Alpine Research 28(3): 388-400.

Van Wagner, C.E. 1977. Effect of slope on fire spread rate. Canadian Forestry Service, Bimonthly Research notes 33(1): 7-8.

van Wagtendonk, J. W., Root, R. R., Key, C. H. 2004. Comparison of AVIRIS and Landsat ETM+ detection capabilities for burn severity. Remote Sensing of the Environment 92(3): 397-408.

Viereck, L. A. 1973. Wildfire in the taiga of Alaska. Quaternary Research 3: 465-495.

Yarie, J. 1981. Forest fire cycles and life tables: a case study from interior Alaska. Canadian Journal of Forest Research 11(3): 554-562.

Zackrisson, O. 1977. Influence of forest fires on the North Swedish boreal forest. Oikos 29: 22-32.

Zasada, J. C., Norum, R. A., Van Veldhuizen, R. M., Teutsch, C. E. 1983. Artificial regeneration of trees and tall shrubs in experimentally burned upland black spruce/feather moss stands in Alaska. Canadian Journal of Forest Research 13: 903-913.

CHAPTER 3

STAND AGE DYNAMICS OF THE ALASKAN BOREAL FOREST

3.1 Abstract

The boreal forest of interior Alaska contains approximately 60 million burnable hectares. Fire is the dominant disturbance mechanism and statistical modeling has shown that for the period 1950-2003 roughly 80% of the inter-annual variability in the logarithm of area burned in Alaska is explained by monthly weather and teleconnection indices. Here we use a statistical model of fire-weather relationships coupled with a historical climatic and area burned dataset to reconstruct annual area burned in Alaska for the period 1860-2000. This reconstruction is used in conjunction with a historical fire record to calibrate a spatially explicit cellular automata model (ALFRESCO) that simulates fire and successional dynamics across interior Alaska. Using both simulated and field data, the following hypotheses are tested: 1) Flammability of forest vegetation is a function of time-since last fire; 2) Anthropogenic disturbance has a significant impact on tree-age distributions; and 3) The mean and variance of the stand age distribution of the Alaskan boreal forest are stationary. This work shows that there is little evidence for changes in flammability as a function of time since last fire for the first 30 years after fire. Additionally, anthropogenic disturbance in the early 1900's has left a distinct, yet localized impact on stand age distributions. Finally, we conclude that significant temporal trends in both the mean and variance of the stand age distribution are an intrinsic property of the Alaskan boreal forest. Collectively, these results suggest that the strong link between climate and fire drives non-stationarity of stand age distributions through time. This non-stationarity precludes distributional modeling but enables simulation-based depiction of stand age dynamics across the interior Alaskan boreal forest through time.

3.2   Introduction

Interactions among climate, vegetation, and disturbance factors control ecosystem dynamics in the boreal forest (Chapin et al. 2006a). The sub-arctic climate experiences changes occurring at decadal and greater timescales that are differentially impacted by factors ranging from fluctuations in atmospheric trace gas concentrations to large-scale shifts in atmospheric circulation (Niebauer 1998, IPCC 2001, McBean et al. 2004). Abrupt changes in synoptic climate patterns can cause short-term interactions resulting from feedbacks among climate, vegetation, and disturbance. These interactions may persist for decades to centuries after an abrupt climate change (Kittel et al. 2000) because of the lags caused by species migrations (Rupp et al. 2001), soil development (Trumbore and Harden 1997, Harden et al. 2000, Ping et al. 2006), and impacts on permafrost (Osterkamp and Romanovsky 1999, Osterkamp et al. 2000, Hinzman et al. 2006). Many of these interactions are dictated by disturbance and consequently, there is a pressing need to characterize the sensitivities and potential responses of the disturbance regime of the boreal forest to climatic change (Schimel et al. 1997, Fosberg et al. 1999, Gower et al. 2001). As a place with a well-documented disturbance regime that has also experienced pronounced warming over the past several decades (Serreze et al. 2000), the boreal forest of interior Alaska is an ideal location to explore interactions and feedbacks among climate, vegetation, and disturbance factors.

Relative to the other disturbance mechanisms in Alaska, fire dominates at the landscape-scale (Van Cleve et al. 1991, Payette 1992). The annual area burned in Alaska is largely determined by monthly weather and atmospheric teleconnection indices (Duffy et al. 2005); however interactions between fire and vegetation play an important role in the structure (Johnstone et al. 2004, Johnstone and Kasischke 2005, Duffy et al. accepted) and function (McGuire et al. 2004, Csiszar et al. 2004) of the boreal forest. These interactions can result in succession-initiated shifts in stand age structure and dominant species (Johnstone et al. 2004, Johnstone and Kasischke 2005). As a result, the spatio-

temporal distribution of forest vegetation and stand ages across interior Alaska is a constantly changing mosaic driven by interactions among differentially flammable vegetation, topography, and fire-initiated succession (Payette 1992, Chapin et al. 2006b). A critical component of this mosaic that remains unquantified in Alaska is the change in flammability of forest vegetation as a function of time since fire. Hence, a key question in the ongoing conceptual model development relating fire-disturbance and carbon flux in the Alaskan boreal forest is: Does stand flammability change as a function of time since last fire?

Anthropogenic activity is playing an increasingly important role in the stand age distribution of boreal forests. As a consequence of its relatively sparse population, the northern boreal forest is a biome that has historically experienced minimal human impact. Aboriginal settlements have existed across interior Alaska for at least 12,000 years, and to some extent, this activity can be considered part of the "natural" fire regime since it is thought to have been relatively low impact with respect to area burned (Natcher 2004). On the other hand, recent human activity has been linked to important changes in the fire regime. Areas experiencing significant population growth in Alaska have seen a corresponding increase in the number of fire ignitions coupled with increased fire suppression resulting in a reduction of the area burned (DeWilde and Chapin, in press). Because of the critical role of fire, an increasing population can potentially influence fire activity and hence stand age distributions in complex ways (Fastie et al. 2003, Drobyshev et al. 2004, Bergeron et al. 2004, Grenier et al. 2005). One of the goals of this work is to assess the impact of mining-related anthropogenic disturbance that has occurred within the past century in interior Alaska.

The primary goal of this analysis is to understand which factors most strongly influence the shape of stand age distributions in the boreal forest. To that end, this work characterizes critical linkages among humans, climate, fire, and the distribution of forest stand ages across the landscape of interior Alaska. This is done through the refinement

and application of a conceptual model of boreal forest dynamics. ALFRESCO is a spatially explicit cellular automata model that depicts a simple representation of the current conceptual model of the Alaskan boreal forest. The stand age maps generated by ALFRESCO are a consequence of the assumptions within the conceptual model; consequently various aspects of the conceptual model are tested by comparing the simulated stand age distributions with field data collected from across interior Alaska.

3.3 Methods

3.3.1 Overview

The methods in this work support the testing of three main hypotheses. The first main hypothesis is tested using analyses of observed fire perimeters from 1950-2002. Hypothesis 1: *Flammability of forest vegetation is a function of time since last fire (TSLF)*, determines the way that flammability of vegetation is represented in the spatially explicit cellular automata model ALFRESCO. To test this hypothesis, patterns of intersection from observed fire perimeters are compared with the corresponding expectation under a spatial independence model. Hypothesis 2: *Anthropogenic disturbance has left a significant impact on stand age distributions*, is used to identify areas where mining related anthropogenic disturbance has impacted the stand age distribution. Areas that have experienced significant anthropogenic impacts on the stand age distribution are excluded from the observed stand age dataset that is used to validate ALFRESCO output. The results of the first two hypothesis tests provide information for the application of ALFRESCO, which is used here to simulate interactions among climate, fire and vegetation. Finally, hypothesis 3: *The mean and variance of the stand age distribution of the Alaskan boreal forest are stationary*, examines the stationarity of the mean and variance of the stand age distribution from 1860-2000. These results collectively refine the conceptual model of stand age dynamics in the Alaskan boreal forest. Specific methods for the three hypotheses are presented below.

3.3.2 Hypothesis 1: Flammability of Forest Vegetation is a Function of Time Since Last Fire

To test the hypothesis that flammability of vegetation is a function of the TSLF, we used fire perimeters from the Large Fire Database (LFDB) of the Alaska Fire Service (http://agdc.usgs.gov/data/blm/fire/index.html) in ArcView GIS and quantified the areas of fire intersection for pairs of time intervals. There are some fires in this dataset that are missing spatial perimeter information; however almost all of the fires that have burned over the past fifty years are represented. A complete description of this dataset and its quality is presented by Kasischke et al. (2002). We partitioned the period 1950-2002 into thirteen intervals, each with length of four years. The exception to this is the earliest interval, which is five years long (1950-1954). Under the null hypothesis that flammability is independent of TSLF, the spatial locations (i.e., the region within each fire perimeter) of fires in distinct time periods should be random. The null hypothesis was tested by comparing the *observed* spatial area covered by intersections of fire perimeters for a pair of time intervals with the area of intersection that would be *expected* under an independence model (i.e., the null hypothesis). Specifically, the test statistic of interest is (Observed-Expected)/sqrt(Expected). This is similar to a Chi-Square statistic often used to test for independence except that the form here preserves information regarding the direction of difference (i.e., was more or less area of intersection observed than would be expected). This method is robust to most of the major shortcomings in the LFDB because it is based only on the fires used in the analysis, so fires that are omitted because they were not reported or were excluded because of uncertain perimeters do not affect the calculation.

With these thirteen intervals, there are seventy-eight = (13*(13-1)/2) distinct, unique pairs of intervals considered. For each of these interval pairs, the observed area burned in the intersection was computed using fire perimeters from the LFDB. Firescars that are recorded in the LFDB without exact boundaries are omitted from this analysis. Based on the respective area burned in each time interval within a pair, the expected area

of overlap (under an independence model) was computed (Table 3.1). For example, consider the comparison of the pair of intervals 1950-1954 (the only five year interval) and 1955-1958. The observed intersected area burned based on the fire perimeters in the LFDB was 14,970 hectares. The expected intersected area burned is calculated as the product of the areas burned in each time period, divided by the total area of the region of interest. In the period 1950-1954, 1,897,811 hectares burned. In the period 1955-1958, 2,436,414 hectares burned. The burnable area in Alaska is assumed to be 62,000,000 hectares (about 240,000 mi^2). Hence, for the comparison of the intervals 1950-1954 and 1955-1958, under an independence assumption we would expect to observe a burned area of

$$\frac{(1,897,811 \times 2,436,414)}{62,000,000} = 74,578 \quad \text{hectares} \qquad [3.1]$$

This datum shows that less area re-burned than would be expected under an independence model and hence provides some evidence that once an area has burned it is somewhat less likely to burn than would be expected just by chance. Null distributions were generated by repeatedly (10,000 times) randomizing the time periods associated with each of the intervals (i.e., interval of the initial burn and interval of the subsequent burn) and re-computing the value of the test statistics for each time interval. Hence for each time interval (e.g., 4, 8, 12, etc) a distribution of values for the test statistic was generated.

P-values were computed by comparing the observed value of the test statistic to the distribution simulated under the null hypothesis. These p-values were then used to test the null hypothesis that fire perimeters occur independently as a function of TSLF. This is a two-sided test and p-values can be a consequence of either more or less observed

intersection of fire perimeters than would be expected under the null hypothesis. More intervals of smaller temporal duration are available (e.g., there are thirteen intervals of length four years, twelve intervals of length eight years, etc.) hence the results for longer intervals are relatively less reliable since fewer data are available.

A second step in this analysis examines the impact of the total area burned (within the earlier of the two time intervals) on the relationship between observed and expected burn area. Specifically, we look at the relationship between the maximum observed test statistic (for a given initial burn period) and the total area burned in the earlier of the two time intervals. This relationship was quantified using a linear regression. Time intervals with a greater area burned are more likely to have experienced larger fires, since annual area burned is positively correlated with both the number and size of fires (Kasischke et al. 2002). Changes in burn severity associated with increased fire size (Duffy et al. accepted) have the potential to influence the likelihood of reburning. Practically, this portion of the analysis quantifies the potential for differences in burn severity that are associated with fire size (Duffy et al. accepted) to impact the likelihood of reburning.

3.3.3 Hypothesis 2: Anthropogenic Disturbance Has Left a Significant Impact on Stand Age Distributions

3.3.3.1 Observed Stand Age Data

Two distinct stand age data sets are used in these analyses. We collected the first data set as part of a Joint Fire Science Program (JFSP) project. These are referred to as the JFSP data. We sampled within three main regions along a climatic gradient of growing season temperature and precipitation within interior Alaska (Figure 3.1). Numerous transects were sampled within each region. Each transect has five nodes that were separated by roughly a kilometer and each node consists of five samples. The five sample sites exist at the corners and center (node) of a square with sides equal to roughly 100 meters. At each sample site, several (3-6) of the largest trees were sampled. At

sample sites where distinct age cohorts of different species were present, samples were collected from each species. A total of 728 sites and 3,851 trees were sampled. Sampling occurred over the course of three summers (2002 to 2004) and ages were corrected in order to assemble a stand age distribution that is consistent in time. For example, samples collected in 2004 had two years subtracted from the ages so that they were consistent with the samples collected in 2002, etc.

Because of delays in post-fire recruitment and, in the case of black spruce, the existence of adventitious root systems (DesRochers and Gagnon, 1997) there is uncertainty regarding the accuracy of tree-ages as estimators of time since last fire. Because of this, a correction factor was estimated for both the coniferous and deciduous simulated vegetation classes. The correction factors are based on both the JFSP field data and additional sampling that took place in burns of known age within interior Alaska. Stand age samples were collected in areas located within historical fire perimeters of known age. Stand ages from four separate sites were used resulting in ninety-four ages for the coniferous class and seventy-four ages for the deciduous class. The recruitment delay (in years) was modeled using Poisson distributions with a mean of 3.91 and 8.19 for the deciduous and coniferous vegetation classes, respectively. Specifically, each stand age on the simulated landscape was corrected by subtracting a realization (i.e., randomly generated value) from the corresponding Poisson distribution. In this way, differences between observed and simulated stand age distributions that are a consequence of delays in post-fire recruitment and the existence of adventitious root systems are minimized.

The second stand age data set resides at the US Forest Service PNW Experiment Station - Anchorage Forest Sciences Laboratory and was collected over the course of several decades as part of the Forest Inventory and Analysis (FIA) program. This dataset will be referred to as the FIA data. Some FIA sites lie within fire perimeters that have burned (based on GIS representations of fire perimeters in the LFDB) since the sites were sampled. At these sites, the original datum of the stand age was removed and replaced

with the time that has elapsed since the fire minus a realization from the Poisson distribution (see previous paragraph). The stand ages in this dataset are recorded in discrete decadal intervals (e.g., 50-60 years old). Within each acre, trees were sampled at three pre-determined locations. From the trees sampled at these three locations, the maximum tree age was taken as the stand age for that plot. Hence, stand age is assessed for the spatial unit of one acre. For comparison purposes, the JFSP data used a spatial sampling frequency of five ages per 100 square meters, which is roughly equivalent to 2.5 acres. So the JFSP data had a spatial sampling frequency of roughly twice that of the FIA data. The FIA was performed over the course of several decades, and an appropriate correction has been added to the stand age in order to represent the stand age distribution at present. For example, if a stand was sampled two decades ago, twenty years were added to that stand age in order to represent those data at present.

We examined stand ages for evidence of anthropogenic impacts on the fire regime during the early 20th century in two areas that were intensively occupied by gold miners. The first is the Fairbanks area, which was sampled as part of the FIA. Gold was discovered in Fairbanks in 1902 and the population in the town rapidly grew to about 18,000 people within the next ten years. The second area sampled was part of the JFSP project and located in the Ruby-Poorman mining district. Large gold strikes in this area occurred in 1907 and 1911 resulting in a local population that grew to over 1,000 miners over the course of the next several decades.

Both these areas were compared with the closest areas in the respective datasets that did not experience anthropogenic disturbance. Distribution comparison tests were performed to quantify differences in the forest stand age distributions between the areas that experienced anthropogenic disturbance and those that did not. To assess changes in different portions of the distributions, we tested subsets of the distributions by removing ages less than a threshold age. This approach allows for an estimate of the time when the anthropogenic impact occurred. If the impact is observed near the time that increases in

populations were recorded, this strengthens the case for modification of stand age distributions as a consequence of mining-related anthropogenic disturbance. Fourteen different thresholds were assessed from 50 to 180 years before present (Table 3.2). The comparisons were performed using a test statistic equal to the sum of the squared differences between relative proportions of each age class [Equation 3.2]

$$D = \sum_{i=1}^{N} \left(p_{1i} - p_{2i}\right)^2 \qquad [3.2]$$

Where, N is the total number of age classes used in the comparison, p_{1i} is the relative proportion from the 1st data set that is in the ith age class and p_{2i} is the relative proportion from the 2nd data set that is in the ith age class. By squaring the differences, only the relative (as opposed to directional) difference is used in the calculation of the test statistic. This is essentially equivalent to summing the squared differences that would be observed for each age class in a comparison of two histograms. The null distribution is generated by repeatedly (100,000 times) computing the test statistic for samples (with replacement) taken from the locations that were sampled but assumed to have no anthropogenic disturbance. This resampling process results in stability of the p-values out to the hundredths place (i.e., if we repeatedly performed this analysis, p-values would be identical out to the hundredths place). To ensure appropriate representation of variances, sample sizes for the computation of the p_i's in [3.2] were identical to those in the original dataset.

3.3.4 Hypothesis 3: The Mean and Variance of the Stand Age Distribution of the Alaskan Boreal Forest are Stationary

This hypothesis was assessed using output from ALFRESCO, a spatially explicit cellular automata model that was used here to simulate fire-initiated changes in stand age across actual topography over annual time steps (Rupp et al. 2000a, 2000b, 2002, in press). The output from ALFRESCO consists of spatially explicit annual maps of stand ages across interior Alaska. The stationarity assessment is performed by examining the mean and variance of stand ages through time from an ensemble of ALFRESCO runs.

ALFRESCO output was both calibrated and validated. The calibration consisted of two main parts. First, historical data from 1950-2000 were used to ensure realism of the size distribution of fires simulated by ALFRESCO. The second part of the calibration focused on observed versus simulated annual area burned. Historical data for annual area burned are available for 1950-2000. A statistical model relating weather/climate to annual area burned for the period 1950-2000 was developed, as described below. This statistical model explains 75% of the observed variability in the natural logarithm of annual area burned for 1950-2000, and was used to generate a climatically driven (described below) point estimate backcast of annual area burned from 1860-1949. This backcast was then compared to annual area burned simulated by ALFRESCO for 1860-1949.

Once calibrated, ALFRESCO was used to generate 100 spatially explicit maps of stand age from 1860-1949. Each of these 100 maps was then subjected to burning according to the spatially explicit historical record of fires from 1950-2000. This results in an ensemble of 100 spatially explicit stand age maps for the year 2000. Stand ages from the 100 maps were sampled from four regions corresponding in both extent and location to field sampling. These simulated stand ages were then validated against observed stand age distributions using distributional comparison tests. Once validated, a subset of the annual spatially explicit maps of stand ages was used to characterize changes in the average and variance of the stand age distribution from 1860-2000. In

order to assess changes throughout the entire region of interior Alaska, the sampling of simulated stand ages for use in this portion of the analysis was more comprehensive in spatial extent.

3.3.4.1 ALFRESCO Overview

ALFRESCO is a spatially explicit cellular automata model that is used here to simulate annual fire and successional dynamics at a 1km spatial resolution across the landscape of interior Alaska. ALFRESCO represents the empirical relationship between growing-season climate (e.g., average temperature and total precipitation for May through September) and total annual area burned (i.e., the spatial footprint of fire on the landscape), but does not explicitly model fire behavior. The effect of climate on the likelihood of cell ignition was computed using a two-parameter (i.e., growing season temperature and growing season precipitation) linear regression model similar to that used by Kasischke et al. (2002).

Annual fire occurrence is simulated stochastically and is driven by both climate and vegetation type (Rupp et al. 2000a). The burn algorithm in ALFRESCO employs a recursive cellular automaton approach with a first-order neighborhood. In other words, an ignited pixel may spread to any of the eight surrounding neighbor pixels. Ignition of a pixel is determined by testing a randomly generated number against the flammability value of that pixel for a given year. Fire spread depends on the flammability of pixels in the first-order neighborhood and any effects of natural firebreaks including non-vegetated mountain slopes and large water bodies, which do not burn. ALFRESCO also allows for changes in flammability that occur during succession through a flammability coefficient that changes with vegetation type (Chapin et al. 2003).

This model version has three vegetation types: upland tundra, spruce forest and deciduous vegetation. The spruce vegetation type in this ALFRESCO application corresponds to black spruce, since this represents the majority of spruce in the interior.

Succession is initiated exclusively by fire and occurs as a transition from either deciduous or spruce forest to early successional deciduous vegetation (Rupp et al. 2000b). The deciduous vegetation type is conceptually an early successional spruce forest stage and succeeds to spruce forest accordingly. The exception to this occurs when repeated burning or climatic conditions preclude the transition from deciduous to spruce (Rupp et al. 2000a). Transitional ages for succession from deciduous to spruce were identified using both the literature (Viereck et al. 1986, Van Cleve et al. 1991, Kurkowski et al. submitted) and observed data from the JFSP sampling. These transitions are determined stochastically in the model application. Details for the tundra frame are not provided as the scenarios in this study assume the treeline ecotone to be static. A complete and detailed description of ALFRESCO can be obtained from the literature (Rupp et al. 2000a, 2000b, 2001, 2002).

3.3.4.2 Climate Data

Two spatially explicit (0.5 degree by 0.5 degree) datasets were used to collectively represent weather in Alaska from 1860-2000. Both contain monthly averages for temperature and precipitation yet have different temporal periods of coverage. The Potsdam Institute for Climate Impact Research (PICIR) dataset is a modified version of that presented in Leemans and Cramer (1991). The modification is presented in McGuire et al. (2001) and covers the period 1860-1995 and the Climate Research Unit (CRU: http://www.cru.uea.ac.uk/~timm/grid/CRU_TS_2_0.html) data from 1900-2000. For these analyses, the PICIR data were used from 1860-1899 and the CRU data were used for 1900-2000. Since both the PICIR and CRU data sets exist at 0.5 degree by 0.5 degree resolution, each 1km cell on the ALFRESCO landscape is assigned a temperature and precipitation value based on the corresponding 0.5 degree by 0.5 degree PICIR/CRU cell. These climate records were used in two distinct and independent models. The first model is a modified version of that presented by Duffy et al. (2005). Based on the relationship between climate and fire between 1950-2000, this statistical model generates a point estimate 'backcast' of the annual area burned from 1860-1949. This 'backcast' was then

used in conjunction with an historical record from 1950-2000 as a baseline in the calibration of ALFRESCO. Once calibrated, ALFRESCO simulates a spatially and temporally explicit representation of the 'backcast' using these same climate data integrated across months to represent growing season temperature and precipitation.

3.3.4.3 Backcasting with the Statistical Model

The statistical model used in this work is a modified version of that presented by Duffy et al. (2005). It is a linear regression model that uses monthly temperature and precipitation values along with a Pacific Decadal Oscillation (PDO) index to estimate the annual area burned across interior Alaska. Since the PICIR and CRU datasets are spatially explicit, point estimates of monthly temperature and precipitation were calculated by integrating across the spatial domain of interior Alaska to generate explanatory variables for the regression, which is a point model. The Pacific Decadal Oscillation (PDO) metric for the months of January and February (PDOWIN) was used as an explanatory variable for the statistical regression model. PDO indices from 1900-present are available from the Joint Institute for the Study of the Atmosphere and Ocean (JISAO: http://jisao.washington.edu/pdo/PDO.latest). In order to extend the backcast to 1860, an estimate of the PDO calculated from tree-ring based reconstructions generated by D'Arrigo (2001) was used in the model. The resolution from the tree-ring based PDO reconstruction is annual but the correlation between PDOWIN and the average PDO index for the year (based on the PDO data available from JISAO) is greater than 0.70; hence, the use of the annual resolution estimates for the explanatory variable representing the PDO from 1860-1899 was sufficient to drive the statistical backcast. Additionally, annual area burned estimates for 1940 to 1949 were taken from documentation in Alaska Fire Control Service records. The result of the statistical backcast and the historical data is a reconstruction of the area burned for each year from 1860-2000.

3.3.4.4 Model Spinup

In order to approximate ecologically realistic initial conditions with respect to the distribution and composition of vegetation, ten different randomly generated initial age/vegetation maps were simulated by running ALFRESCO for 1,000 years. This time span is roughly five times the length of the longest reported fire return interval in interior Alaska (Yarie 1981, Van Cleve et al. 1991, Chapin et al. 2003). Climate for the spinups was assembled in a manner consistent with Barber et al. (2004). From each of these ten initial age/vegetation maps, ten different simulations from 1860-1949 were run. Each of these 100 maps was then subjected to burning from 1950-2000 according to the spatially explicit historical record in the LFDB. This process results in the generation of 100 different final maps of stand ages across interior Alaska. These 100 maps consist of an ensemble of spatially explicit realizations of stand ages. Collectively, this ensemble provides a probabilistic context for the interpretation of observed stand age distributions.

3.3.4.5 ALFRESCO Calibration

The relationship between climate and fire in ALFRESCO was calibrated using metrics that focus on the most important characteristics of the fire regime at large spatial scales. The calibration is performed by comparing different aspects of model output to the corresponding historical data from the Large Fire Database (LFDB) (Kasischke et al. 2002).

3.3.4.6 Fire Sizes

The spatial record of fires in the historical database consists of perimeters. The estimates of area burned that are based on these perimeters are likely over-estimates due to the existence of unburned inclusions within fire perimeters. Work in Alberta has shown that the percentage of area that remains unburned within a fire perimeter increases with the size of the fire, and fires greater than 2,000 ha often have roughly 5% unburned area (Eberhart and Woodard 1987). Using this information along with the examination of aerial photographs and remotely sensed imagery from interior Alaska, it was determined that the calibration should match the size distribution of historical record with a slight

bias of the simulated fires being smaller in total area (roughly 5%) than those in the historical record.

An important characteristic of the fire size distribution is the relative proportion of area burned by fires of a given size. The historical record shows that most fires are small but the majority of the area burned comes from a small percentage of fires that are orders of magnitude larger than the rest (Kasischke et al. 2006). Specifically, roughly half the total area burned from 1950-2000, came from fires larger than 55,000 ha (Figure 3.2a). However, fires greater than 55,000 ha accounted for less than 3% of the total number of fires that occurred during this same period (Figure 3.2b-d). Consequently, the comparison of the distribution of fire sizes for the historical versus simulated data is focused on tails of the distribution since the majority of the area burned occurs as a consequence of the largest fires, which account for a relatively small percentage of the total number of fires.

Differences in the distributions of the natural logarithm of fire sizes for the historical data and ALFRESCO simulations were assessed using two nonparametric distribution comparison tests. These tests respectively focus on differences between two distributions that exist at a given quantile (e.g., 80th percentile) (Johnson et al. 1987) and the maximum (Rosenbaum 1954). These combinatorially based distribution comparison tests are one-sided and set up so that the null hypotheses guard against the 80th percentile and maximum of the simulated distribution of fire sizes being statistically greater than the 80th percentile and maximum of observed distribution of fire sizes, respectively. This was done to accommodate the assumed 5% overestimation of the annual area burned based on the fire perimeters recorded in the LFDB. All ALFRESCO output used in this analysis failed to reject (at $\alpha = 0.05$) the null hypotheses that for the period of 1950-2000, the 80th percentile and maximum of the distribution of simulated fire sizes is significantly greater than 80th percentile and maximum of the actual fire sizes.

3.3.4.7 Comparison of Simulated versus Historical Annual Area Burned

For each of the 100 realizations generated by ALFRESCO (e.g., Figure 3.3), a comparison of simulated annual area burned to the observed annual area burned data from the 1950-2000 historical record was performed (Figure 3.4). The average of the annual area burned from the 100 realizations was regressed on the historical data from 1950-2000, and the R-squared was 0.31. Additionally, the simulated annual area burned by ALFRESCO from 1860-1949 was compared to the point estimates from the statistical backcast (Figure 3.5). The R-squared between the average across 100 realizations from ALFRESCO and point estimates from the statistical model for 1860-1949 was 0.44. Essentially, ALFRESCO is used here to provide a spatial representation of the point estimates from the reconstruction of annual area burned from 1860-2000.

The annual area burned for interior Alaska is highly variable and spans several orders of magnitude, and consequently regression assumptions regarding constant variance are violated (Duffy et al. 2005). Because of this, the natural logarithm transformation was applied to both the historical/backcast annual area burned and simulated annual area burned data. The transformed variables were then used in the regression. The result is that for each temporal subset of ALFRESCO model output (i.e., 1860-1949 and 1950-2000) a regression model was fit. One regression was performed using only the historical data as a response variable and the second regression used the historical data (1950-2000) in conjunction with the backcast (1860-1949) as a response variable. The p-values from these regression models provides a metric to assess the fit of the simulation output to either the historical data or the backcast, respectively. Specifically, it provides a test of whether the coefficient for the explanatory variable (i.e., simulated annual area burned) is equal to zero. All simulation results used in subsequent analyses presented here had p-values <0.001.

3.3.4.8 Model Validation: Field Data versus Simulated Data

ALFRESCO was calibrated using both the historical data and the statistical backcast in order to ensure the simulation of realistic landscapes with fire legacies from which stand ages could be analyzed. Hence, ALFRESCO provides spatial representation of the point estimates from the reconstruction of annual area burned from 1860-2000. In order to quantify the realism of the simulated stand age distributions, comparisons identical to those used to assess the impact of anthropogenic disturbance (i.e., Hypothesis 2) were performed with the JFSP and FIA data (Figure 3.6, Table 3.3). The stand age maps generated by ALFRESCO were sampled in three regions corresponding in both extent and location to JFSP field sampling (Figure 3.1). Additionally, a fourth region in the south-eastern portion of the interior was sampled from the simulated stand age maps to correspond to the FIA samples. This approach allows the regional climatic anomalies in the historical record to manifest through localized fire activity in the simulations. The observed data set is composed of both the JFSP and FIA data that did not experience anthropogenic disturbance (Hypothesis 2). The tests were performed on decadal subsets of the data for stand ages >180 years down to the entire dataset. This allows for identification of where the distributions diverge. A maximum stand age of 280 years was used in this analysis.

The result is a list of p-values, which correspond to comparisons of different subsets of the observed and simulated stand age distributions (Table 3.3). The size of the subsets used for this comparison was arbitrarily selected as 250 samples. Since p-values are essentially a function of sample size in this context, the use of classical statistical techniques for the analysis of simulation results (where sample sizes can be arbitrarily large) will almost always produce a significant result (i.e., significant differences are observed). Specifically, as the sample size increases, p-values (Table 3.3) will converge to 0. In this case the results of the distributional comparison tests (Table 3.3) should be used only to assess relative significance between different decadal subsets of the data.

3.3.4.9 Stationarity Assessment

Once the model is calibrated and validated, there is a reasonable degree of assurance that the simulated stand age distributions provide realistic spatial representations of stand ages across both space and time. In order to assess the stationarity assumptions that are implicit in classical statistical analyses of stand age distributions, the simulated stand ages are examined from 1860-2000. In contrast to the relatively localized sampling of simulated stand age maps used for validation in conjunction with the JFSP and FIA data, more comprehensive spatial sampling of simulated stand age maps was used to assess temporal trends in the mean and variance of the stand age distribution. For each of ten random sets of realizations from 1860-2000, the mean and variance of the stand age distribution is computed. The goal of this portion of the analysis is to test the hypothesis that t*he mean and variance of the stand age distribution of the Alaskan boreal forest are stationary*. The presence of significant trends in the average stand age distribution through time provides evidence against the stationarity assumptions needed for classical statistical analyses.

3.4   Results

3.4.1   Hypothesis 1: Flammability of Forest Vegetation is a Function of Time Since Last Fire

The comparison between observed and expected burn area for different 4-year intervals shows that there is only one interval (16-year) with a significant p-value (Figure 3.7). The significance was driven by the observed area of intersection exceeding the expectation under the independence model. Overall, there is not significant evidence to conclude that age-dependent flammability in the first few decades after fire significantly modifies patterns of burn intersections across the interior. Additionally, larger values of total area burned are associated with larger maximum values of the test statistic (Figure 3.8). This provides some evidence that time intervals where a larger area burns are more

likely to experience burning (in subsequent time intervals) that exceeds the expectation under an independence model.

3.4.2   Hypothesis 2: Anthropogenic Disturbance has Left a Significant Impact on Stand Age Distributions

The distribution comparisons of regions impacted by anthropogenic disturbance with unimpacted regions performed on both the FIA and the JFSP datasets yield similar results. Specifically, the stand age distributions of impacted and unimpacted areas are not significantly different until subsets of the data with ages greater than 70 and 80 years, respectively, are considered (Table 3.2). There is also a general trend of decreasing p-values as the minimum stand age considered decreases. In both cases (JFSP and FIA) these differences are due to fewer stand ages in the 90 to 120 age classes (Figure 3.9). These results provide evidence that anthropogenic disturbance in the early 20th century resulted in increased tree mortality and reduced recruitment for several decades. These impacts are evident in current stand age distributions by the under-representation of the 90 to 120 year age classes.

3.4.3   Hypothesis 3: The Mean and Variance of the Stand Age Distribution of the Alaskan Boreal Forest are Stationary

Quantitative and graphical comparisons (Table 3.3 and Figure 3.6, respectively) of the observed versus simulated stand ages show relatively good agreement between the observed versus simulated stand age distributions. Differences between the observed and simulated stand age distributions are most pronounced for the youngest age class (Figure 3.6). A time series plot of the simulated average stand age (Figure 3.10) shows a lack of stationarity due to significant changes in average stand age through time. Simulated estimates of average stand age decreased from 1860-1880. Then, there was a fairly slow but steady increase from 1880 until roughly 1990 with a short decrease between 1940-1950. Average stand age then decreased between 1990-2000. The variance associated with stand age distribution changes significantly as well and behaves in a manner roughly

opposite of the average stand age (Figure 3.11). Comparison of the simulated stand age distributions for years with the youngest and oldest average stand age (1878 and 1988, respectively) demonstrates significant variability in the stand age distributions through time (Figure 3.12). Collectively, these results provide strong evidence to reject the hypothesis that stand age distributions are stationary through time. Essentially, the strength of the link between climate and fire drives the lack of stationarity. Practically, the non-stationarity demonstrates the importance of landscape flammability and accentuates the potential impacts of climatic change on boreal forest structure and function. Finally, the simulation output provides a probabilistic estimate of the stand age distribution in year 2000 (Figure 3.13).

3.5   Discussion

3.5.1   Hypothesis 1: Flammability of Forest Vegetation is a Function of Time Since Last Fire

One of the fundamental aspects of a fire regime is the relationship between stand age and flammability. In theory, significant age-dependent flammability influences both the probability distribution (van Wagner 1978) and spatial pattern formation of stand ages within the boreal forest (Johnson 1995). In the boreal forest of Alaska, the majority of the observed variability in annual area burned is explained by weather and teleconnection indices (Duffy et al. 2005). Coupled with the fact that fire is the dominant landscape-scale disturbance mechanism in the Alaskan boreal forest; this implies that stand dynamics are largely determined by climate through its impact on area burned. As a consequence, the potential importance of structural differences among stands (e.g., fuel-build-up associated with age-dependent flammability) with respect to fire-vegetation interactions is limited. The analysis of the observed versus expected fire intersections failed to find conclusive evidence of age-dependent flammability within the first several decades after fire (Figure 3.7). Specifically, if flammability did increase monotonically with stand age, we would expect to see a corresponding monotonic decreasing trend of

significant p-values for the tests of significant fire perimeter intersection as a function of TSLF.

This does not mean that the changes in flammability do not occur later than several decades after fire. One possible scenario where this can occur is in stands where deciduous vegetation ultimately transitions to coniferous vegetation. This will result in an increase in stand flammability that is essentially a consequence of changing dominant vegetation but also corresponds to increasing time since last fire. In this scenario, the threshold in stand age effects would occur as stands shift from deciduous to coniferous dominance, which takes longer than thirty years. In this work a conceptual distinction is made between changes in flammability that occur as a function of shifts in the dominant species, as opposed to changes in flammability that result from age-dependent accumulation of fuel. In stands where shifts from deciduous to coniferous vegetation occur, the transition can take as long as sixty years to begin. Hence, this analysis does not address succession-initiated changes in stand flammability (Cumming 2001) due to the limited temporal extent of the available data.

Along with the lack of trend in the p-values, this fire intersection analysis reveals interesting aspects of fire-vegetation interactions. Specifically, there is some evidence that, in general, it is more likely for the observed area of intersection to exceed that of the expectation under an independence model (Table 3.1). Practically, this means that there is evidence (non-statistically significant) that once a stand burns it is more likely to reburn than we would expect by just random chance. Additionally, within the first three decades after a fire, the magnitude of the area burned is related to patterns of re-burning (Figure 3.8), whereas the time since fire is not (Figure 3.7). The importance of the area burned may be a consequence of the existence of sub-regions of the landscape that are more susceptible to repeated burning.

Burn severity influences successional trajectory (Johnstone et al. 2004, Johnstone and Kasischke 2005), which can provide strong feedback to subsequent flammability. However, topography also influences interactions between vegetation and burn severity (Duffy et al. accepted). In places where the physical characteristics (poorly drained, north facing sites) of the landscape preclude the post-fire colonization of less flammable deciduous vegetation (Van Cleve and Viereck 1983), a higher likelihood of both burning and subsequent reburning would result. Conversely, sites with characteristics that favor post-fire regeneration by less flammable deciduous vegetation (Cumming 2001) are relatively less likely to re-burn.

In places where succession is most strongly determined by burn severity, rather than topographic influences on vegetation, short-term feedbacks between fire scars and convective development could influence the likelihood of reburning. Specifically, higher rates of reburning may be a consequence of changes in albedo that are associated with burn scars on the landscape (Dissing and Verbyla 2003). Post-fire albedo is related to burn severity, which is also correlated to fire size (Duffy et al. accepted). Additionally, the relative distribution of burn severity within a fire changes as a function of fire size (Duffy et al. accepted). Hence, it is possible that certain fire sizes may be associated with distributions of burn severity that are optimal with respect to feedbacks on convective development. As a potential example of this, the fires that burned in 1971-1974 experienced greater reburning than expected for all subsequent time intervals (Table 3.1). One possible explanation for the anomalous rates of reburning associated with the 1971-1974 period is that the weather conditions supported fire sizes and corresponding severities that were conducive to subsequent reburning.

3.5.2 Hypothesis 2: Anthropogenic Disturbance has Left a Significant Impact on Stand Age Distributions

Humans modify disturbance regimes in virtually all ecosystems, and in the boreal forest the affected disturbance is fire. While fire has historically been used by native

Alaskans (Natcher 2004), anthropogenic disturbance related to mining activity brought what was almost certainly an unprecedented level of human impact with respect to both logging and increased fire activity (Wurtz et al. 2006). The importance of this hypothesis is two-fold. First, for the purposes of forest management, there is a need to better understand the potential impacts of recent anthropogenic disturbance and the legacy that these impacts leave on stand age distribution of the boreal forest. Second, in order to most effectively assess the link between climate initiated fire disturbance and stand ages, field data from places where anthropogenic disturbance has impacted the stand age distribution should be excluded from subsequent analyses (i.e., validation of stand ages simulated by ALFRESCO).

The use of two independently collected datasets (FIA and JFSP) allows for a rigorous assessment of historical impacts of mining related anthropogenic disturbance on current stand age distribution. Both the FIA and JFSP datasets contain subsets of the data collected in and around places known to have experienced high levels of anthropogenic pressure as a consequence of mining operations in the early 1900's. Because of the availability of both impacted and adjacent unimpacted sites, the JFSP and FIA datasets provide unique opportunities to assess the legacy of mining related anthropogenic disturbance on stand age distributions. Comparisons performed with both datasets provide relatively strong evidence that anthropogenic disturbance in the early 1900's has left an impact on the stand age distribution of the forest that is still detectable today _ (Table 3.2 and Figure 3.9).

In both the JFSP and FIA datasets, anthropogenic disturbances have left a distinctive yet localized impact on stand age distributions. The most striking feature of the differences between the distributions of the impacted and unimpacted sites is the under-representation of the 90-120 year stand age classes. This is likely due to an abrupt and persistent increase in human-initiated fire and logging activity that started in the early 20th century (Wurtz et al. 2006). The 90-120 year old cohort would have been a 0-30 year

old cohort 90 years ago. The lack of stand ages between 90-120 years in the current stand age distribution is likely a consequence of increased fire ignitions corresponding to anthropogenic disturbance associated with land clearing.

The impact of the mining related anthropogenic disturbance was localized. In the case of the JFSP data used for this portion of the analysis, the closest sites from the impacted and unimpacted areas are roughly 100 km apart. In the case of the FIA data, the subregions used in the analysis are spatially distinct with the centers roughly 100 km apart as well. Based on the historical fire data from the past five decades, only the very largest fires would span this distance. Since the main impact of anthropogenic disturbance was likely increased ignitions, it follows that sites separated by a buffer roughly equivalent to the diameter of the largest fires would be independent in some sense. However, the subregions of the FIA data essentially border one another, so there is no buffer between them. This may account for the lack of monotonicity of p-values as a function of decreasing minimum age considered for the FIA comparisons. With respect to the subsequent analyses that use the observed stand age distributions for comparison to the simulated stand age distributions from ALFRESCO, the distinct pattern of ages observed in the impacted distributions in both the JFSP and FIA datasets provides justification for the exclusion of these data from validation of ALFRESCO.

3.5.3 Hypothesis 3: The Mean and Variance of the Stand Age Distribution of the Alaskan Boreal Forest are Stationary

A fundamental component of any assessment of change is the characterization of the historical state of the system of interest. Since fire-initiated disturbance shapes the structure and function of the Alaskan boreal forest, the strength of the link between climate and fire is used as the cornerstone of the characterization of historical stand age dynamics. The simulation results demonstrate changes in both the average and variance of stand ages through time and show that the stand age distribution of the Alaskan boreal forest is not stationary at time scales of several hundred years. These changes imply that

landscape flammability can change significantly through the modification of differentially flammable vegetation across the landscape. Additionally, these results suggest that as a consequence of the strong-link between climate and fire, the Alaskan boreal forest is likely to experience significant changes in structure as a consequence of future climatic change.

3.5.3.1 ALFRESCO Validation

The validation of ALFRESCO with the observed stand age data provides two important results. First, the general agreement between observed and simulated stand ages from four distinct regions of the interior shows that by using a relatively simple depiction of the interactions among climate, fire, and vegetation, ALFRESCO reasonably depicts temporal changes in stand age dynamics across interior Alaska. Despite the general agreement in observed and simulated stand ages, there is a significant difference between observed and simulated stand age data in the 0-10 year age class (Figure 3.6, Table 3.3). The youngest age classes are under-represented in the field data relative to the ALFRESCO output. Hence, the second important result from the validation is that despite the seemingly large regions covered by the JFSP and FIA sampling, the simulation results provide evidence that regional and localized sampling can result in significant differences with respect to characterization of stand age distribution of the entire interior (Figure 3.13, Table 3.3). This is likely a consequence of the spatial variability in the location of fire activity through time. There are significant differences in the stand age distributions for sub-regions within interior Alaska. Consequently, with respect to the characterization of stand age dynamics for interior Alaska as a whole, the main utility of the observed data lies in the validation of ALFRESCO output.

Another possible source of the discrepancy between the observed and simulated stand ages of the 0-10 year age class is heterogeneity with respect to tree mortality within a burn perimeter. If the area represented by unburned inclusions is significant, then differences in the youngest stand age classes are possibly a consequence of the over-

estimation of the actual area burned in the historical record. Results from the JFSP field sampling shed some light on the role that heterogeneity of tree mortality within fire perimeters plays in the determination of stand age distributions. Several sites within the JFSP sampling campaign took place within fire perimeters that were marked as burned within the past fifty years. Firescars and cohorts of deciduous trees recruited within several years of the fire confirm that fire did occur in the area during the years recorded in the historical database. However, several of the sites within historical fire perimeters also have stands dominated by cohorts that are older than the recorded TSLF. These field observations demonstrate that this heterogeneity needs to be better quantified as a next step in understanding fire-vegetation interactions. Since ALFRESCO was calibrated using the area burned information derived from the historical fire perimeters, the existence of inclusions was not explicitly taken into account. Once spatial patterns of unburned inclusions have been quantified, the next step in this modeling approach is to add a layer that would simulate burn severity and its corresponding impacts on the stand age distribution.

To put the differences between the observed and simulated stand age distributions in the context of the historical fire data from 1950-2000, consider that fact that the total area burned in Alaska according to the LFDB from 1950-2000 is 14,083,284 ha. Assuming that the total burnable area in Alaska is 62,000,000 ha, and for the sake of simplicity, assume that no reburning has occurred (i.e., all fires in the period 1950-2000 are spatially distinct), then we would expect that 14,083,284/62,000,000 = 23% of the age class distribution should be less than 50 years old. Allowing for intersection of fire scar perimeters within the past five decades would result in less than 23% of the age class distribution being less than 50 years old. Alternatively, the estimated percentage of stand ages less than 50 years old based on the observed and simulated data used for the validation is 17% and 13%, respectively. So although the discrepancy between observed and simulated validation stand age distributions is statistically significant for the youngest age class (Table 3.3), the differences with respect to the proportion of the

overall distribution is moderate. Additionally, the observed and simulated data used for the validation are consistent in their discrepancy with the historical data. Conversely, the comprehensive sampling of the simulated stand age distributions resulted in 23.8% of simulated stand ages that were less than 50 years old. Collectively, the validation results provide strong evidence that climatically driven fire activity dictates the stand age dynamics of the Alaskan boreal forest.

3.5.3.2 Depicting Disturbance Regimes

In forests where fire is the dominant disturbance, survival analyses have been used to infer properties of the fire regime such as the hazard of burning (van Wagner 1978). This approach has often been applied to assess changes in flammability as a function of stand age and "shifts" in fire frequency (Larsen 1997, Reed 1997, Reed et al. 1998, Reed 1998, Polakow and Dunne 1999, Bergeron 2000, Weir et al. 2000, Parisien and Sirois 2003, Bergeron et al. 2004, Grenier et al. 2005). The change in flammability through time is presumably due to changes in the quantity and structure of fuels in stands through time (e.g., fuel build-up). However, variability in weather has been shown to play a more important role than the variability in fuel loads (Bessie and Johnson, 1995), and consequently the existence of fuel build-up in boreal forests has been questioned (Johnson et al. 1998). The concept of age-dependent flammability in the boreal forest is confounded by the existence of both self-replacement and stand-dominance relay successional trajectories. In stands undergoing stand dominance relay succession, changes in flammability through time are a consequence of the shift from early to late (i.e., deciduous and coniferous, respectively) successional forest types. The dominant influence of monthly weather and teleconnection indices on annual area burned in Alaska (Duffy et al. 2005) provides evidence against, but does not rule out, the importance of age-dependent flammability in the determination of stand age distributions. However, when coupled with the results of hypothesis 1, the evidence against the existence of age-dependent flammability in the boreal forest of Alaska during the first thirty years after fire is quite strong.

Analyses using distributional models of TSLF data allow inference regarding properties of the fire regime (e.g., hazard functions) in the area of interest. However, the application of standard parametric methods requires not only the selection of a distributional model for the data but also that the underlying process being studied is stationary. Stationarity in this context refers to the mean and variance being roughly constant through at least the time period of interest. Since stand ages are used for this type of analysis, the stationarity must exist for several hundred years. The utility of subsequent analyses rests on not only the degree to which the selected model fits the observed data but also the validity of the stationarity assumption. Due to the strong relationship between annual area burned and short term weather that exists in the boreal forest (Skinner et al. 1999, Hess et al. 2001, Skinner et al. 2002, Girardin et al. 2004, Duffy et al. 2005), there is often a significant lack of fit between stand age data and corresponding distributional models (Boychuk et al. 1997).

In Alaska, the distribution of annual area burned is skewed with the majority of the area burned coming in a relatively small percentage of the years (Kasischke et al. 2006). Even when interior Alaska as a whole is considered as the region of interest, climatic anomalies and the corresponding large areas burned from decades ago produce spikes in the distribution of stand ages (Figure 3.12). These spikes drive a significant lack of fit for distributional models (Boychuk et al.1997, Johnson et al. 1998). When different subregions of the interior are considered, the impact from single large fire events is increased and these issues become even more pronounced. Ignoring a lack of fit and proceeding with distributional modeling can convey a false impression about the intrinsic variability and more importantly potential stationarity of the fire regime. Even when non-parametric approaches are used to obviate the necessity of a distributional model, the stationarity of the mean and variance of stand ages needs to be considered.

The lack of stationarity in the mean and variance of the stand ages calls into question the meaning of some of the fundamental descriptors of the fire regime. Since annual area burned in Alaska is driven largely by the climate signals that vary on time scales ranging from decades to centuries, the concept of fire frequency must be considered with caution. The low frequency variability associated with these climate signals makes the variance estimates used in statistical distribution models unreliable. The use of parametric statistical models for the estimation of fire frequency and quantification of the uncertainty associated with these estimates conveys a sense of stationarity regarding the fire regime that simply does not seem to exist. For example, approximately 10% of the boreal forest in interior Alaska burned during the fire seasons of 2004 and 2005. The level of fire activity was unprecedented in the fifty-year historical record. The inclusion of these two years into estimates of fire frequency based on classical statistical analyses will have a dramatic impact on estimates of fire frequency and its corresponding variability. The fire activity in these two years provides strong evidence against the validity of stationarity assumptions.

The first step towards a better understanding of the dynamics of the stand age distribution in Alaska lies in the characterization of changes in the average stand age distribution through time. The non-stationarity of the average stand age is likely a manifestation of the variability of climatic patterns across spatio-temporal scales. In the period from 1860-1880, fire activity resulted in a decrease in average stand age, which is consistent with analyses of the Canadian boreal forest (McGuire et al. 2004). From 1880 to roughly 1990, average stand age increased by approximately 25 years. Again a corresponding increase through 1970 has been noted for Canada as well (Kurz and Apps 1999). One might argue that the relative stability of the mean and variance of stand age from 1900-1940 provides evidence that the stationarity assumptions are somewhat reasonable. The length of time required for the mean and variance to remain relatively constant in order to satisfy stationarity assumptions is arbitrary. However, most locations within the interior go more than 30 years without burning, and ideally, the period of

relative stability in the mean and variance should be at least several times as long as the average fire interval observed across the region within that time span.

The strong forcing of climate on the fire regime of the Alaskan boreal forest precludes the use of parametric models for stand age analyses due to lack of fit and absence of stationarity in stand age distributions. Despite this, the link between climate and fire also provides an opportunity to explicitly model stand age dynamics across a simulated landscape. Because of this, the ALFRESCO modeling framework provides a tool that can be used to characterize stand age distributions across interior Alaska through time. These distributions can be used to better understand the role of the Alaskan boreal forest in a number of different contexts. For example, the unprecedented magnitude of area burned in 2004 and 2005, combined with the simulation results for average stand age (Figure 3.10), suggests that the current stand age distribution of the Alaskan boreal forest is likely equal to what it was around 1970. As the stand age distribution of the landscape shifts, there are potentially important feedbacks to the atmosphere via modification of exchanges of radiatively active gases and water/energy (McGuire and Chapin 2006). Perhaps most importantly, the ALFRESCO modeling framework provides a way to assess the impact of future climate change scenarios on stand age dynamics; hence allowing an explicit representation of the linkages among climate, fire and vegetation. These results can subsequently be coupled with other models that depict feedbacks between climate and vegetation.

3.6   Conclusion

In the vast forested ecosystem of Interior Alaska, disturbance is dominated by climatically driven fire occurrence. The extremely skewed distributions of both annual area burned and fire sizes result in pulses of stand ages that propagate along stand age distributions through time. As a consequence, the utility of distributional models with respect to characterization of properties such as fire frequency is limited due to lack of fit and a violation of stationarity assumptions. Although the strong link between climate and

fire makes distributional models less useful, it also allows for the development of a spatially explicit model (ALFRESCO) with simple rules regarding flammability and succession. The rules governing ALFRESCO are representations of post-fire succession and flammability as a function of stand type and climate. By calibrating with historical data and validating with field data we show that ALFRESCO can accurately depict stand age dynamics within the Alaskan boreal forest across both space and time. These results can be used in conjunction with other ecosystem models to assess the impacts of changes in stand age distributions on feedbacks to the atmosphere via modification of exchanges of radiatively active gases and water/energy. Additionally, assuming that the linkages among climate, fire and vegetation within Alaska remain relatively stable through time, ALFRESCO can be used to assess the impact of climatic change on stand age distributions and subsequent structure and function of the forest.
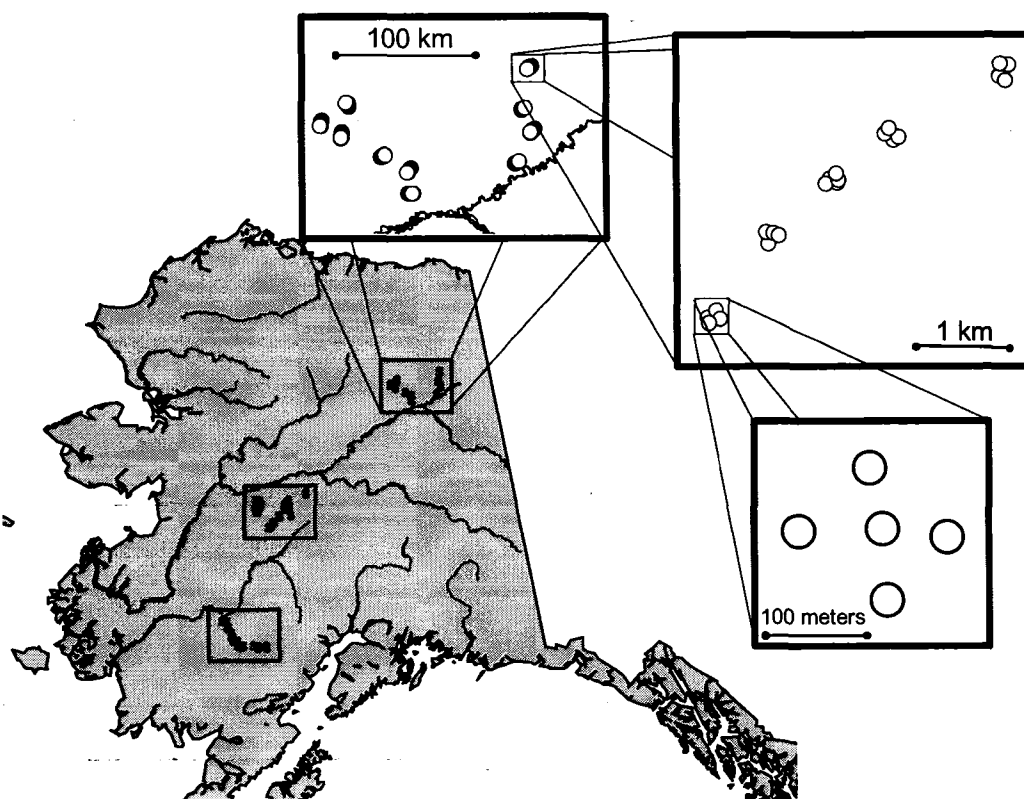
3.7   Figures

Figure 3.1   Location of three study regions across a climatic gradient within interior Alaska. Numerous transects were sampled within each region. Two transects are shown in the first step-out box with the 100 km scale. Each transect had five nodes that were separated by a little over a kilometer, as shown in the second step-out box with the 1 km scale. Each node is associated with five sample sites as shown in the third step-out box with the 100-meter scale. The five sample sites exist at the corners and center of a square with sides equal to roughly 100 meters.
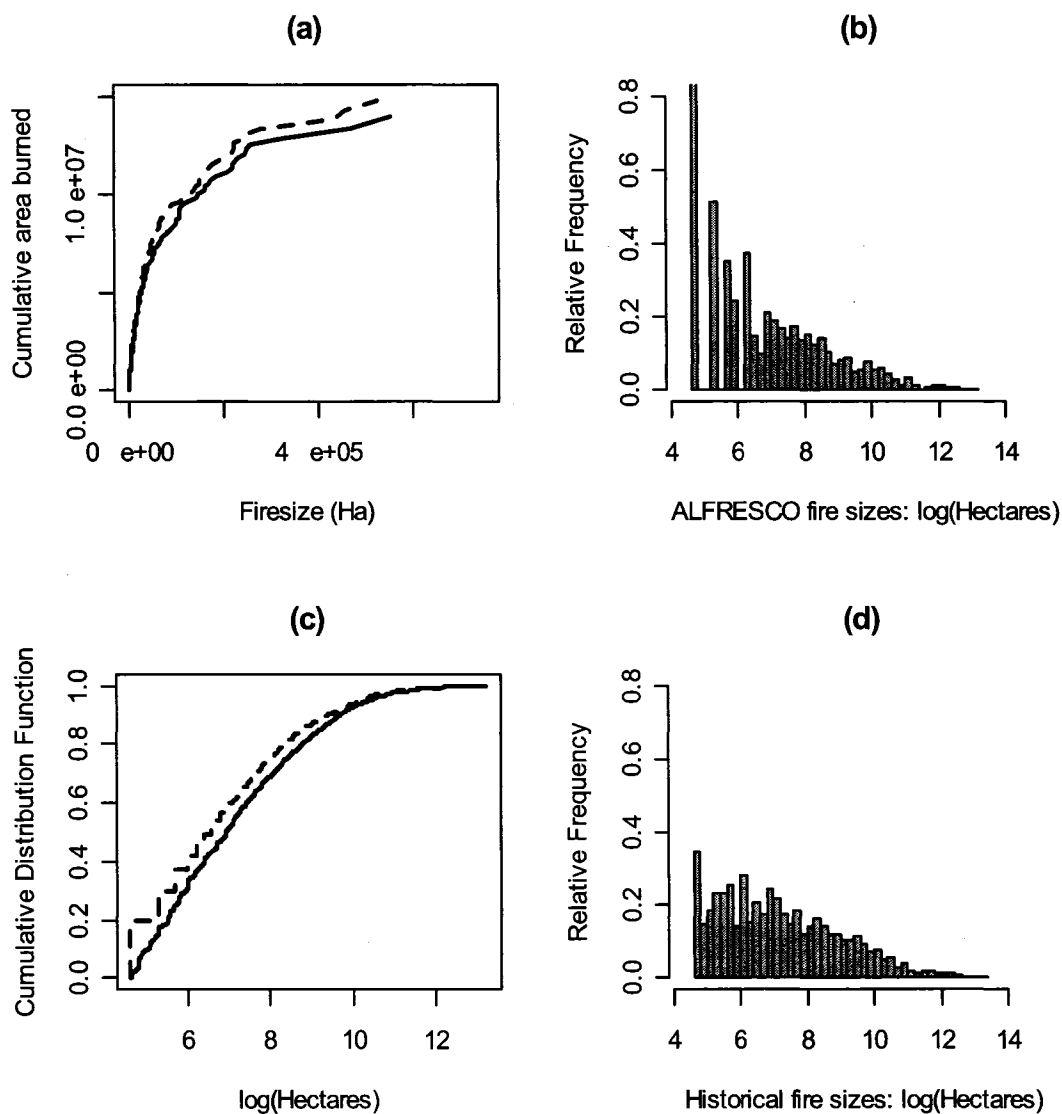
Figure 3.2   Fire size distribution plots for historical (solid) and ALFRESCO simulated (dashed) data: (a) Cumulative area burned as a function of fire size; (b) Histogram of the logarithm of fire sizes from ALFRESCO; (c) Cumulative distribution functions for both historical (solid) and simulated (dashed) data; and (d) Histogram for the logarithm of fire sizes from the historical record. ALFRESCO results correspond to a single set of realizations from 1950-2000.

Figure 3.3 Spatial representation of historical fire perimeters (white polygons) and ALFRESCO output (black polygons) from a single set of realizations for the period 1990-2000. This period of time was chosen due to the high quality of fire perimeter tracking available after 1990.
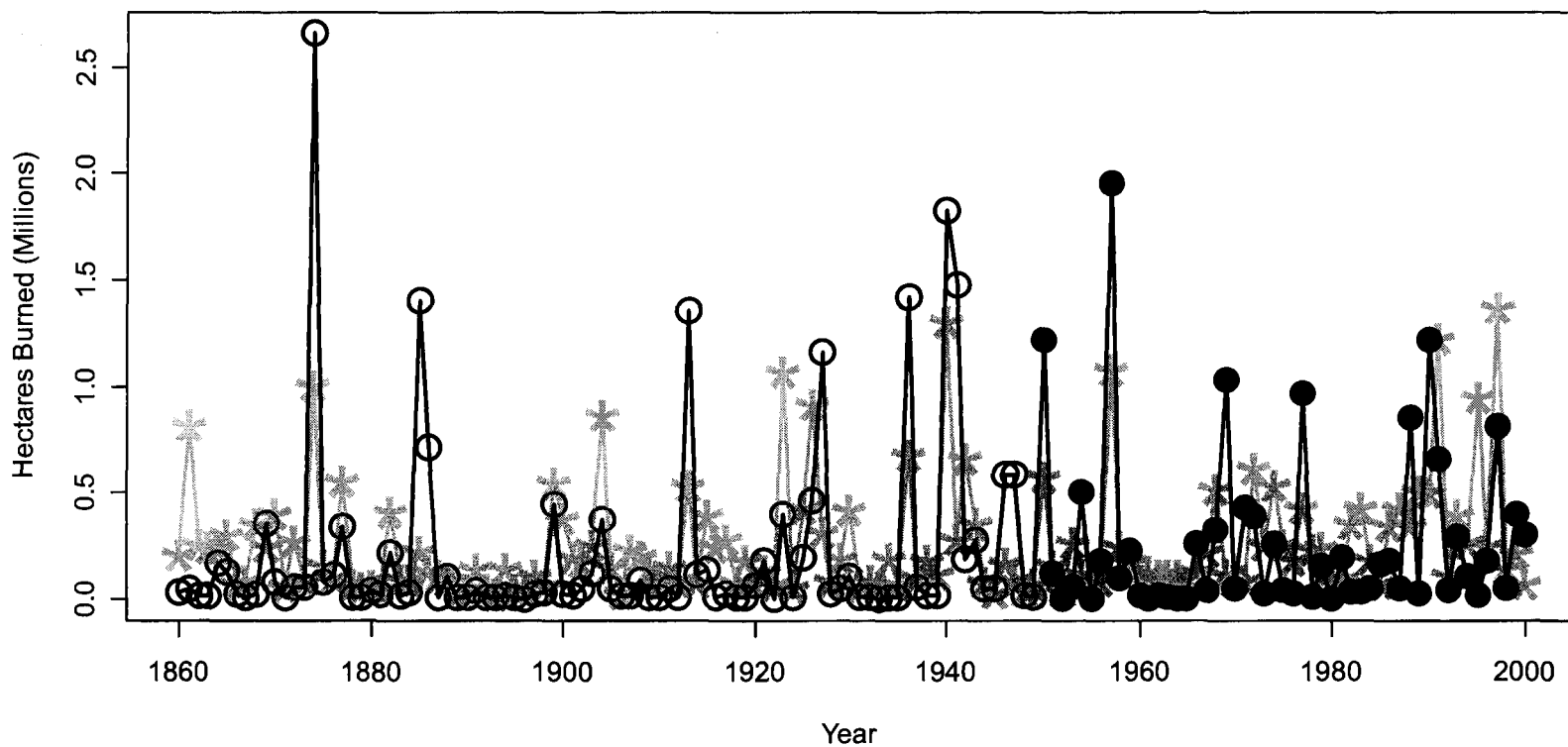
Figure 3.4   Backcast of annual area burned for interior Alaska from 1860-2000. The data from 1950-2000 (closed circles) are taken from the Large Fire Database (Kasischke et al.2002). Data from 1860-1949 (open circles) are point estimates from a modified version of the model presented in Duffy et al (2005). The backcast is used to calibrate the ALFRESCO output (Asterisks connected with grey lines), which simulates a spatially explicit representation of the annual area burned. ALFRESCO output presented here is from a single realization
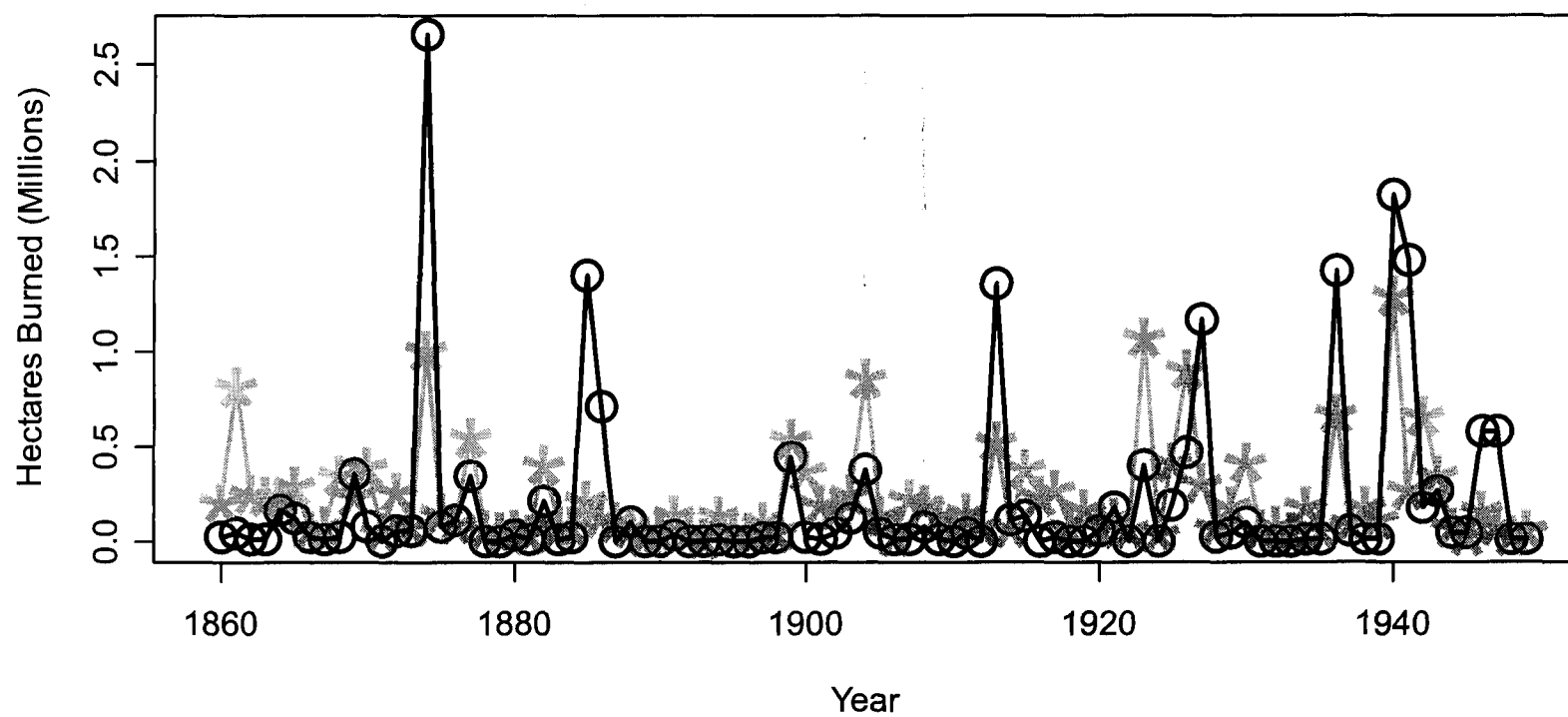
Figure 3.5   Comparison of annual area burned estimates from a statistical point model (open circles) and spatially explicit ALFRESCO output (Asterisks connected with grey lines). ALFRESCO output is represented by the average of 100 ALFRESCO realizations. The r-squared is 0.44.
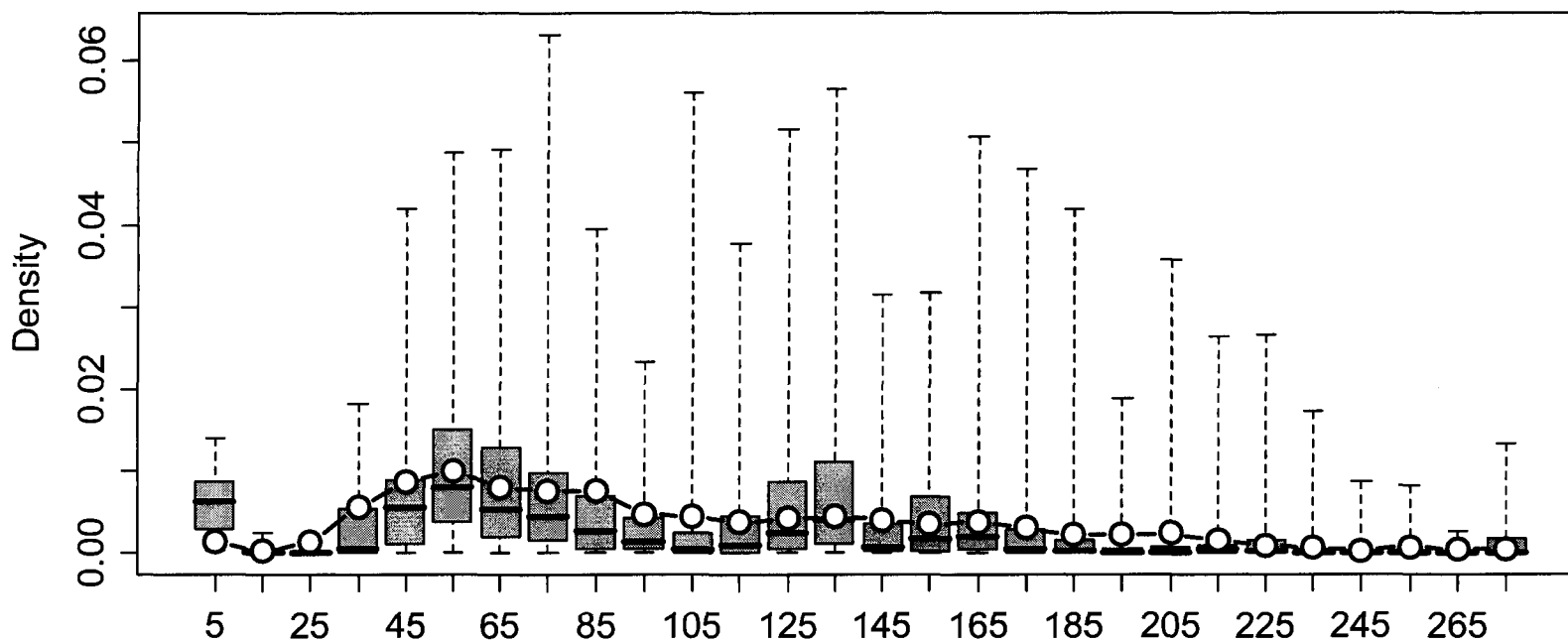
Figure 3.6   Comparison of observed (JFSP and FIA data) and simulated (ALFRESCO) stand age distributions from four subregions of interior Alaska. The observed distribution of stand ages is represented by black open dots with connecting lines. The collection of realizations from ALFRESCO simulations is represented with boxplots for each decadal interval. For each realization, there is a different distribution of stand ages; hence for each decadal interval there is a distribution. Shaded portions of the boxplot represent the interquartile range and horizontal bars represent the median. Whiskers extend to the maximum value of each decadal class across all simulation.
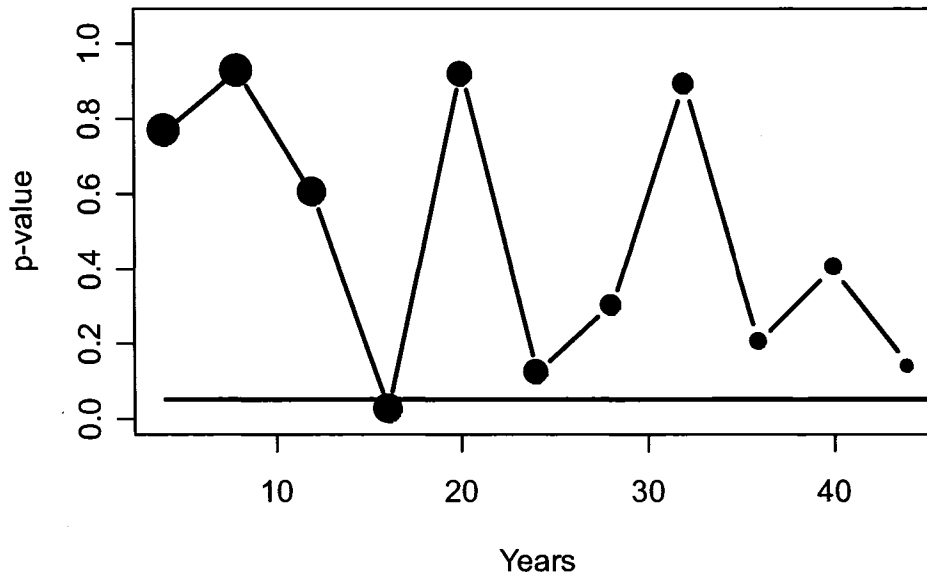
Figure 3.7   P-values corresponding to the tests of the null hypothesis that the spatial locations of fire polygons occur independently as a function of time since last fire (TSLF). Small p-values can be a consequence of either more or less intersection of fire polygons than would be expected under the null hypothesis. The test was performed at four-year intervals using fire perimeter data from 1950-2002. More intervals of smaller temporal duration are available (e.g there are thirteen intervals of length four years, twelve intervals of length eight years, etc.) and hence the size of the points corresponds to the number of intervals used to compute the p-value. The results for longer intervals are less reliable since fewer data are available.
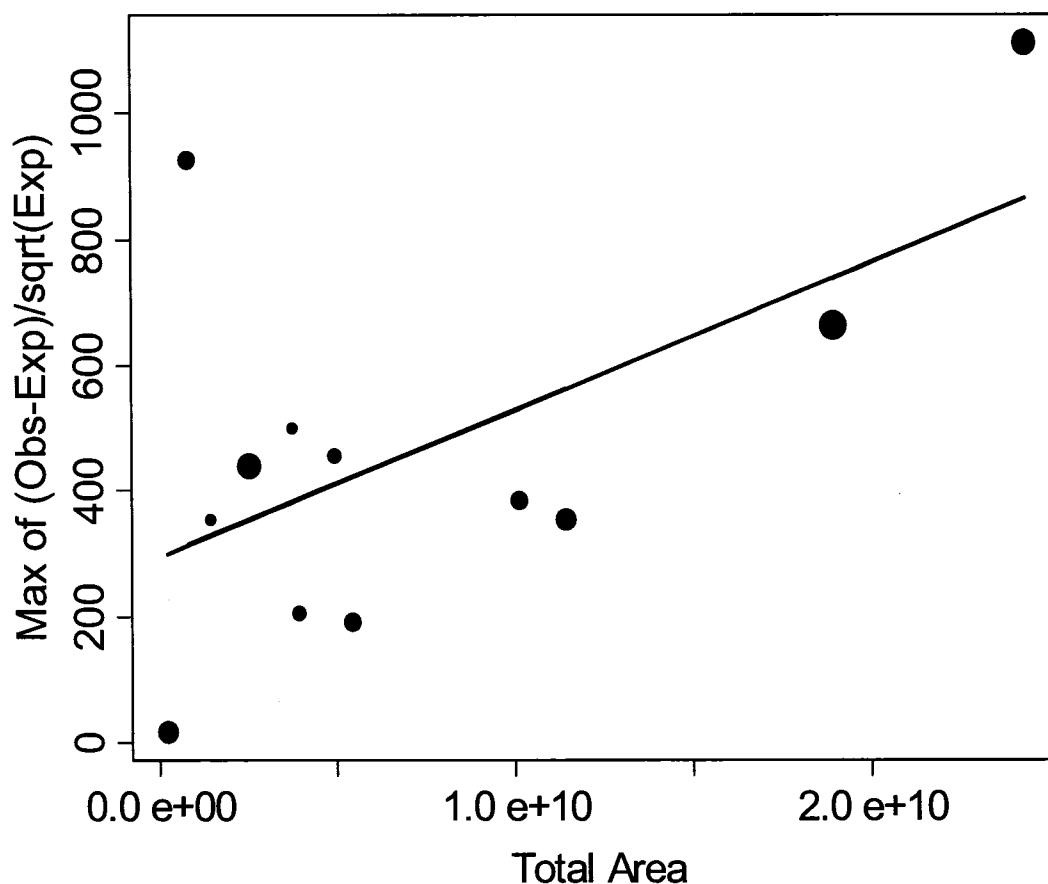
Figure 3.8   Scatterplot of total area burned (ha) in 4-year intervals versus the maximum value of the statistic [(Observed-Expected)/sqrt(Expected)] for the same 4-year interval (Table 2). Observed and expected values refer to intersections of fire perimeters. Expectation is computed based on a model of spatial independence. Size of each point corresponds to the number of observations available for each interval. Larger values of total area burned are associated with larger maximum values of the test statistic. The p-value for the regression significance is 0.05. This provides some evidence that time intervals where a larger initial area burns are more likely to experience burning in subsequent time intervals that exceeds the expectation under an independence model.

FIA (Impacted)

JFSP (Impacted)

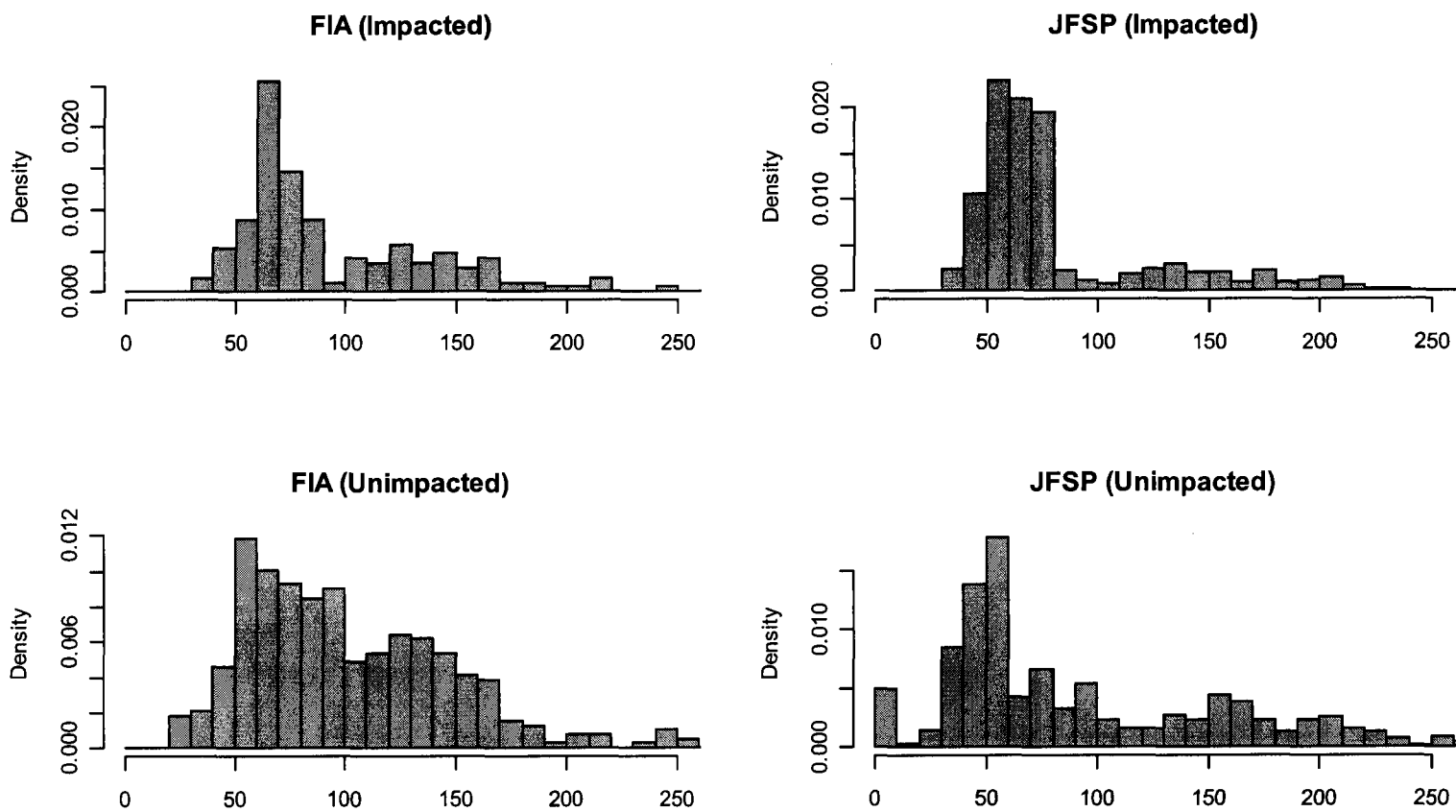**FIA (Unimpacted)**

JFSP (Unimpacted)

Figure 3.9   Histograms of two paired datasets (subsets of the FIA and JFSP datasets) where each pair contains both an impacted and unimpacted site. Impacts are associated with mining-related anthropogenic disturbance occurring around 1920. There is a distinct lack of stand ages in the 90-120 age range in both impacted sites.

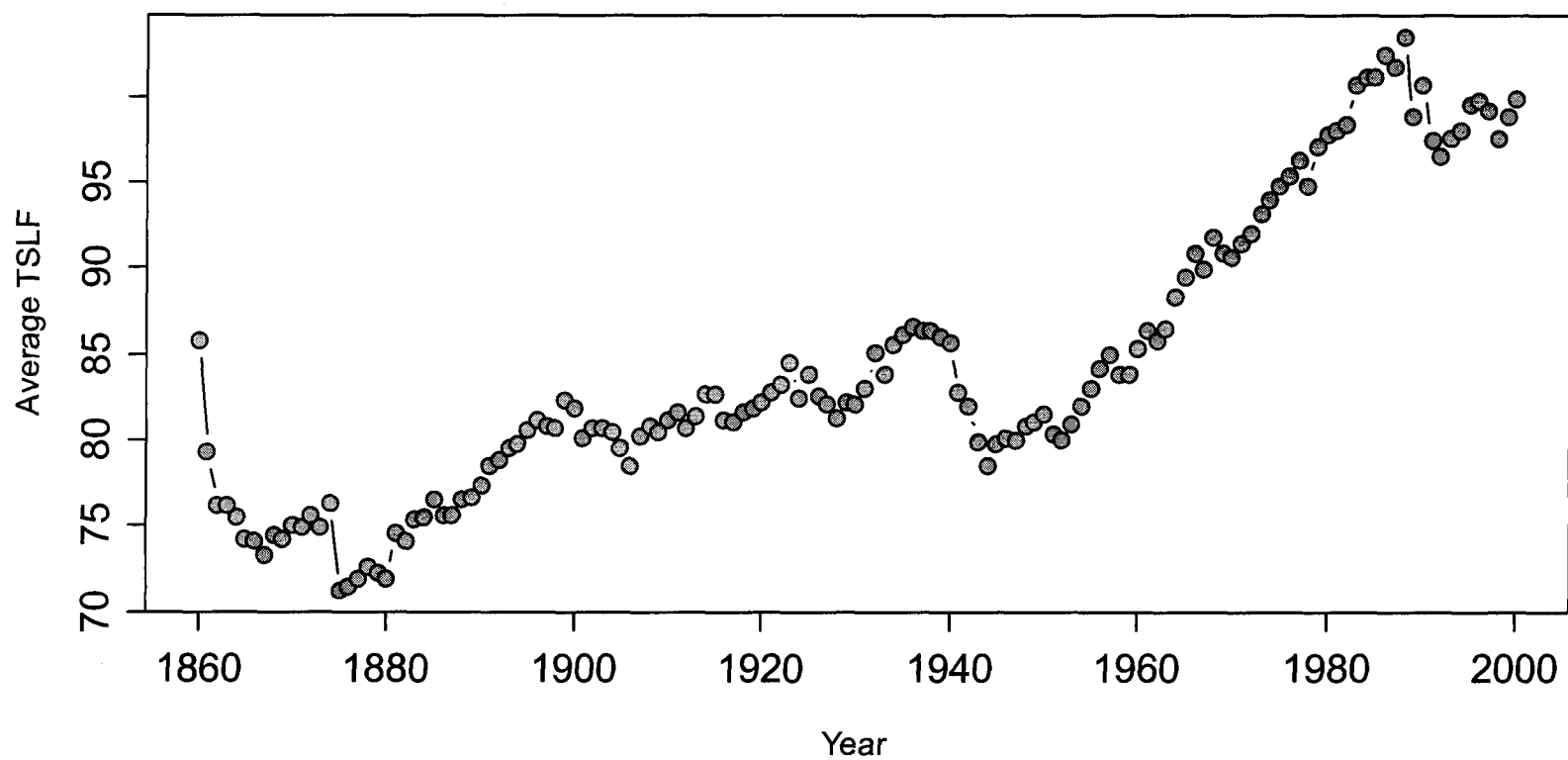**Figure 3.10** Time series plot of the average stand age sampled from ALFRESCO output. This plot shows that the average stand age can change significantly over the course of several decades.
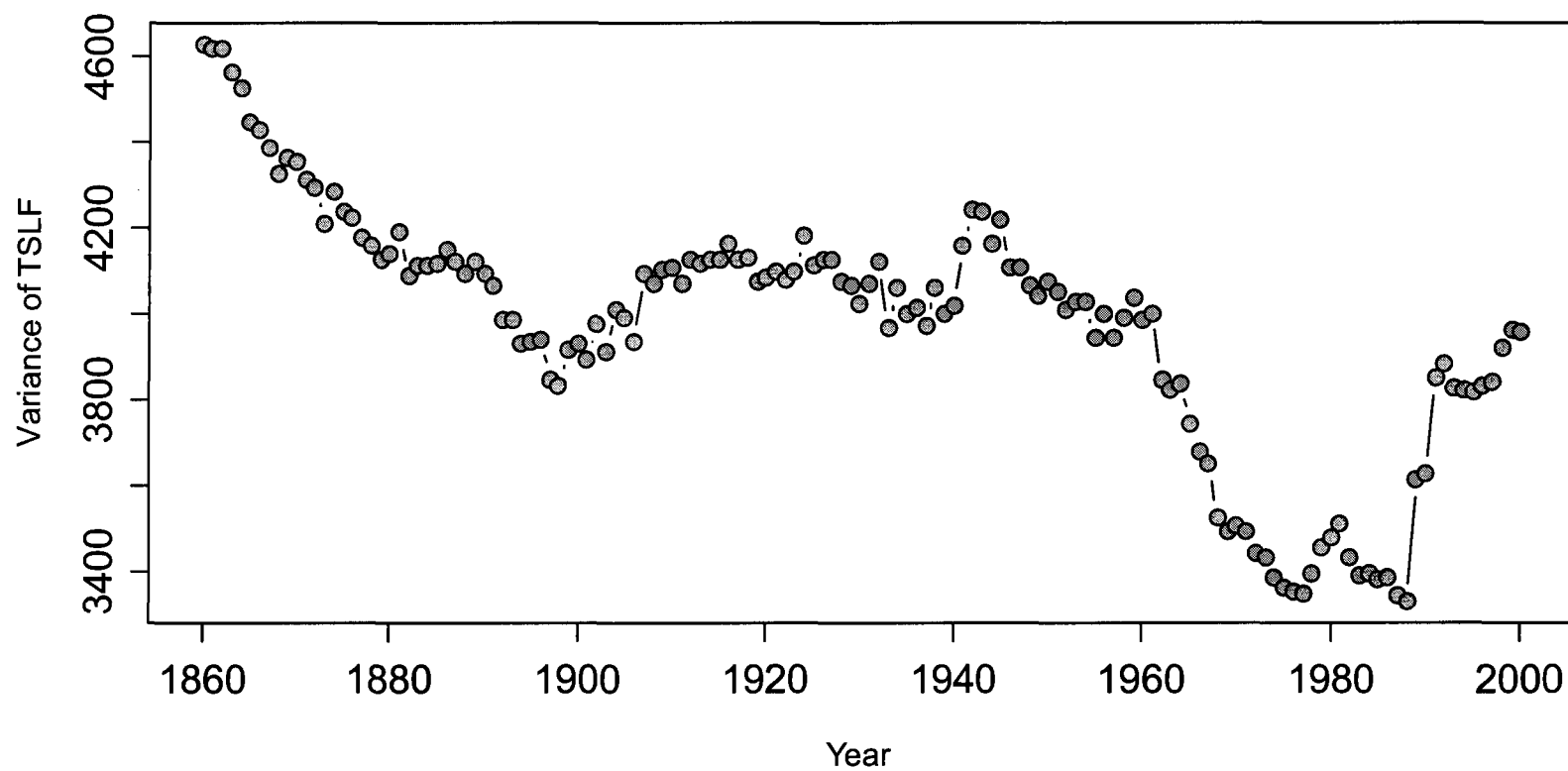
Figure 3.11   Time series plot of the variance of stand ages sampled from ALFRESCO output. This plot shows that based on the simulation results the assumption of stationarity of variance is questionable.
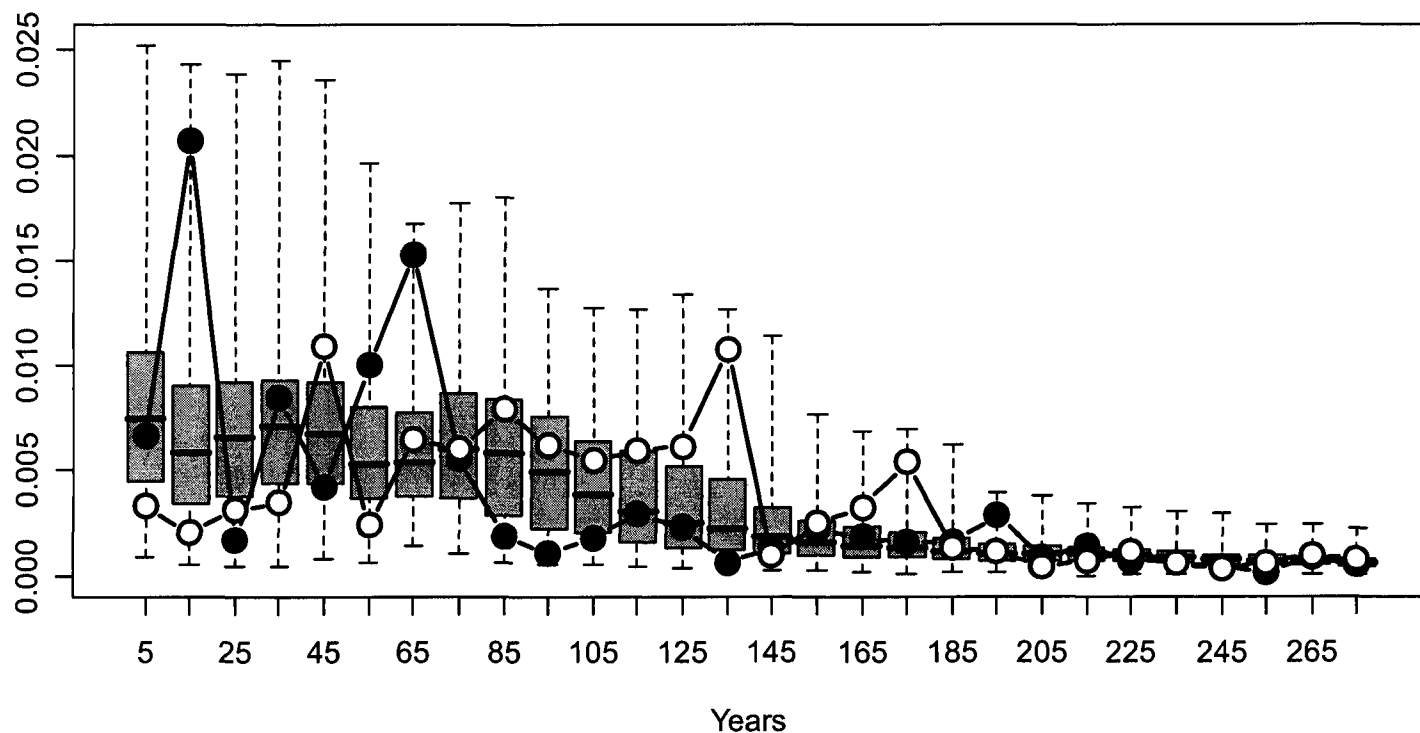
Figure 3.12   Boxplots of stand age distributions through time. For each year (1860-2000) within each set of ALFRESCO output there is a different distribution of stand ages; hence for each decadal interval there is a distribution. These boxplots represent the variability of stand age distributions at decadal intervals across each year from 1860-2000. This plot provides a temporal context that can be used to interpret observed stand age distributions. As an example of how stand ages can significantly change through time, the years with the oldest (1878 with open circles) and youngest (1988 with solid circles) average stand ages (see Figure 3.10) are represented.

Figure 3.13   Boxplots of simulated stand age distribution for the year 2000. Dots with connecting lines represent the stand age distribution estimate based on the JFSP and FIA data.

3.8 Tables

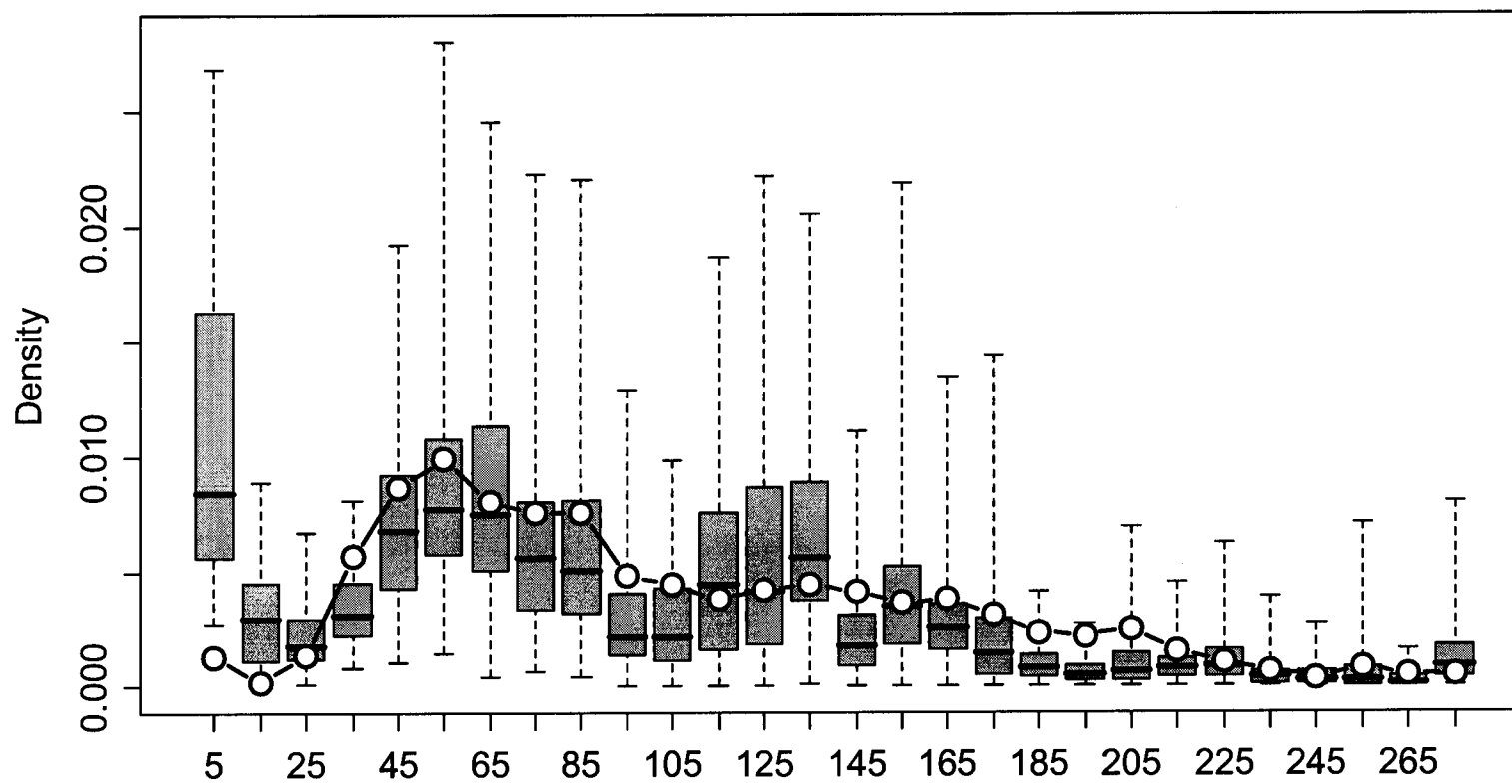**Table 3.1** Observed intersected area burned with expectation under an independence model in round parentheses. The value of the statistic [(Observed-Expected)/sqrt(Expected)] is presented in italics and the maximum value of this statistic for each time interval is presented in bold. Grey font indicates observed was less than expected.

	1950-1954	1955-1958	1959-1962	1963-1966	1967-1970	1971-1974	1975-1978	1979-1982	1983-1986	1987-1990	1991-1994	1995-1998
55-58	14969 (74578) *-218.3*	---	---	---	---	---	---	---	---	---	---	---
59-62	0 (7818) *-88.4*	0 (10037) *-100.2*	---	---	---	---	---	---	---	---	---	---
63-66	0 (705) *-26.6*	328 (905) *-19.2*	0 (94) *-9.7*	---	---	---	---	---	---	---	---	---
67-70	53342 (35024) *97.9*	1995 (44964) *-202.6*	2816 (4714) *-27.6*	0 (425) *-20.6*	---	---	---	---	---	---	---	---
71-74	1804 (2519) *-14.2*	66440 (3234) ***1111.4***	8452 (339) ***440.6***	0 (30) *-5.5*	125 (1519) *-35.8*	---	---	---	---	---	---	---
75-78	13222 (31032) *-101.1*	38643 (39839) *-6.0*	18258 (4176) *217.9*	0 (376) *-19.4*	6115 (18710) *-92.1*	7996 (1345) *181.3*	---	---	---	---	---	---
79-82	7450 (16684) *-71.5*	6287 (21419) *-103.4*	885 (2245) *-28.7*	0 (202) *-14.2*	3253 (10059) *-67.9*	4711 (723) *148.3*	0 (8912) *-94.4*	---	---	---	---	---
83-86	4613 (12127) *-68.2*	5251 (15569) *-82.7*	4763 (1632) *77.5*	0 (147) *-12.1*	16584 (7311) *108.4*	1676 (525) *50.2*	475 (6478) *-74.6*	955 (3483) *-42.8*	---	---	---	---
87-90	96804 (15178) ***662.5***	37932 (19486) *132.1*	2764 (2042) *16.0*	0 (184) *-13.6*	36080 (9151) *281.5*	17443 (658) *654.2*	28697 (8108) *228.7*	4047 (4359) *-4.72*	5072 (3168) *33.8*	---	---	---
91-94	29446 (4444) *375.0*	22096 (5705) *217.0*	3440 (598) *116.2*	0 (53) *-7.3*	21075 (2679) ***355.4***	1228 (192) *74.6*	4977 (2374) *53.4*	3710 (1276) *68.1*	4773 (927) *126.2*	1984 (1161) *24.2*	---	---
95-98	21113 (11486) *89.9*	21545 (14746) *56.0*	2408 (1546) *21.9*	0 (139) *-11.8*	5254 (6925) *-20.1*	21186 (498) *926.9*	582 (6136) *-70.9*	14199 (3299) ***189.8***	6064 (2398) *74.9*	17599 (3001) *266.5*	11372 (878) *354.0*	---
99-02	39257 (13391) *223.5*	91629 (17191) *567.7*	1240 (1802) *-13.2*	381 (162) *17.2*	9090 (8073) *11.3*	18712 (580) *752.4*	39573 (7153) ***383.3***	1983 (3846) *-30.0*	13625 (2795) *204.8*	30520 (3498) *456.8*	9040 (1024) *250.4*	28364 (2647) ***499.8***

Table 3.2   P-values for distributional comparisons of human-impacted versus unimpacted sites.

Minimum age	JFSP (Impacted vs. unimpacted)	FIA (Impacted vs. unimpacted)
> 180	0.94	0.55
> 170	0.98	0.57
> 160	0.59	0.59
> 150	0.59	0.62
> 140	0.60	0.65
> 130	0.51	0.71
> 120	0.33	0.78
> 110	0.33	0.82
> 100	0.35	0.84
> 90	0.15	0.22
> 80	**0.01**	0.10
> 70	**0.00**	**0.00**
> 60	**0.00**	**0.00**
> 50	**0.00**	**0.00**

Table 3.3 P-values for distributional comparisons of subsets of simulated (ALFRESCO) versus observed (JFSP and FIA) stand age distributions. Samples of size 250 were repeatedly taken from each dataset and the difference was assessed relatively to a null distribution generated by comparison of samples taken only from the simulated stand age data. Tests were performed on both validation and comprehensive simulated dataset. Validation dataset corresponds to the spatial extent and location of field sampling. The comprehensive dataset was obtained through sampling of much larger regions across interior Alaska. Since p-values are essentially a function of sample size in this context, the use of classical statistical techniques for the analysis of simulation results (where sample sizes can be arbitrarily large) will almost always produce a significant result (i.e., significant differences are observed). Specifically, as the sample size increases, p-values in Table 3 will converge to 0. In this case the results of the distributional comparison tests should be used only to assess relative significance between different decadal subsets of the data.

Minimum age	Validation vs. observed	Comprehensive vs. observed
> 180	0.44	0.51
> 170	0.40	0.58
> 160	0.46	0.59
> 150	0.43	0.50
> 140	0.43	0.53
> 130	0.24	0.22
> 120	0.30	0.18
> 110	0.24	0.21
> 100	0.23	0.19
> 90	0.18	0.17
> 80	0.13	0.16
> 70	0.16	0.21
> 60	0.16	0.16
> 50	0.15	0.22
> 40	0.14	0.21
> 30	0.10	0.19
> 20	0.09	0.15
> 10	0.08	0.08
All data	**0.03**	**0.00**

3.9 Acknowledgements

3.10   Literature Cited

Literature Cited

Barber, V. A., Juday, G. P., Finney, B. P., Wilmking, M. 2004. Reconstruction of summer temperatures in interior Alaska from tree-ring proxies: Evidence for changing synoptic climate regimes. Climatic Change 63: 91-120.

Bergeron, Y. 2000. Species and stand dynamics in the mixed woods of Quebec's southern boreal forest. Ecology 81(6): 1500-1516.

Bergeron, Y., Gauthier, S., Flannigan, M., Kafka, V. 2004. Fire regimes at the transition between mixedwood and coniferous boreal forest in Northwestern Quebec. Ecology 85(7): 1916-1932.

Bessie, W. C., Johnson, E. A. 1995. The relative importance of fuels and weather on fire behavior in subalpine forests. Ecology 76(3): 747-762.

Boychuk, D., Perera, A. H., Ter-Mikaelian, M. T., Martell, D. L., Li, C. 1997. Modeling the effect of spatial scale and correlated fire disturbances on forest age distribution. Ecological Modeling 95: 145-164.

Chapin III, F. S., T. S. Rupp, A. M. Starfield, L. DeWilde, E. S. Zavaleta, N. Fresco, J. Henkelman, and A. D. McGuire. 2003. Planning for resilience: modeling change in human fire interactions in the Alaskan boreal forest. Frontiers in Ecology and the Environment 1: (255-261).

Chapin III, F. S., Yarie, J., Van Cleve, K., Viereck, L. A. 2006a. The conceptual basis for LTER studies in the Alaskan boreal forest. in 'Alaska's Changing Boreal Forest'. (Eds. F. S. Chapin, III, M. W. Oswood, K. Van Cleve, L. A. Viereck, and D. L. Verbyla), Oxford University Press.

Chapin III, F. S., Viereck, L. A., Adams, P. C., Van Cleve, K., Fastie, C. L., Ott, R. A., Mann, D., Johnstone, J. F. 2006b. Successional processes in the Alaskan boreal forest. in 'Alaska's Changing Boreal Forest'. (Eds. F. S. Chapin III, M. W. Oswood, K. Van Cleve, L. A. Viereck, and D. L. Verbyla), Oxford University Press.

Csiszar, I., C. O. Justice, A. D. McGuire, M. A. Cochrane, D. P. Roy, F. Brown, S. G. Conard, P. G. H. Frost, L. Giglio, C. Elvidge, M. D. Flannigan, E. S. Kasischke, D. J. McRae, T. S. Rupp, B. J. Stocks, and D. L. Verbyla. 2004. Land use and fires. in 'Land Change Science: Observing, Monitoring, and Understanding Trajectories of Change on the Earth's Surface'. (Eds. Gutman, G., Janetos, A. C., Justice, C. O., Moran, E. F., Mustard, J. F., Rindfuss, R. R., Skole, D., Turner II, B. L., Cochrane, M. A.), pp. 329-350, Dordrecht, Netherlands, Kluwer Academic Publishers.

Cumming, S. G. 2001. Forest type and wildfire in the Alberta boreal mixedwood: What do fires burn? Ecological Applications 11(1): 97-110.

D'Arrigo, R., Villalba, R., Wiles, G. 2001. Tree-ring estimates of Pacific decadal climate variability. Climate Dynamics 18: 219-224.

DesRochers, A., Gagnon, R. 1997. Is ring count at ground level a good estimation of black spruce age? Canadian Journal of Forest Research 27: 1263-1267.

Dissing, D., Verbyla, D. L. 2003. Spatial patterns of lightning strikes in interior Alaska and their relations to elevation and vegetation. Canadian Journal of Forest Research 33: 770-782.

Drobyshev, I., Niklasson, M., Angelstam, P., Majewski, P. 2004. Testing for anthropogenic influence on fire regime for a 600-year period in the Jaksha area, Komi Republic, East European Russia. Canadian Journal of Forest Research 34(10): 2027-2036.

Duffy, P. A., Walsh, J. E., Graham, J. M., Mann, D. H., Rupp, T. S. 2005. Impacts of large-scale atmospheric-ocean variability on Alaskan fire season severity. Ecological Applications 15(4): 1317-1330.

Duffy, P. A., Epting, J., Graham, J. M., Rupp, T. S., McGuire, A. D. (accepted). Analysis of Alaskan burn severity patterns using remotely sensed data. International Journal of Wildland Fire

Eberhart, K. E., Woodard, P. M. 1987. Distribution of residual vegetation associated with large fires in Alberta. Canadian Journal of Forest Research 17: 1207-1212.

Fastie, C. L., Lloyd, A. H., Doak, P. 2003. Fire history and postfire forest development in an upland watershed of interior Alaska. Journal of Geophysical Research 108(D1), 8150: FFR 6-1, 6-13.

Fosberg, M. A., Cramer, W., Brovkin, V., Fleming, R., Gardner, R., Gill, A. M., Goldammer, J. G., Keane, R., Koehler, P., Lenihan, J., Neilson, R., Sitch, S., Thornicke, K., Venevski, S., Weber, M. G., Wittenberg, U. 1999. Strategy for a fire module in dynamic global vegetation models. International Journal of Wildland Fire 9(1): 79-84.

Girardin, M.-P., Tardif, J., Flannigan, M. D., Wotton, B. M., Bergeron, Y. 2004. Trends and periodicities in the Canadian Drought Code and their relationships with atmospheric circulation for the southern Canadian boreal forest. Canadian Journal of Forest Research 34: 103-119.

Gower, S. K., O. Olson, R.J., Apps, M., Linder, S., Wang, C. 2001. Net primary production and carbon allocation patterns of boreal forest ecosystems. Ecological Applications 11(5): 1395-1411.

Grenier, D. J., Bergeron, Y., Kneeshaw, D., Gauthier, S. 2005. Fire frequency for the transitional mixedwood forest of Timiskaming, Quebec. Canadian Journal of Forest Research 35(3): 656-666.

Harden, J. W., Trumbore, S. E., Stocks, B. J., Hirsch, A., Gower, S. T., O'Neill, K. P., Kasischke, E. S. 2000. The role of fire in the boreal carbon budget. Global Change Biology 6(Supplement 1): 174-184.

Hess, J. C., Scott, C. A., Hufford, G. L., Fleming, M. D. 2001. El Nino and its impact on fire weather conditions in Alaska. International Journal of Wildland Fire 10: 1-13.

Hinzman, L. D., Viereck, L. A., Adams, P. C., Romanovsky, V. E., Yoshikawa, K. 2006. Climate and permafrost dynamics of the Alaskan boreal forest. in 'Alaska's Changing Boreal Forest'. (Eds. F. S. Chapin III, M. W. Oswood, K. Van Cleve, L. A. Viereck, and D. L. Verbyla), Oxford University Press.

IPCC 2001. Climate Change 2001: Technical Summary of the Working Group I Report. WMO/UNEP. Cambridge, Cambridge University Press.

Johnson, E. A. 1995. Fire and vegetation dynamics: Studies from the North American boreal forest, Cambridge University Press.

Johnson, E. A., Miyanishi, K., Weir, J. M. H. 1998. Wildfires in the western Canadian boreal forest: Landscape patterns and ecosystem management. Journal of Vegetation Science 9: 603-610.

Johnson, R. A., Verrill, S., Moore II, D. H. 1987. Two-sample rank tests for detecting changes that occur in a small proportion of the treated population. Biometrics 43(3): 641-655.

Johnstone, J. F., Chapin III, F. S., Foote, J., Kemmett, S., Price, K., Viereck, L. 2004. Decadal observations of tree regeneration following fire in the boreal forest. Canadian Journal of Forest Research 34: 267-273.

Johnstone, J. F., Kasischke, E. S. 2005. Stand-level effects of soil burn severity on postfire regeneration in a recently burned black spruce forest. Canadian Journal of Forest Research 35(9): 2151-2163.

Kasischke, E. S., Williams, D., Barry, D. 2002. Analysis of the patterns of large fires in the boreal forest region of Alaska. International Journal of Wildland Fire 11: 131-144.

Kasischke, E. S., Rupp, T.S., Verbyla, D.L. 2006. Fire trends in the Alaskan boreal forest. in 'Alaska's Changing Boreal Forest'. (Eds. F. S. Chapin III, M. W. Oswood, K. Van Cleve, L. A. Viereck, and D. L Verbyla), Oxford University Press.

Kittel, T. G. F., Steffen, W. L., Chapin III, F. S. 2000. Global and regional modeling of Arctic-boreal vegetation distribution and its sensitivity to altered forcing. Global Change Biology 6(Supplement 1): 1-18.

Kurkowski, T. A., Rupp, T. S., Mann, D. H., Verbyla, D. L. (submitted). Quantifying the relative importance of different secondary succession processes in the Alaskan boreal forest.

Kurz, W. A., Apps, M. J. 1999. A 70-year retrospective analysis of carbon fluxes in the Canadian forest sector. Ecological Applications 9(2): 526-547.

Larsen, C. P. S. 1997. Spatial and temporal variations in boreal forest fire frequency in northern Alberta. Journal of Biogeography 24: 663-673.

Leemans, R., Cramer, W. P., 1991. The IIASA database for mean monthly values of temperature, precipitation and cloudiness of a global terrestrial grid. International Institute for Applied Systems Analysis: RR-91-18.

McBean, G., Alekseev, G., Chen, D., Forland, E., Fyfe, J., Groisman, P. Y., King, R., Melling, H., Vose, R., Whitfield, P. H. 2004. Arctic climate: Past and present. In 'Arctic Climate Impact Assessment - Scientific Report'. (Eds. C. Symon, Arris, L., Heal, B.), Cambridge.

McGuire, A. D., S. Sitch, J. S. Clein, R. Dargaville, G. Esser, J. Foley, M. Heimann, F. Joos, J. Kaplan, D. W. Kicklighter, R. A. Meier, J. M. Melillo, B. Moore III, I. C. Prentice, N. Ramankutty, T. Reichenau, A. Schloss, H. Tian, L. J. Williams, and U. Wittenberg. 2001. Carbon balance of the terrestrial biosphere in the twentieth century: Analyses of CO2, climate and land-use effects with four process-based ecosystem models. Global Biogeochemical Cycles 15: 183-206.

McGuire, A. D., M. Apps, F. S. Chapin III, R. Dargaville, M. D. Flannigan, E. S. Kasischke, D. Kicklighter, J. Kimball, W. Kurz, D. J. McRae, K. McDonald, J. Melillo, R. Myneni, B. J. Stocks, D. L. Verbyla, and Q. Zhuang, Ed. 2004. Land cover disturbances and feedbacks to the climate system in Canada and Alaska. In 'Land Change Science: Observing, Monitoring, and Understanding Trajectories of Change on the Earth's Surface'. (Eds. Gutman, G., Janetos, A. C., Justice, C. O., Moran, E. F., Mustard, J. F., Rindfuss, R. R., Skole, D., Turner II, B. L., Cochrane, M. A.), pp. 139-161. Dordrecht, Netherlands, Kluwer Academic Publishers.

McGuire, A.D., F. S. Chapin III. 2006. Climate Feedback in the Alaskan Boreal Forest. in 'Alaska's Changing Boreal Forest'. (Eds. F. S. Chapin III, M. W. Oswood, K. Van Cleve, L. A. Viereck, and D. L. Verbyla), Oxford University Press.

Natcher, D. C. 2004. Implications of fire policy on native land use in the Yukon Flats, Alaska. Human Ecology 32(4): 421-441.

Niebauer, H. J. 1998. Variability in Bering Sea ice cover as affected by a regime shift in the North Pacific in the period 1947-1996. Journal of Geophysical Research 103(c12): 27171-27737.

Osterkamp, T. E., Romanovsky, V. E. 1999. Evidence for warming and thawing of discontinuous permafrost in Alaska. Permafrost and Periglacial Processes 10(1): 17-37.

Osterkamp, T. E., Viereck, L., Shur, Y, Jorgenson, M. T., Racine, C., Doyle, A., Boone, R.D. 2000. Observations of thermokarst and its impact on boreal forests in Alaska, USA. Arctic, Antarctic and Alpine Research 32(3): 303-315.

Parisien, M.-A., Sirois, L. 2003. Distribution and dynamics of tree species across a fire frequency gradient in the James Bay region of Quebec. Canadian Journal of Forest Research 33(2): 243-256.

Payette, S. 1992. Fire as a controlling process in the North American boreal forest. in 'A systems analysis of the Global Boreal Forest'. (Eds. Shugart, H. H., Leemans, R., Bonan, G. B.), Cambridge, Cambridge University Press.

Ping, C. -L., Boone, R. D., Clark, M. H., Packee, E. C., Swanson, D. K. 2006. State factor control of soil formation in interior Alaska. In 'Alaska's Changing Boreal Forest'. (Eds. F. S. Chapin III, M. W. Oswood, K. Van Cleve, L. A. Viereck, and D. L. Verbyla), Oxford University Press.

Polakow, D. A., Dunne, T. T. 1999. Modeling fire-return interval T: Stochasticity and censoring in the two-parameter Weibull model. Ecological Modeling 121: 79-102.

Reed, W. J. 1997. Estimating the historic probability of stand-replacement fire using the age-class distribution of undisturbed forest. IMAJ Math Applied Medical Biology 14: 71-83.

Reed, W. J., Larsen, C. P. S., Johnson, E. A., MacDonald, G. M. 1998. Estimation of temporal variations in historical fire frequency from time-since-fire map data. Forest Science 44(3): 465-475.

Reed, W. J. 1998. Determining changes in historical forest fire frequency from a time-since fire map. Journal of Agricultural, Biological and Environmental Statistics 3(4): 430-450.

Rosenbaum, S. 1954. Tables for a nonparametric test of location. Annals of Mathematical Statistics 25(1): 146-150.

Rupp, T. S., Starfield, A. M., Chapin III, F. S. 2000a. A frame-based spatially explicit model of subarctic vegetation response to climatic change: comparison with a point model. Landscape Ecology 15: 283-400.

Rupp, T. S., Chapin III, F. S., Starfield, A. M. 2000b. Response of subarctic vegetation to transient climatic change on the Seward Peninsula in North-West Alaska. Global Climate Change 6: 541-555.

Rupp, T. S., Chapin III, F. S., Starfield, A. M. 2001. Modeling the influence of topographic barriers on treeline advance at the forest-tundra ecotone in Northwestern Alaska. Climatic Change 48: 399-416.

Rupp, T. S., A. M. Starfield, F. S. Chapin III, P. Duffy. 2002. Modeling the impact of black spruce on the fire regime of Alaskan boreal forest. Climatic Change 55: 213-133.

Rupp, T. S., Olson, M., Adams, L. G., Dale, B.W., Joly, K., Henkelman, J., Collins, W. B., Starfield, A. M. 2006. Simulating the influences of various fire regimes on caribou winter habitat. (in press).

Schimel, D. S., VEMAP participants, Braswell, B.H. 1997. Continental scale variability in ecosystem processes: Models, data, and the role of disturbance. Ecological Monographs 67(2): 251-271.

Serreze, M. C., Walsh, J. E., Chapin III, F. S., Osterkamp, T., Dyurgerov, M., Romanovsky, V., Oechel, W.C., Morison, J., Zhang, T., Barry, R.G. 2000. Observational evidence of recent change in the Northern high-latitude environment. Climatic Change 46(1/2): 159-207.

Skinner, W. R., Stocks, B. J., Martell, D. L., Bonsal, B., Shabbar, A. 1999. The association between circulation anomalies in the mid-troposphere and the area burned by wildfire in Canada. Theoretical and Applied Climatology: 3-17.

Skinner, W. R., Flannigan, M. D., Stocks, B. J., Martell, D. L., Wotton, B. M., Todd, J. B., Mason, J. A., Logan, K. A., and Bosch, E. M. 2002. A 500 hPa synoptic wildland fire climatology for large Canadian forest fires, 1959-1996. Theoretical Applied Climatology 71: 157-169.

Trumbore, S. E., Harden, J. W. 1997. Accumulation and turnover of carbon in organic and mineral soils of the BOREAS northern study area. Journal of geophysical research 103(D24): 28.

Van Cleve, K., Viereck, L. A. 1983. A comparison of successional sequences following fire on permafrost-dominated and permafrost-free sites in interior Alaska. Permafrost: Fourth International Conference, Proceedings: 1286-1291.

Van Cleve, K., Chapin III, F. S., Dyrness, C. T., Viereck, L. A. 1991. Element cycling in Taiga forests: State-factor control. Bioscience 41(2): 78-88.

Van Wagner, C. E. 1978. Age-class distribution and the forest fire cycle. Canadian Journal of Forest Research 8: 220-7.

Viereck, L. A., Van Cleve, K., Dryness, C. T. 1986. Forest ecosystem distribution in the Taiga environment. in 'Forest Ecosystems in the Alaskan Taiga: A synthesis of structure and function'. (Eds. K. Van Cleve, Chapin III, F. S., Flanagan), New York, Springer-Verlag: 22-43.

Weir, J. M. H., Johnson, E. A., Miyanishi, K. 2000. Fire frequency and the spatial age mosaic of the mixed-wood boreal forest in Western Canada. Ecological Applications 10(4): 1162-1177.

Wurtz, T. L., Ott, R. A., Maisch, J. C. 2006. Timber harvest in interior Alaska. in 'Alaska's Changing Boreal Forest'. (Eds. F. S. Chapin III, M. W. Oswood, K. Van Cleve, L. A. Viereck, and D. L. Verbyla), Oxford University Press.

Yarie, J. 1981. Forest fire cycles and life tables: a case study from interior Alaska. Canadian Journal of Forest Research 11(3): 554-562.

Conclusion

In the vast forested ecosystem of interior Alaska, disturbance is dominated by climatically driven fire occurrence. As a consequence, forest vegetation is a constantly changing mosaic governed by interactions among fire, climate, and vegetation. This work strengthens several critical components of the conceptual model of the Alaskan boreal forest through the development and testing of numerous hypotheses. An over-riding focus of this work is the explicit recognition of the relevant spatial and temporal scales for the various interactions that are characterized. This allows for a better understanding of the mechanisms that drive these interactions. Additionally, the recognition of spatio-temporal scaling allows for the development of a simulation model, which facilitates the testing of hypotheses regarding changes across different regions of the boreal forest through time.

The most important result among those presented in this work, is the link between climate and fire. Specifically, the use of monthly temperature, precipitation, and atmospheric teleconnection indices in a regression model results in the explanation of roughly 80% of the inter-annual variability of the natural logarithm of annual area burned in Alaska from 1950-2003. June temperature plays a critical role in the magnitude of area burned, as it alone explains roughly a third of the observed variability. This statistical model can be used to generate both forecasts and backcasts of annual area burned in Alaska. Due to the strong dependence of area burned on weather, forecasts produced by the regression model are only as reliable as the forecasts for temperature and precipitation used in the model. Attempts to forecast area burned in Alaska should focus on identifying those atmospheric mechanisms that most strongly influence June temperature.

The statistical model is used in conjunction with a historical climate record and historical fire data to calibrate a spatially explicit cellular automata model (ALFRESCO). ALFRESCO is a virtual laboratory, which allows for the design of experiments that can test assumptions within the conceptual model of the boreal forest of Alaska. In this work,

ALFRESCO simulates fires at an annual temporal resolution across the landscape of interior Alaska. Flammability of a given cell within the model is a function of growing season temperature, precipitation and vegetation. There is a simple successional model where burned cells are recruited by deciduous vegetation the year after fire. In the absence of fire the deciduous cells stochastically transition to a more flammable conifer state between 60 and 120 years. Once calibrated, spatially explicit historical climate data from 1860-2000 were used to drive ALFRESCO simulations that depict stand age distributions across interior Alaska. The simulated stand-ages were validated using field data from across interior Alaska.

The ALFRESCO simulation results suggest that significant changes in both the average and variance of stand ages have occurred from 1860-2000. Specifically, the average stand age has increased and the variance has decreased. These model results indicate that the patches of highly flammable conifer vegetation that currently exist on the landscape are unprecedented over the past 140 years. These changes imply that the forest is currently in a state where the arrangement of differentially flammable vegetation across the landscape will likely result in increased fire activity and size within the next several decades.

This change in flammability demonstrates that although climate plays the dominant role with respect to annual area burned, the distribution of differentially flammable vegetation across the landscape of interior Alaska is important with respect to impacts of fire. As a consequence, interactions among vegetation, burn severity and topography were explored. This portion of the analysis found that average burn severity increases with the logarithm of fire size. Fire size can be considered a proxy for the climatic conditions that are favorable for burning. Specifically, fires that are large tend to burn later in the season. We also found that fires burning in the flats show significant differences between average burn severities among vegetation classes. Conversely, fires burning in more complex terrain were less likely to have significant differences between

average burn severities as a function of vegetation type. These results will guide future modeling efforts in ALFRESCO that account for the role of fire size and topography as modifiers of fire-vegetation interactions.

In summary, climatically driven fire is the crux of interactions among climate, fire, and vegetation in the Alaskan boreal forest. The majority of the variability in annual area burned across Alaska can be explained using monthly climatic indices. The remaining variability that is unexplained by climatic indices can, for the most part, be attributed to the distribution of differentially flammable vegetation across the landscape of interior Alaska. Topography plays an important role in the modification of interactions between dominant forest vegetation and burn severity, which can consequently modify spatial pattern formation of dominant forest vegetation across the Alaskan boreal forest. Collectively, these results were incorporated in the ALFRESCO model. Spatially explicit simulations of stand-age distributions through time suggest that the Alaskan boreal forest is currently in an elevated state of flammability due to the unprecedented level of homogenous, highly flammable coniferous vegetation. Coupled with the forecast climatic warming for high latitudes, these results indicate that the next several decades will exhibit fire activity outside the range of historical activity observed over the past five decades.